2013

Orchestrating cancer cell migration: Quantatitive analysis of protrusion, adhesion and contraction dynamics regulated by epidermal growth factor and collagen

Yue Hou
Iowa State University

Orchestrating cancer cell migration: Quantitative analysis of protrusion, adhesion and contraction dynamics regulated by epidermal growth factor and collagen

by

Yue (Ariel) Hou

A dissertation submitted to the graduate faculty

in partial fulfillment of the requirements for the degree of

DOCTOR OF PHILOSOPHY

Major: Chemical Engineering

Program of Study Committee:

Ian C. Schneider, Major Professor

Surya Mallapragada

Jacqueline V. Shanks

Sanjeevi Sivasankar

Emily Smith

Iowa State University

Ames, Iowa

2013

DEDICATION

I would like to dedicate this thesis to my husband Cansheng, my father Tianping and my mother Songjun, without whose support and love I would not have been able to complete this work.

I would also like to dedicate this thesis to my son Lee, without whom this work would have been finished two months earlier.

Finally, I would like to thank my friends and other family members for their loving and caring encouragement during the writing of this work.

TABLE OF CONTENTS

LIST OF TABLES

LIST OF FIGURES

ACKNOWLEDGEMENTS

I would like to take this opportunity to express my thanks to those who helped me with various aspects of conducting research and the writing of this thesis.

First and foremost, I would like to express my deepest gratitude to my advisor Professor Ian C. Schneider for his guidance, patience and support throughout this research and the writing of this thesis. His inspired suggestions, patient guidance and encouraging words have not only supported me in completing my PhD education but also taught me how to be an independent researcher.

I would also like to thank my committee members for their efforts and contributions to this work: Professor Surya Mallapragada, Professor Jacqueline V. Shanks, Professor Sanjeevi Sivasankar, Professor Emily Smith and Professor Anastasios Matzavinos. Their remarkable advice and comments have motivated me in designing experiments and modifying my thesis.

In addition, I thank Professor Surya Mallapragada, Professor Charles E. Glatz and Professor Laura Jarboe for your kindness in providing access to equipment for my research.

Last but not least, many thanks to my lab mates: Amanda Haage, Laura Lara Rodriguez, Juan Wang, Nicholas R. Romsey, Justin Adams, Dr. Bingqi Zhang, Dr. Yanjie Zhang, Dr. Latrisha Petersen as well as all the undergraduate and high school students whom I have supervised. It was such a pleasure to work with all of you.

ABSTRACT

Cell migration plays an important role in cancer metastasis. Traditional diagnostic methods often involve obtaining tissue biopsies and examining the morphology of the cells and the molecular composition of the microenvironment in static microscopy images. A link between dynamic cellular processes and static microenvironmental inputs must be made. This connection is often made qualitatively with a lack of quantitative information. Therefore, the aims of this work are to investigate how subcelluar dynamics of cell migration such as protrusion and adhesion are quantitatively modulated under different environmental inputs such as epidermal growth factor (EGF) and collagen.

There are two major subcellular processes of migration, protrusion and adhesion. Protrusion is a dynamic movement of the cell edge and adhesion is mediated through macromolecular complexes called focal adhesions (FA). EGF concentration is an input that regulates FA and protrusion dynamics, whereas cell speed is an output that integrates information determined by inputs such as EGF. Several FA signatures and protrusion waves are associated with fast migration, but not necessarily with EGF. This suggests that other factors like contractility or extracellular matrix (ECM) might alter protrusion and FA for fast migration. Because fast migrating cells are usually invasive and cause metastasis, I designed a high-throughput method to identify the fast cells for determining what differences in cell properties such as protein expression level lead to the cell-to-cell variability. As mentioned above, contractility and ECM adhesivity are other inputs that affect migration. Although their effects on migration may be similar, upstream responses may vary. For example, both increasing adhesivity and decreasing contractility decreased migration speed, but their impact on protrusion and adhesion were distinct. Adhesivity affects migration not only on uniform substrates, but also under contact guidance. Both increasing adhesivity and the number of lines a cell contacted resulted in decreased directionality with more protrusion waves, which suggest that adhesivity and line

spacing drive the efficiency of contact guidance through the presence of protrusion waves. In summary, quantification of protrusion and FA properties might provide signatures that relate short timescale dynamics to long timescale migrational properties, making them ideal measurements for cancer diagnosis.

CHAPTER 1. INTRODUCTION

1.1 Cancer Metastasis and its Diagnosis

Breast cancer is the most common type of cancer in women. Most of the primary tumors can be removed relatively easily by irradiation and surgery, but when a primary tumor colonizes distant organs to form secondary tumors, cancer is much harder to treat (van Nimwegen, Verkoeijen et al. 2005). This entire process is called metastasis and it causes about 90% of the deaths in breast cancer patients. Metastasis relies on moving cells from one point to another, making it an intrinsically dynamic cellular process. However, traditional diagnostic pathology methods often involve obtaining tissue biopsies and examining the morphology of the cells and the molecular composition of the microenvironment in static microscopy images. A link between dynamic cellular processes and static microenvironmental inputs must be made. Often times this connection has been made qualitatively with a dramatic lack of quantitative information. However, this quantitative information is critically important to the correct diagnosis of potentially fatal, invasive cancer. Correct diagnosis means not only avoiding under diagnosis that could lead to a patient′s death, but also over diagnosis that could expose the patient to unneeded medical procedures. The following sections will describe what dynamic cellular (and subcellular) processes must be measured and some of the microenvironmental inputs that control these dynamic processes during metastasis, including epidermal growth factor (EGF) and extracellular matrix (ECM).

Cell migration is an important dynamic cell behavior that drives cancer metastasis (Friedl and Gilmour 2009). Cells migrate from the primary tumor to blood and lymph vessels and eventually to the secondary tumor. This migration is stimulated by microenvironmental factors like growth factors or extracellular matrix (ECM). As mentioned above one goal of this work

is to provide a link between cellular dynamics like cell migration and the state of the microenvironment. Perhaps this link might inform models to predict migration behavior from static images of tissue biopsies (Anderson, Weaver et al. 2006), thus improving cancer diagnostics. The inhibition of cell migration is also an appropriate goal for cancer treatment, to be employed in conjunction with other approaches that target tumor cell proliferation (Wells, Kassis et al. 2002). **In order to provide a link between cell migration and the state of the microenvironment, I quantitatively characterized migration behavior of single cells as well as the underlying subcellular dynamics under different microenvironmental conditions (Chapters 2, 3, 4 and 6).**

The progression of carcinomas not only relies on single cell behavior, but also on the assembly and disassembly process of clusters of cells. The primary tumor develops as cluster of attached epithelial cells, but at some point these cells scatter and break off the primary tumor as single cells or clusters of cells. These single cells or clusters of cells metastasize to distant organs and form nascent secondary tumors (Hanahan and Weinberg 2000). Many clinical and experimental observations suggest that both the weakening of cell-cell contacts and enhanced migration lead to metastasis driven by single cells (Friedl and Wolf 2003, Vincent-Salomon and Thiery 2003). However, others have found less invasive clusters of cells in lymph nodes (Cavallaro and Christofori 2001). This suggests that multicellular clusters can escape from the primary tissues and form emboli in either blood vessels or lymph nodes (Tomlinson, Alpaugh et al. 2001). The idea that metastases might be in fact multicellular clusters provides motivation for the work showing carcinoma cells can escape suspension-induced apoptosis by forming multicelluar clusters. Single cells in suspension that do not form clusters undergo apoptosis (Zhang, Lu et al. 2004, Zhang, Xu et al. 2010). Therefore, cell clustering plays an important role in the formation of secondary tumor site by either assembling the cancer cells themselves or reorganizing stromal cells. **Although many studies have been designed to probe the qualitative properties of the clustering of cells with strong cell-cell adhesions, little work has been done on quantifying the clustering behavior of cells that lack robust cell-cell junctions and investigating the underlying mechanisms. Consequently, I show data quantifying the clustering behavior. Furthermore, I apply reaction and**

transport principles to understand whether clustering is caused by differences in proliferation or cell migration rates (Chapter 5).

1.2 The Role of Protrusion, Adhesion and Contraction During Migration

Cell migration can be considered a cyclic series of distinct but concerted biophysical processes, including protrusion, adhesion, contraction and retraction (Lauffenburger and Horwitz 1996). Each of these processes depends on reorganization of the actin cytoskeleton and involves both external and internal signaling pathways (Wells, Kassis et al. 2002). First, the cell polarizes and protrudes at the leading edge, which is driven by actin polymerization and stabilized by adhesion. The protrusion adheres to the surroundings through specific interactions between integrins and the extracellular matrix (ECM) (Giancotti and Ruoslahti 1999). Once adhered, cells generate traction forces against the substratum through actomyosin contraction. These contractile forces allow the cell to disassemble and release adhesions at the cell rear, causing the whole cell body to move forward (Ridley, Schwartz et al. 2003).

During protrusion, traveling waves have been observed, which are cycles of protrusion and retraction at the leading edge that travel both laterally along or rearward from the cell edge (Giannone, Dubin-Thaler et al. 2004, Machacek and Danuser 2006, Giannone, Dubin-Thaler et al. 2007, Barnhart, Lee et al. 2011). The mechanisms of these traveling waves have just begun to be studied. The generation of the traveling wave is associated with actin polymerization and treadmilling. For example, Barnhart et al. found that the fish keratocytes exhibit traveling waves of protrusion when crawling on highly adhesive substrates and lateral wave propagation speed was similar to the actin polymerization speed (Barnhart, Lee et al. 2011). The termination behind the traveling wave is associated with depletion of an F-actin promoter on a slower timescale than initiation of the waves. Machacek et al. found that the persistence of waves depends on the relative abundance of activated Arp2/3 and polymerizable G-actin (Machacek and Danuser 2006). Protrusion waves are subcellular signatures not only biophysically linked with cell migration, but also mechanically linked with subcellular processes such as myosin activity and adhesion-site formation. Giannone et al. found periodic rearward protrusion waves that are formed when F-actin flows from the front to the rear when it reaches newly assembled

myosin II, contraction occurs, initiating the next cycle. These periodical lamellipodial waves connect myosin motors with the initiation of adhesion sites (Giannone, Dubin-Thaler et al. 2007).

The processes of protrusion, adhesion, contraction and retraction are temporally and spatially connected via a series of feedback loops (Fig. 1.1)(Bailly, Yan et al. 1998, Totsukawa, Wu et al. 2004, Machacek and Danuser 2006, Nayal, Webb et al. 2006, Giannone, Dubin-Thaler et al. 2007, Vicente-Manzanares, Zareno et al. 2007, Cirit, Krajcovic et al. 2010, Ronde, Deramaudt et al. 2011), which occur through altering adhesive attachments called focal adhesions (FAs) (Han, Li et al. , Peppelenbosch, Tertoolen et al. 1993, Segall, Tyerech et al. 1996, Harms, Bassi et al. 2005, Katz, Amit et al. 2007). FAs are dynamic, macromolecular structures, which serve as both mechanical linkages and centers of intracellular signal transduction. The maturation of nascent adhesions to stable FAs constitutes a functional switch. This switch changes how much force the adhesion can bare as well as whether it signals for additional protrusion (Cirit, Krajcovic et al. 2010). For example, nascent adhesions can active Rac through integrin-mediated signaling pathways, which promote the formation of broad, flat membrane structures called lamellipodia and thus enhance protrusion (DeMali, Barlow et al. 2002, Zaidel-Bar, Ballestrem et al. 2003, Valles, Beuvin et al. 2004, Nayal, Webb et al. 2006, Serrels, Serrels et al. 2007). Nascent adhesions also function as traction points that resist the force arising from the retrograde flow and shunt the force to the substrates, resulting in increased protrusion (Beningo, Dembo et al. 2001, Gardel, Sabass et al. 2008). This coupling between FAs and protrusion is regulated by a clutch-like mechanism (Jay 2000). When the clutch between FAs and retrograde flowing actin is engaged, rates of forward protrusion increase while the FAs undergo force-dependent maturation. The efficiency of this clutch is different among cells. Mature FAs serve as stable physical linkages between ECM and actin cytoskeleton, through which myosin II motors generate contractile force and promote retraction (Geiger, Zamir et al. 1999, Balaban, Schwarz et al. 2001, Choi, Leong et al. 2008, Vicente-Manzanares, Choi et al. 2008, Stricker, Aratyn-Schaus et al. 2011).

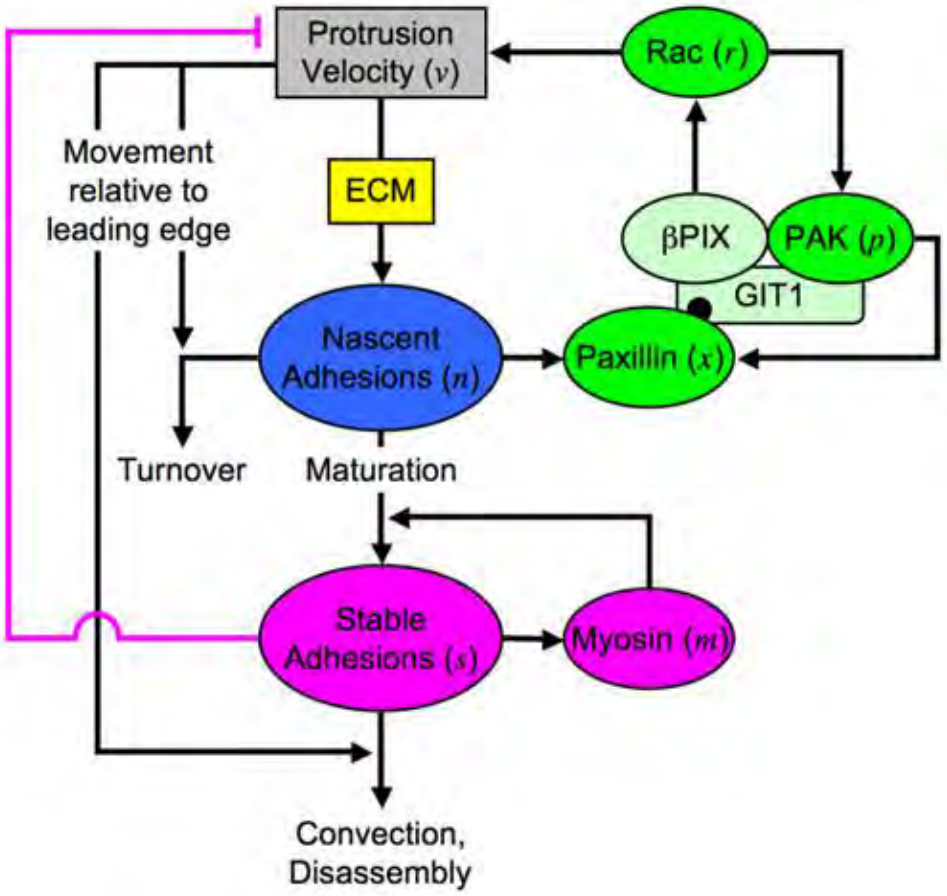

Figure 1.1 **A schematic model describes the feedback loops between protrusion and adhesion.** The rates of nascent adhesion formation and turnover depend on the velocity of membrane protrusion (v), and the density and composition of ECM. Nascent adhesions promote protrusion by mediating activation of Rac, utilizing a pathway that is reinforced by positive feedback loops. Those nascent adhesions that are not turned over mature to form stable adhesions, a process that is reinforced by myosin-mediated feedback loop. Stable adhesions either directly antagonize protrusion or disassemble over a relatively long time scale, and their influence on protrusion is also diminished by convective (v-dependent) transport (Cirit, Krajcovic et al. 2010).

FAs exist in different maturation states. This FA assembly, maturation and disassembly is a continuous process driven by actin polymerization and myosin II-genetrated tension (Parsons, Horwitz et al. 2010). The assembly of nascent adhesions requires Arp2/3 complex-mediated actin polymerization, which is regulated by the Rho GTPases Rac and Cdc42 (Choi, Vicente-Manzanares et al. 2008). The disassembly of nascent adhesions is driven by severing and disassembly of branched actin structures (Parsons, Horwitz et al. 2010). The maturation of nascent adhesions is driven by either new actin polymerization or the reorganization of existing actin filaments along an α-actinin and actin crosslinking template that elongates centripetally from nascent adhesions (Choi, Vicente-Manzanares et al. 2008). The activity of myosin II and the resulting tension exerted on FAs seem to be important factors in determining the balance between FA maturation and disassembly (Geiger, Spatz et al. 2009, Wolfenson, Henis et al. 2009). For example, inhibiting myosin II with blebbistatin prevents adhesion maturation and greatly increases nascent adhesions. Conversely, myosin IIA overexpression in CHO cells inhibits leading edge protrusion and increases nascent adhesion maturation to focal complexes (Vicente-Manzanares, Koach et al. 2008). Finally, tension and actin reorganization contribute to FA disassembly at both the front and the rear of the cell (Broussard, Webb et al. 2008). At the front of the cell, disassembly of FAs is driven by actin depolymerization and reorganization. At the rear of the cell, disassembly of FAs is driven by retraction, which is usually accompanied by the adhesion sliding. Although not fully understood, the adhesion sliding seems to be a Rho GTPase and myosin II dependent form of treadmilling, in which the peripheral edge of the FA disassembles while the central edge assembles, causing the whole cell body to move forward (Ballestrem, Hinz et al. 2001, Digman, Brown et al. 2008). Thus, initial nascent adhesion assembly is mechanically and kinetically linked to actin polymerization at the edge of the cell, whereas myosin II activity and tension exerted on actin further back in the cell contribute to the maturation of nascent adhesions to FAs and the disassembly of FAs.

Several morphological characteristics, such as FA size, lifetime and elongation, have been used to describe maturation states (Fig. 1.2). Nascent adhesions are small, short-lived and minimally elongated (Parsons, Horwitz et al. 2010, Zaidel-Bar and Geiger 2010). Focal complexes are slightly larger than nascent adhesions (0.2-0.8 μm^2) and persist for several minutes

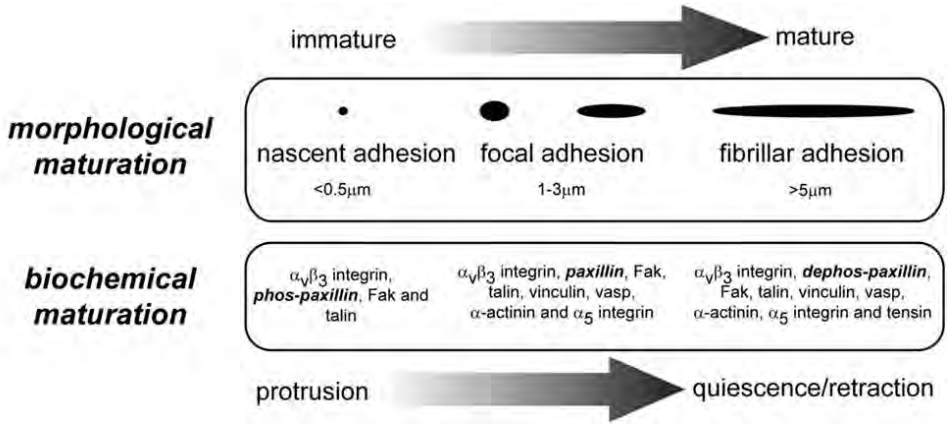

Figure 1.2 **The morphology and composition of FA change during maturation process.** (Gardel, Schneider et al. 2010)

(Parsons, Horwitz et al. 2010). Focal complexes mature to stable FAs, which are typically larger (0.8-10 μm^2) (Zimerman, Volberg et al. 2004). FAs mature to fibrillar adhesions characterized by long lifetimes and a highly elongated structure. Additionally, other characteristics such as FA protein density, speed and number have been used to predict the magnitude of force transmission to the surroundings (Balaban, Schwarz et al. 2001, Beningo, Dembo et al. 2001, Stricker, Aratyn-Schaus et al. 2011). Cells with many FAs that are stationary and dense with proteins tend to transmit large forces to the surroundings and correspond to non-migratory cells (Smilenov, Mikhailov et al. 1999), whereas cells with many FAs that are highly dynamic and turnover rapidly tend to migrate fast (Nayal, Webb et al. 2006). **While characteristics that drive the maturation and turnover of FAs have begun to be quantitatively measured, the quantitative correlation between these characteristics and cell migration behavior is largely unknown. In addition, protrusion waves and their functional relevance are only starting to be characterized now. Therefore I characterize protrusion/retraction and FA dynamics and link these signatures with cell migration under either epidermal growth factor stimulation, substrate adhesiveness, contractility and organized patterns of collagen (Chapters 2, 4 and 6). A key to this process is to appreciate FA characteristics as distributions and not mere averages and standard deviations.**

1.3 Growth Factor-Induced Migration

Growth factors are proteins that process growth-stimulating signals and promote the cells to proliferate and migrate. In cancer cells, the proteins involved in the growth-stimulating signaling pathways are overactive and thus cause cancer cells to proliferate or migrate much faster than normal cells. Some cancer cells overproduce growth factors or overexpress abnormal receptor proteins that are constitutively activated.

One of the most well-studied growth factors is epidermal growth factor (EGF) and it is known to stimulate sustained cell migration, which is crucial for tumor cell invasion (Wells, Kassis et al. 2002). A number of clinical data indicate that epidermal growth factor receptor (EGFR) overexpression and signaling correlates to tumor invasion (Wells, Kassis et al. 2002). High levels of EGFR are visualized in the regions of the tumors that are actively invading the microenvironment while the regions distant or adjacent to the tumors expressed lower physiological levels of EGFR (Rao, Hemstreet et al. 1993). Additionally, EGFR inhibition very effectively decreases metastasis in breast cancer (Herbst 2004). Finally, increased levels of EGFR expression has been suggested to increase cell motility and proliferation required for tumor progression (Xie, Turner et al. 1995, Turnert, Chen et al. 1996, Arteaga 2002).

The migration speed response to EGF is dose dependent. For example, there was a 2.5-4.5 fold increase in migration speed in a log-linear manner, with a maximum concentration at 1.6-8 nM EGF (Ando and Jensen 1993) in keratinocytes stimulated with various doses of EGF. Joslin et al. found that the average speed of human mammary epithelial cells increased with increasing concentrations of exogenous EGF, from 0.2 to 2nM (Joslin, Opresko et al. 2007). Celestino et al. investigated the dose response of EGF (0, 0.16, 1.6, 8, 16, or 32 nM) on the growth of caprinepreantral follicles and found that the low concentrations of EGF maintain caprine follicular viability and promote the transition from primordial to primary follicles (Celestino, Bruno et al. 2009). Similarly, a low concentration of EGF (0.16 nM) has a stimulatory effect on trophoblast migration, whereas high concentrations of EGF (16 nM) shows an inhibitory effect (Han, Li et al.). Interestingly, EGF stimulation can also be biphasic. For example, MDA-MB-231 cells demonstrated a characteristic bell-shaped chemo-migratory

curve toward EGF (0.1616 nM), with an optimal concentration of 1.6 nM (Price, Tiganis et al. 1999). Maheshwari et al. found that EGF can either decrease or increase fibroblast speed depending on the concentration of fibronectin surface (Maheshwari, Wells et al. 1999). Furthermore, the distribution in migration speed and persistence time appears to be dependent on EGF stimulation (Ware, Wells et al. 1998), suggesting that EGF controls not only the mean response, but also the cell-to-cell variability in response. The diversity in response to EGF at the level of cell migration speed indicates that other characteristics that define a particular cell state might modulate the response to EGF. A couple of these characteristics include adhesion to the substrate, whether specific or non-specific, and contractile force generated by the cell. These regulate protrusion and FA dynamics which are determining factors that lead to migration.

EGF′s control of cell motility originates from its regulation of membrane protrusion and retraction (Zhang, Yang et al. , Lichtner, Wiedemuth et al. 1993, Bailly, Condeelis et al. 1998, Harms, Bassi et al. 2005). For example, addition of EGF stimulates MTLn3 cells to extend actin-filled lamellipodia within 1 to 3 minutes (Segall, Tyerech et al. 1996). As described for migration, EGF does not always uniformly stimulate protrusion. For example, in poorly motile and weakly metastatic A431 cells, binding of EGF leads to increases in ruffling retraction and the velocity of protrusion doesn′t change (Chinkers, McKanna et al. 1979, Chinkers, McKanna et al. 1981). However, in more motile, metastatic MTLn3 cells, EGF stimulates protrusion (Wyckoff, Insel et al. 1998). Furthermore, the effect of EGF on protrusion depends on the ECM concentration. Fractional membrane protrusion and retraction activity vary with surface fibronectin concentration in the presence of EGF but not in its absence (Maheshwari, Wells et al. 1999).

This EGF-mediated protrusion and retraction occurs through altering the formation and disruption of FA (Han, Li et al. , Peppelenbosch, Tertoolen et al. 1993, Segall, Tyerech et al. 1996, Xie, Pallero et al. 1998, Harms, Bassi et al. 2005, Katz, Amit et al. 2007, Schneider, Hays et al. 2009). EGF stimulates the formation and maturation of FAs, which stabilize lamellipod protrusion. At the same time, the preexisting FAs prior to EGF stimulation disassemble and disappear. This coordination of FA turnover with lamellipod protrusion is proposed to result in polarized cell motility in response to gradients of EGF (Bailly, Condeelis et al. 1998, Bailly,

Yan et al. 1998). There is a dose dependency of FA disassembly in response to decreased adhesiveness of substrates under EGF stimulation, which is mediated by Erk through calpain to promote proteolysis of focal adhesion proteins and thus drive adhesion disassembly (Xie, Pallero et al. 1998). EGF also alters phosphorylation of Fak and paxillin, which promote FA assembly and cell migration, however, the context of this regulation may be important since reports differ as to whether EGF promotes phosphorylation or dephosphorylation of these proteins (Tapia, Camello et al. 1999, Sieg, Hauck et al. 2000, Lu, Jiang et al. 2001, Schneider, Hays et al. 2009).

Although much is known about EGF-induced cell migration, protrusion and FA dynamics, very little work has been done to examine how protrusion and FA dynamics are quantitatively altered in response to EGF. As a result, I designed experiments to quantify the protrusion dynamics as well as FA properties under EGF stimulation and investigate how protrusion and FA coordinately mediate cell migration in response to EGF (Chapters 2 and 4).

1.4 Cell-to-Cell Variability in Migration

Cell-to-cell variability has been widely observed in mammary cells and has drawn much attention due to its influence on physiology (Monine and Haugh 2008), pathology (Anderson, Weaver et al. 2006) and pharmacology (Niepel, Spencer et al. 2009). This heterogeneity arises from both intrinsic and extrinsic noise in intracellular processes (Kim and Price , Rao, Wolf et al. 2002, Raj and van Oudenaarden 2008). The noise can be traced to heterogeneity in protein level (Rinott, Jaimovich et al. , Yuan, Wulf et al.), membrane organization (Wieser, Weghuber et al. 2009) and cytoskeletal organization (Lacayo, Pincus et al. 2007) and is enhanced through extracellular stimuli (Colman-Lerner, Gordon et al. 2005). People have dissected and measured sources of variation in system output, analyzing thousands of individual, genetically identical cells and found that only a small portion of total cell-to-cell variability is caused by random fluctuations in intrinsic noises. Instead, variation is dominated by differences in the capacity of individual cells to transmit signals through signaling pathways leading to gene expression (Colman-Lerner, Gordon et al. 2005).

While the above examples relate to non-migratory processes, cell-to-cell variability also has impact on cell migration (Sorger, Niepel et al. 2009). For example, Lacayo et al. found that variations in cell migration and morphology are consequences of changes in underlying cytoskeletal organization and dynamics. They used mathematical modeling to elucidate the global cell variations in shape and speed from knowledge of local effects of multiscale protein interactions (Lacayo, Pincus et al. 2007). These specific phenotypic properties of single cells are strong predictors of cell fate or cellular activity (Pelkmans and Snijder 2011). Consequently, cell-to-cell variability has also begun to permeate mathematical models (Anderson, Weaver et al. 2006, Monine and Haugh 2008), where even small changes in the distribution of protein concentrations yield enhanced wound healing or metastasis due to the selection of an optimal subpopulation. Yuan et al. found that Akt activity is bimodal in response to EGF stimulation and correlates with Phosphoinositide 3-kinase (PI3K) protein level. MCF-10A cells with high and low levels of PI3K protein have distinct cellular functions and only cells with high PI3K can active Akt (Yuan, Wulf et al.). Changes in these protein levels will alter signaling that might impact both FA growth and turnover as well as protrusion and retraction dynamics. **Therefore I examined an approach that could be used to assess cell-to-cell variability in migration speed in a high throughput system (Chapter 3).**

1.5 Extracellular Matrix-Induced Migration

The ECM constitutes the structural organization for cells and is the main regulator of cell behavior processes such as scattering, clustering and migration (de Rooij, Kerstens et al. 2005, Shields, Dangi-Garimella et al. 2011, Pope and Asthagiri 2012, Shields, Krantz et al. 2012). Cells adhere to the ECM via the integrin family of transmembrane receptors, which signal to control mammary specific gene expression and regulate cell migration and proliferation (Keely, Wu et al. 1995, Streuli, Schmidhauser et al. 1995, Tsai and Kam 2009). During tumor formation, the ECM is extensively remodeled and signaling through integrins is altered such that cells become proliferative and invasive. A key regulator of whether integrin-mediated adhesion will promote tumor formation is the stiffness of the stromal ECM. Increased ECM density results in the increase in matrix stiffness. Cells sense the stiffness of their surrounding

ECM by Rho-mediated contraction of the actin-myosin cytoskeleton (Totsukawa, Yamakita et al. 2000). The Rho-mediated contractility then activates integrin-mediated pathways and promotes cell proliferation and clustering (Salmenpera, Kankuri et al. 2008, Rhee, Ho et al. 2010, da Rocha-Azevedo, Ho et al. 2013). In clustering, the ECM determines the speed and persistence of cell migration, which can act to cluster cells (Pope and Asthagiri 2012). The stiffness of ECM is also important regulator of cell scattering (de Rooij, Kerstens et al. 2005, Gilchrist, Darling et al. 2011). For example, epithelial cell scattering is enhanced on collagen and fibronectin, as compared with laminin I and rigid substrates that produce high traction forces promoted scattering, in comparison to more compliant substrates (de Rooij, Kerstens et al. 2005).

Collagen is an ECM protein that assembles into fibers. These fibers can be crosslinked and can entangle to form dense networks or can be assembled into higher ordered, bundled fibers (Kadler, Holmes et al. 1996). The aligned collagen fibers often times direct *in vivo* migration. For instance, metastatic carcinoma cells translate along collagen fibers as they exit the tumor (Wolf, Mazo et al. 2003, Sahai, Wyckoff et al. 2005, Provenzano, Eliceiri et al. 2008). This migration behavior is called contact guidance (Dunn and Heath 1976). If the contact guidance cue is weak, cell migration is only weakly biased and not all migration steps are in the direction of the cue. If the contact guidance cue is strong, cell migration is strongly biased and most or all steps are in the direction of the cue. Early in the development of the tumor, collagen is organized circumferentially around the tumor mass. During tumor progression, these collagen fibers are reorganized by surrounding stromal cells resulting in large fiber bundles that extend radially from the tumor mass. This new collagen fiber morphology can then direct migration of cells out of the tumor (Provenzano, Eliceiri et al. 2006). While protease activity and fiber reorganization are both vital to the overall process of invasion and metastasis, protease activity seems to be most important during penetration through the basement membrane during initial exit out of the epithelial tissue or entrance into endothelial tissue of blood and lymph vessels (Mierke, Rosel et al. 2008). This suggests that between these two points, cancer cell migration is determined to a large extent by the existing ECM. How fast cells migrate in that environment (speed) and how well the aligned fibers bias migration direction (directionality) are two primary

indicators of if or how fast metastatsis will occur. Environmental characteristics such as fiber density (fiber-to-fiber spacing) and the concentration of charged accessory molecules in and around the ECM will impact both speed and directionality.

The ECM impacts speed and directionality by altering protrusion and FA dynamics, which plays an important role in the adhesion-based modulation of directionality, because a cell must form nascent FAs and extend an adherent new leading protrusion to change its direction of locomotion. Protrusion can either occur continuously in spatially confined regions as in keratocyte migration or it can occur in cycles or waves of protrusion that move laterally along the edge (Dbereiner, Dubin-Thaler et al. 2006, Machacek and Danuser 2006, Hou, Hedberg et al. 2012). These protrusions adhere to the surrounding ECM through receptors or other non-specific charge-based interactions. Collagen is also recognized by integrins and activates various intracellular signaling pathways related to protrusion (Martins and Kolega, 2006), adhesion (Tamariz and Grinnell, 2002) and cell migration (Gaudet et al., 2003). Integrins constitute one large family of receptors, which bind specifically to ECM proteins such as fibronectin, laminin and collagens. However, cell adhesion can also be made through non-specific interactions between charged ligands and surface proteoglycans or other receptors (Massia and Hubbell 1992, Mager, LaPointe et al. 2011). While these charge-based interactions can cooperate to adhere new protrusion to the substrate, they lack in the ability to form FAs (Massia and Hubbell 1992, Lehnert, Wehrle-Haller et al. 2004). On the other hand, integrin interactions with ECM readily form FAs that can be attached to the actin cytoskeleton for structural support and can engage in intracellular signaling that can drive continued protrusion (Zaidel-Bar, Ballestrem et al. 2003, Nayal, Webb et al. 2006). At fast migrational speeds, changing either adhesion or contractility (or matrix stiffness) can lead to decreased cell migration speed, resulting in a biphasic response (Dimilla, Barbee et al. 1991, Peyton and Putnam 2005, Gupton and Waterman-Storer 2006, Zaman, Trapani et al. 2006).

Developing *in vitro* environments where collagen organization can be controlled and cell clustering, migration, protrusion and FA characteristics can be measured will be a powerful approach to understand how cells sense both uniform and directional ECM cues. Therefore, I investigated how collagen attachment to the

substrates controls cell clustering through migration (Chapter 5) and how adhesion strength, contractility as well as aligned collagen patterns drive the efficiency of contact guidance and cell migration through protrusion and FA dynamics (Chapters 4 and 6).

1.6 Objectives

Understanding how cells migrate and form clusters in response to multiple environmental cues has broad impact on many pathological and physiological processes including cancer. Although many studies have focused on qualitatively describing migration and clustering, many fewer attempt to quantify the migration and clustering behavior and link them to subcellular processes mechanistically. Therefore, the aims of this research are to investigate how cancer cell migration and clustering are quantitatively modulated under different environmental conditions.

It is well known that cell migration is mediated through protrusion and FA dynamics and EGF plays an important role in this process. However, it is not known how FA maturation, FA dynamics and protrusion dynamics are regulated during EGF-induced migration. In chapter 2, I describe experiments that use total internal reflection fluorescence (TIRF) microscopy and image analysis to quantify FA properties and protrusion dynamics under different doses of EGF stimulation and to investigate whether differences in FA and protrusion dynamics correlate with differences in migration speed under EGF stimulation.

Fast migrating cells have particular importance in cancer metastasis because of their invasive phenotype, but individual cells vary dramatically in their cell migration speeds. Indeed, in Chapter 2 I demonstrated that EGF enhances cell-to-cell variability. Few experimental platforms exist to assess whether this variability is due to intrinsic gene expression or variability in the microenvironment. Therefore, I began to optimize a high-throughput approach to identify fast migrating cells out of other cells and study changes in cell-to-cell variability under EGF stimulation. In chapter 3, I present a method that combines a QD-based phagokinetic assay and flow cytometry to select the fast migrating cells and potentially examining expression profiles of migratory proteins.

EGF is not the only microenvironmental stimulant for cell migration, but adhesion to the extracellular matrix and cell contractility contribute too. Adhesion and contraction are often described as linked processes, where tuning either results in similar changes in cell behavior. In Chapter 2, I found certain protrusion and FA signatures that were present in EGF-stimulated cells and between fast and slow migrating cells. In Chapter 4, I present experiments where I examined whether changing either adhesion or contraction result in the same changes in cell migration behavior, protrusion dynamics and FA properties.

Cells can assemble into large clusters and these clusters are important in several different steps during cancer progression. Although cell scattering and clustering is a well-described process, much of the quantitative work has focused on the analysis of clustering between cells with strong cell-cell junctions. Much less is known about how cells assemble with weak cell-cell contact. Therefore, in Chapter 5, I quantify the clustering in response to different approaches to attach collagen to surfaces. In addition, I examine what mechanisms contribute to clustering and rule out cell-cell communication as an approach to assemble cell clusters using a scaling approach that describes clustering and a transport-limited reaction.

Finally, *in vivo* migration is not random, but often times directed by extracellular cues such as aligned collagen fibers. Although directed migration has been well studied, little work has been done on how directed migration is mediated through protrusion dynamics and FA properties. In chapter 6, I present characterization of the directed migration of cells on substrates where I could probe how fiber density and surrounding chemical composition regulate the ability of cells to organize protrusion and adhesion in order to migrate directionally.

1.7 References

Anderson, A. R. A., A. M. Weaver, P. T. Cummings and V. Quaranta (2006). "Tumor morphology and phenotypic evolution driven by selective pressure from the microenvironment." Cell 127(5): 905-915.

Ando, Y. and P. J. Jensen (1993). "Epidermal growth-factor and insulin-like growth factor-I enhance keratinocyte migration." Journal of Investigative Dermatology 100(5): 633-639.

Arteaga, C. L. (2002). "Epidermal Growth Factor Receptor Dependence in Human Tumors: More Than Just Expression?" The Oncologist 7(suppl 4): 31-39.

Bailly, M., J. S. Condeelis and J. E. Segall (1998). "Chemoattractant-induced lamellipod extension." Microscopy Research and Technique 43(5): 433-443.

Bailly, M., L. Yan, G. M. Whitesides, J. S. Condeelis and J. E. Segall (1998). "Regulation of protrusion shape and adhesion to the substratum during chemotactic responses of mammalian carcinoma cells." Experimental Cell Research 241(2): 285-299.

Balaban, N. Q., U. S. Schwarz, D. Riveline, P. Goichberg, G. Tzur, I. Sabanay, D. Mahalu, S. Safran, A. Bershadsky, L. Addadi and B. Geiger (2001). "Force and focal adhesion assembly: a close relationship studied using elastic micropatterned substrates." Nature Cell Biology 3(5): 466-472.

Ballestrem, C., B. Hinz, B. A. Imhof and B. Wehrle-Haller (2001). "Marching at the front and dragging behind: differential alpha-V beta 3-integrin turnover regulates focal adhesion behavior." Journal of Cell Biology 155(7): 1319-1332.

Barnhart, E. L., K.-C. Lee, K. Keren, A. Mogilner and J. A. Theriot (2011). "An Adhesion-Dependent Switch between Mechanisms That Determine Motile Cell Shape." PLoS Biol 9(5): e1001059.

Beningo, K. A., M. Dembo, I. Kaverina, J. V. Small and Y.-l. Wang (2001). "Nascent Focal Adhesions Are Responsible for the Generation of Strong Propulsive Forces in Migrating Fibroblasts." The Journal of Cell Biology 153(4): 881-888.

Broussard, J. A., D. J. Webb and I. Kaverina (2008). "Asymmetric focal adhesion disassembly in motile cells." Current Opinion in Cell Biology 20(1): 85-90.

Cavallaro, U. and G. Christofori (2001). "Cell adhesion in tumor invasion and metastasis: loss of the glue is not enough." Biochimica Et Biophysica Acta-Reviews on Cancer 1552(1): 39-45.

Celestino, J. J. H., J. B. Bruno, I. B. Lima-Verde, M. H. T. Matos, M. V. A. Saraiva, R. N. Chaves, F. S. Martins, L. F. Lima, K. P. O. Name, C. C. Campello, J. R. V. Silva, S. N. Bao and J. R. Figueiredo (2009). "Recombinant Epidermal Growth Factor Maintains Follicular Ultrastructure and Promotes the Transition to Primary Follicles in Caprine Ovarian Tissue Cultured In Vitro." Reproductive Sciences 16(3): 239-246.

Chinkers, M., J. McKanna and S. Cohen (1981). "Rapid rounding of human epidermoid carcinoma cells A-431 induced by epidermal growth factor." The Journal of Cell Biology 88(2): 422-429.

Chinkers, M., J. A. McKanna and S. Cohen (1979). "Rapid induction of morphological changes in human carcinoma cells A-431 by epidermal growth factors." The Journal of Cell Biology 83(1): 260-265.

Choi, C. K., M. Vicente-Manzanares, J. Zareno, L. A. Whitmore, A. Mogilner and A. R. Horwitz (2008). "Actin and alpha-actinin orchestrate the assembly and maturation of nascent adhesions in a myosin II motor-independent manner." Nature Cell Biology 10(9): 1039-U1036.

Choi, J. S., K. W. Leong and H. S. Yoo (2008). "In vivo wound healing of diabetic ulcers using electrospun nanofibers immobilized with human epidermal growth factor (EGF)." Biomaterials 29(5): 587-596.

Cirit, M., M. Krajcovic, C. K. Choi, E. S. Welf, A. F. Horwitz and J. M. Haugh (2010). "Stochastic Model of Integrin-Mediated Signaling and Adhesion Dynamics at the Leading Edges of Migrating Cells." Plos Computational Biology 6(2).

Colman-Lerner, A., A. Gordon, E. Serra, T. Chin, O. Resnekov, D. Endy, C. Gustavo Pesce and R. Brent (2005). "Regulated cell-to-cell variation in a cell-fate decision system." Nature 437(7059): 699-706.

da Rocha-Azevedo, B., C.-H. Ho and F. Grinnell (2013). "Fibroblast cluster formation on 3D collagen matrices requires cell contraction dependent fibronectin matrix organization." Experimental Cell Research 319(4): 546-555.

de Rooij, J., A. Kerstens, G. Danuser, M. A. Schwartz and C. M. Waterman-Storer (2005). "Integrin-dependent actomyosin contraction regulates epithelial cell scattering." The Journal of Cell Biology 171(1): 153-164.

DeMali, K. A., C. A. Barlow and K. Burridge (2002). "Recruitment of the Arp2/3 complex to vinculin: coupling membrane protrusion to matrix adhesion." Journal of Cell Biology 159(5): 881-891.

Digman, M. A., C. M. Brown, A. R. Horwitz, W. W. Mantulin and E. Gratton (2008). "Paxillin dynamics measured during adhesion assembly and disassembly by correlation spectroscopy." Biophysical Journal 94(7): 2819-2831.

Dimilla, P. A., K. Barbee and D. A. Lauffenburger (1991). "Mathematical model for the effects of adhesion and mechanics on cell migration speed." Biophysical Journal 60(1): 15-37.

Dunn, G. A. and J. P. Heath (1976). "New hypothesis of contact guidance in tissue-cells." Experimental Cell Research 101(1): 1-14.

Dbereiner, H. G., B. J. Dubin-Thaler, J. M. Hofman, H. S. Xenias, T. N. Sims, G. Giannone, M. L. Dustin, C. H. Wiggins and M. P. Sheetz (2006). "Lateral membrane waves constitute a universal dynamic pattern of motile cells." Phys Rev Lett 97(3): 038102.

Friedl, P. and D. Gilmour (2009). "Collective cell migration in morphogenesis, regeneration and cancer." Nature Reviews Molecular Cell Biology 10(7): 445-457.

Friedl, P. and K. Wolf (2003). "Tumour-cell invasion and migration: Diversity and escape mechanisms." Nature Reviews Cancer 3(5): 362-374.

Gardel, M. L., B. Sabass, L. Ji, G. Danuser, U. S. Schwarz and C. M. Waterman (2008). "Traction stress in focal adhesions correlates biphasically with actin retrograde flow speed." J Cell Biol 183(6): 999-1005.

Gardel, M. L., I. C. Schneider, Y. Aratyn-Schaus and C. M. Waterman (2010). "Mechanical Integration of Actin and Adhesion Dynamics in Cell Migration." Annual Review of Cell and Developmental Biology, Vol 26 26: 315-333.

Geiger, B., J. P. Spatz and A. D. Bershadsky (2009). "Environmental sensing through focal adhesions." Nature Reviews Molecular Cell Biology 10(1): 21-33.

Geiger, B., E. Zamir, B. Z. Katz, S. Aota, K. M. Yamada and Z. Kam (1999). "Molecular

diversity of cell-matrix adhesions." Journal of Cell Science 112(11): 1655-1669.

Giancotti, F. G. and E. Ruoslahti (1999). "Transduction - Integrin signaling." Science 285(5430): 1028-1032.

Giannone, G., B. J. Dubin-Thaler, H. G. Dobereiner, N. Kieffer, A. R. Bresnick and M. P. Sheetz (2004). "Periodic lamellipodial contractions correlate with rearward actin waves." Cell 116(3): 431-443.

Giannone, G., B. J. Dubin-Thaler, O. Rossier, Y. Cai, O. Chaga, G. Jiang, W. Beaver, H.-G. Dbereiner, Y. Freund, G. Borisy and M. P. Sheetz (2007). "Lamellipodial Actin Mechanically Links Myosin Activity with Adhesion-Site Formation." Cell 128(3): 561-575.

Gilchrist, C. L., E. M. Darling, J. Chen and L. A. Setton (2011). "Extracellular Matrix Ligand and Stiffness Modulate Immature Nucleus Pulposus Cell-Cell Interactions." PLoS ONE 6(11): e27170.

Gupton, S. L. and C. M. Waterman-Storer (2006). "Spatiotemporal feedback between actomyosin and focal-adhesion systems optimizes rapid cell migration." Cell 125(7): 1361-1374.

Han, J., L. Li, J. Hu, L. Yu, Y. Zheng, J. Guo, X. Zheng, P. Yi and Y. Zhou "Epidermal Growth Factor Stimulates Human Trophoblast Cell Migration through Rho A and Rho C Activation." Endocrinology 151(4): 1732-1742.

Hanahan, D. and R. Weinberg (2000). "The hallmarks of cancer." Cell 100(1): 57-70.

Harms, B. D., G. M. Bassi, A. R. Horwitz and D. A. Lauffenburger (2005). "Directional Persistence of EGF-Induced Cell Migration Is Associated with Stabilization of Lamellipodial Protrusions." Biophysical Journal 88(2): 1479-1488.

Herbst, R. S. (2004). "Review of epidermal growth factor receptor biology." International Journal of Radiation Oncology Biology Physics 59(2): 21-26.

Hou, Y., S. Hedberg and I. C. Schneider (2012). "Differences in adhesion and protrusion properties correlate with differences in migration speed under EGF stimulation." BMC Biophys 5: 8.

Jay, D. G. (2000). "The clutch hypothesis revisited: Ascribing the roles of actin-associated proteins in filopodial protrusion in the nerve growth cone." Journal of Neurobiology 44(2): 114-125.

Joslin, E. J., L. K. Opresko, A. Wells, H. S. Wiley and D. A. Lauffenburger (2007). "EGF-receptor-mediated mammary epithelial cell migration is driven by sustained ERK signaling from autocrine stimulation." Journal of Cell Science 120(20): 3688-3699.

Kadler, K. E., D. F. Holmes, J. A. Trotter and J. A. Chapman (1996). "Collagen fibril formation." Biochemical Journal 316: 1-11.

Katz, M., I. Amit, A. Citri, T. Shay, S. Carvalho, S. Lavi, F. Milanezi, L. Lyass, N. Amariglio, J. Jacob-Hirsch, N. Ben-Chetrit, G. Tarcic, M. Lindzen, R. Avraham, Y.-C. Liao, P. Trusk, A. Lyass, G. Rechavi, N. L. Spector, S. H. Lo, F. Schmitt, S. S. Bacus and Y. Yarden (2007). "A reciprocal tensin-3-cten switch mediates EGF-driven mammary cell migration." Nat Cell Biol 9(8): 961-969.

Keely, P., J. Wu and S. Santoro (1995). "The spatial and temporal expression of the alpha-2-beta-1 integrin and its ligands, collagen-I, collagen-IV, and laminin, suggest important roles in mouse mammary morphogenesis." Differentiation 59(1): 1-13.

Kim, P.-J. and N. D. Price "Macroscopic Kinetic Effect of Cell-to-Cell Variation in Biochemical Reactions." Physical Review Letters 104(14): 148103.

Lacayo, C. I., Z. Pincus, M. M. VanDuijn, C. A. Wilson, D. A. Fletcher, F. B. Gertler, A. Mogilner and J. A. Theriot (2007). "Emergence of Large-Scale Cell Morphology and Movement from Local Actin Filament Growth Dynamics." PLoS Biol 5(9): e233.

Lauffenburger, D. A. and A. F. Horwitz (1996). "Cell migration: A physically integrated molecular process." Cell 84(3): 359-369.

Lehnert, D., B. Wehrle-Haller, C. David, U. Weiland, C. Ballestrem, B. A. Imhof and M. Bastmeyer (2004). "Cell behaviour on micropatterned substrata: limits of extracellular matrix geometry for spreading and adhesion." Journal of Cell Science 117(1): 41-52.

Lichtner, R. B., M. Wiedemuth, C. Noeske-Jungblut and V. Schirrmacher (1993). "Rapid effects of EGF on cytoskeletal structures and adhesive properties of highly metastatic rat mammary adenocarcinoma cells." Clinical and Experimental Metastasis 11(1): 113-125.

Lu, Z. M., G. Q. Jiang, P. Blume-Jensen and T. Hunter (2001). "Epidermal growth factor-induced tumor cell invasion and metastasis initiated by dephosphorylation and downregulation of focal adhesion kinase." Molecular and Cellular Biology 21(12): 4016-4031.

Machacek, M. and G. Danuser (2006). "Morphodynamic profiling of protrusion phenotypes." Biophysical Journal 90(4): 1439-1452.

Mager, M. D., V. LaPointe and M. M. Stevens (2011). "Exploring and exploiting chemistry at the cell surface." Nature Chemistry 3(8): 582-589.

Maheshwari, G., A. Wells, L. G. Griffith and D. A. Lauffenburger (1999). "Biophysical integration of effects of epidermal growth factor and fibronectin on fibroblast migration." Biophysical Journal 76(5): 2814-2823.

Massia, S. P. and J. A. Hubbell (1992). "Immobilized amines and basic amino-acids as mimetic heparin-binding domains of cell-surface proteoglycan-mediated adhesion." Journal of Biological Chemistry 267(14): 10133-10141.

Mierke, C. T., D. Rosel, B. Fabry and J. Brabek (2008). "Contractile forces in tumor cell migration." European Journal of Cell Biology 87(8-9): 669-676.

Monine, M. I. and J. M. Haugh (2008). "Cell population-based model of dermal wound invasion with heterogeneous intracellular signaling properties." Cell Adhesion and Migration 2(2): 137-146.

Nayal, A., D. J. Webb, C. M. Brown, E. M. Schaefer, M. Vicente-Manzanares and A. R. Horwitz (2006). "Paxillin phosphorylation at ser273 localizes a GIT1-PIX-PAK complex and regulates adhesion and protrusion dynamics." Journal of Cell Biology 173(4): 587-599.

Niepel, M., S. L. Spencer and P. K. Sorger (2009). "Non-genetic cell-to-cell variability and the consequences for pharmacology." Current Opinion in Chemical Biology 13(5-6): 556-561.

Parsons, J. T., A. R. Horwitz and M. A. Schwartz (2010). "Cell adhesion: integrating cytoskeletal dynamics and cellular tension." Nature Reviews Molecular Cell Biology 11(9): 633-643.

Pelkmans, L. and B. Snijder (2011). "Origins of regulated cell-to-cell variability." Nature Reviews Molecular Cell Biology 12(2): 119-125.

Peppelenbosch, M. P., L. G. J. Tertoolen, W. J. Hage and S. W. de Laat (1993). "Epidermal growth factor–induced actin remodeling is regulated by 5-lipoxygenase and cyclooxygenase products." Cell 74(3): 565-575.

Peyton, S. R. and A. J. Putnam (2005). "Extracellular matrix rigidity governs smooth

muscle cell motility in a biphasic fashion." Journal of Cellular Physiology 204(1): 198-209.

Pollard, T. D. and G. G. Borisy (2003). "Cellular motility driven by assembly and disassembly of actin filaments." Cell 112(4): 453-465.

Ponti, A., A. Matov, M. Adams, S. Gupton, C. M. Waterman-Storer and G. Danuser (2005). "Periodic Patterns of Actin Turnover in Lamellipodia and Lamellae of Migrating Epithelial Cells Analyzed by Quantitative Fluorescent Speckle Microscopy." Biophysical Journal 89(5): 3456-3469.

Pope, M. D. and A. R. Asthagiri (2012). "Short-Lived, Transitory Cell-Cell Interactions Foster Migration-Dependent Aggregation." Plos One 7(8).

Price, J. T., T. Tiganis, A. Agarwal, D. Djakiew and E. W. Thompson (1999). "Epidermal Growth Factor Promotes MDA-MB-231 Breast Cancer Cell Migration through a Phosphatidylinositol 3-Kinase and Phospholipase C-dependent Mechanism." Cancer Research 59(21): 5475-5478.

Provenzano, P. P., K. W. Eliceiri, J. M. Campbell, D. R. Inman, J. G. White and P. J. Keely (2006). "Collagen reorganization at the tumor-stromal interface facilitates local invasion." Bmc Medicine 4: 15.

Provenzano, P. P., K. W. Eliceiri, L. Yan, A. Ada-Nguema, M. W. Conklin, D. R. Inman and P. J. Keely (2008). "Nonlinear Optical Imaging of Cellular Processes in Breast Cancer." Microscopy and Microanalysis 14(6): 532-548.

Raj, A. and A. van Oudenaarden (2008). "Nature, Nurture, or Chance: Stochastic Gene Expression and Its Consequences." Cell 135(2): 216-226.

Rao, C. V., D. M. Wolf and A. P. Arkin (2002). "Control, exploitation and tolerance of intracellular noise." Nature 420(6912): 231-237.

Rao, J. Y., G. P. Hemstreet, R. E. Hurst, R. B. Bonner, P. L. Jones, K. W. Min and Y. Fradet (1993). "Alterations in Phenotypic Biochemical Markers in Bladder Epithelium during Tumorigenesis." Proceedings of the National Academy of Sciences of the United States of America 90(17): 8287-8291.

Rhee, S., C. H. Ho and F. Grinnell (2010). "Promigratory and procontractile growth factor environments differentially regulate cell morphogenesis." Experimental Cell Research 316(2):

232-244.

Ridley, A. J., M. A. Schwartz, K. Burridge, R. A. Firtel, M. H. Ginsberg, G. Borisy, J. T. Parsons and A. R. Horwitz (2003). "Cell migration: Integrating signals from front to back." Science 302(5651): 1704-1709.

Rinott, R., A. Jaimovich and N. Friedman "Exploring transcription regulation through cell-to-cell variability." Proceedings of the National Academy of Sciences 108(15): 6329-6334.

Ronde, P., T. B. Deramaudt, D. Dujardin, A. Hamadi, F. Noulet, K. Kolli, J. De Mey and K. Takeda (2011). "FAK phosphorylation at Tyr-925 regulates cross-talk between focal adhesion turnover and cell protrusion." Molecular Biology of the Cell 22(7): 964-975.

Rotsch, C., K. Jacobson, J. Condeelis and M. Radmacher (2001). "EGF-stimulated lamellipod extension in adenocarcinoma cells." Ultramicroscopy 86(1-2): 97-106.

Sahai, E., J. Wyckoff, U. Philippar, J. E. Segall, F. Gertler and J. Condeelis (2005). "Simultaneous imaging of GFP, CFP and collagen in tumors in vivo using multiphoton microscopy." Bmc Biotechnology 5: 9.

Salmenpera, P., E. Kankuri, J. Bizik, V. Siren, I. Virtanen, S. Takahashi, M. Leiss, R. Fassler and A. Vaheri (2008). "Formation and activation of fibroblast spheroids depend on fibronectin-integrin interaction." Experimental Cell Research 314(19): 3444-3452.

Schneider, I. C., C. K. Hays and C. M. Waterman (2009). "Epidermal Growth Factor-induced Contraction Regulates Paxillin Phosphorylation to Temporally Separate Traction Generation from De-adhesion." Molecular Biology of the Cell 20(13): 3155-3167.

Segall, J., S. Tyerech, L. Boselli, S. Masseling, J. Helft, A. Chan, J. Jones and J. Condeelis (1996). "EGF stimulates lamellipod extension in metastatic mammary adenocarcinoma cells by an actin-dependent mechanism." Clinical and Experimental Metastasis 14(1): 61-72.

Segall, J. E., S. Tyerech, L. Boselli, S. Masseling, J. Helft, A. Chan, J. Jones and J. Condeelis (1996). "EGF stimulates lamellipod extension in metastatic mammary adenocarcinoma cells by an actin-dependent mechanism." Clinical and Experimental Metastasis 14(1): 61-72.

Serrels, B., A. Serrels, V. G. Brunton, M. Holt, G. W. McLean, C. H. Gray, G. E. Jones and M. C. Frame (2007). "Focal adhesion kinase controls actin assembly via a FERM-mediated interaction with the Arp2/3 complex." Nature Cell Biology 9(9): 1046-U1015.

Shields, M. A., S. Dangi-Garimella, S. B. Krantz, D. J. Bentrem and H. G. Munshi (2011). "Pancreatic cancer cells respond to type I collagen by inducing snail expression to promote membrane type 1 matrix metalloproteinase-dependent collagen invasion." J Biol Chem 286(12): 10495-10504.

Shields, M. A., S. B. Krantz, D. J. Bentrem, S. Dangi-Garimella and H. G. Munshi (2012). "Interplay between β1-integrin and Rho signaling regulates differential scattering and motility of pancreatic cancer cells by snail and Slug proteins." J Biol Chem 287(9): 6218-6229.

Sieg, D. J., C. R. Hauck, D. Ilic, C. K. Klingbeil, E. Schaefer, C. H. Damsky and D. D. Schlaepfer (2000). "FAK integrates growth-factor and integrin signals to promote cell migration." Nature Cell Biology 2(5): 249-256.

Smilenov, L. B., A. Mikhailov, R. J. Pelham, E. E. Marcantonio and G. G. Gundersen (1999). "Focal adhesion motility revealed in stationary fibroblasts." Science 286(5442): 1172-1174.

Sorger, P. K., M. Niepel and S. L. Spencer (2009). "Non-genetic cell-to-cell variability and the consequences for pharmacology." Current Opinion in Chemical Biology 13(5-6): 556-561.

Streuli, C., C. Schmidhauser, N. Bailey, P. Yurchenco, A. Skubitz, C. Roskelley and M. Bissell (1995). "Laminin mediates tissue-specific gene-expression in mammary epithelia." Journal of Cell Biology 129(3): 591-603.

Stricker, J., Y. Aratyn-Schaus, P. W. Oakes and M. L. Gardel (2011). "Spatiotemporal Constraints on the Force-Dependent Growth of Focal Adhesions." Biophysical Journal 100(12): 2883-2893.

Tapia, J. A., C. Camello, R. T. Jensen and L. J. Garcia (1999). "EGF stimulates tyrosine phosphorylation of focal adhesion kinase (p125(FAK)) and paxillin in rat pancreatic acini by a phospholipase C-independent process that depends on phosphatidylinositol 3-kinase, the small GTP-binding protein, p21(rho), and the integrity of the actin cytoskeleton." Biochimica Et Biophysica Acta-Molecular Cell Research 1448(3): 486-499.

Tomlinson, J., M. Alpaugh and S. Barsky (2001). "An intact overexpressed E-cadherin/alpha,beta-catenin axis characterizes the lymphovascular emboli of inflammatory breast carcinoma." Cancer Research 61(13): 5231-5241.

Totsukawa, G., Y. Wu, Y. Sasaki, D. J. Hartshorne, Y. Yamakita, S. Yamashiro and F. Matsumura (2004). "Distinct roles of MLCK and ROCK in the regulation of membrane protrusions and focal adhesion dynamics during cell migration of fibroblasts." The Journal of Cell Biology 164(3): 427-439.

Totsukawa, G., Y. Yamakita, S. Yamashiro, D. J. Hartshorne, Y. Sasaki and F. Matsumura (2000). "Distinct roles of ROCK (Rho-kinase) and MLCK in spatial regulation of MLC phosphorylation for assembly of stress fibers and focal adhesions in 3T3 fibroblasts." Journal of Cell Biology 150(4): 797-806.

Tsai, J. and L. Kam (2009). "Rigidity-Dependent Cross Talk between Integrin and Cadherin Signaling." Biophysical Journal 96(6): L39-L41.

Turnert, T., P. Chen, L. J. Goodly and A. Nwells (1996). "EGF receptor signaling enhances in vivo invasiveness of DU-145 human prostate carcinoma cells." Clinical and Experimental Metastasis 14(4): 409-418.

Valles, A. M., M. Beuvin and B. Boyer (2004). "Activation of Rac1 by paxillin-Crk-DOCK180 signaling complex is antagonized by Rap1 in migrating NBT-II cells." Journal of Biological Chemistry 279(43): 44490-44496.

van Nimwegen, M. J., S. Verkoeijen, L. van Buren, D. Burg and B. V. de Water (2005). "Requirement for focal adhesion kinase in the early phase of mammary adenocarcinoma lung metastasis formation." Cancer Research 65(11): 4698-4706.

Vicente-Manzanares, M., C. K. Choi, J. Zareno, L. A. Whitmore, A. Mogilner and A. R. Horwitz (2008). "Actin and alpha-actinin orchestrate the assembly and maturation of nascent adhesions in a myosin II motor-independent manner." Nature Cell Biology 10(9): 1039-U1036.

Vicente-Manzanares, M., M. A. Koach, L. Whitmore, M. L. Lamers and A. F. Horwitz (2008). "Segregation and activation of myosin IIB creates a rear in migrating cells." J Cell Biol 183(3): 543-554.

Vicente-Manzanares, M., J. Zareno, L. Whitmore, C. K. Choi and A. F. Horwitz (2007). "Regulation of protrusion, adhesion dynamics, and polarity by myosins IIA and IIB in migrating cells." The Journal of Cell Biology 176(5): 573-580.

Vincent-Salomon, A. and J. Thiery (2003). "Host microenvironment in breast cancer de-

velopment - Epithelial-mesenchymal transition in breast cancer development." Breast Cancer Research 5(2): 101-106.

Ware, M. F., A. Wells and D. A. Lauffenburger (1998). "Epidermal growth factor alters fibroblast migration speed and directional persistence reciprocally and in a matrix-dependent manner." Journal of Cell Science 111: 2423-2432.

Wells, A., J. Kassis, J. Solava, T. Turner and D. A. Lauffenburger (2002). "Growth Factor-Induced Cell Motility in Tumor Invasion." Acta Oncologica 41(2): 124-130.

Wieser, S., J. Weghuber, M. Sams, H. Stockinger and G. J. Schutz (2009). "Cell-to-cell variability in the diffusion constants of the plasma membrane proteins CD59 and CD147." Soft Matter 5(17): 3287-3294.

Wolf, K., I. Mazo, H. Leung, K. Engelke, U. H. von Andrian, E. I. Deryugina, A. Y. Strongin, E. B. Brocker and P. Friedl (2003). "Compensation mechanism in tumor cell migration: mesenchymal-amoeboid transition after blocking of pericellular proteolysis." Journal of Cell Biology 160(2): 267-277.

Wolfenson, H., Y. I. Henis, B. Geiger and A. D. Bershadsky (2009). "The Heel and Toe of the Cell's Foot: A Multifaceted Approach for Understanding the Structure and Dynamics of Focal Adhesions." Cell Motility and the Cytoskeleton 66(11): 1017-1029.

Wyckoff, J. B., L. Insel, K. Khazaie, R. B. Lichtner, J. S. Condeelis and J. E. Segall (1998). "Suppression of Ruffling by the EGF Receptor in Chemotactic Cells." Experimental Cell Research 242(1): 100-109.

Xie, H., M. A. Pallero, K. Gupta, P. Chang, M. F. Ware, W. Witke, D. J. Kwiatkowski, D. A. Lauffenburger, J. E. Murphy-Ullrich and A. Wells (1998). "EGF receptor regulation of cell motility: EGF induces disassembly of focal adhesions independently of the motility-associated PLC gamma signaling pathway." Journal of Cell Science 111: 615-624.

Xie, H., T. Turner, M.-H. Wang, R. K. Singh, G. P. Siegal and A. Wells (1995). "In vitro invasiveness of DU-145 human prostate carcinoma cells is modulated by EGF receptor-mediated signals." Clinical and Experimental Metastasis 13(6): 407-419.

Yuan, T. L., G. Wulf, L. Burga and L. C. Cantley "Cell-to-Cell Variability in PI3K Protein Level Regulates PI3K-AKT Pathway Activity in Cell Populations." Current Biology 21(3):

173-183.

Zaidel-Bar, R., C. Ballestrem, Z. Kam and B. Geiger (2003). "Early molecular events in the assembly of matrix adhesions at the leading edge of migrating cells." Journal of Cell Science 116(22): 4605-4613.

Zaidel-Bar, R. and B. Geiger (2010). "The switchable integrin adhesome." Journal of Cell Science 123(9): 1385-1388.

Zaman, M. H., L. M. Trapani, A. Siemeski, D. MacKellar, H. Y. Gong, R. D. Kamm, A. Wells, D. A. Lauffenburger and P. Matsudaira (2006). "Migration of tumor cells in 3D matrices is governed by matrix stiffness along with cell-matrix adhesion and proteolysis." Proceedings of the National Academy of Sciences of the United States of America 103(29): 10889-10894.

Zhang, F., H. Yang, Z. Pan, Z. Wang, J. M. Wolosin, P. Gjorstrup and P. S. Reinach "Dependence of Resolvin-Induced Increases in Corneal Epithelial Cell Migration on EGF Receptor Transactivation." Investigative Ophthalmology and Visual Science 51(11): 5601-5609.

Zhang, X., L. H. Xu and Q. Yu (2010). "Cell aggregation induces phosphorylation of PECAM-1 and Pyk2 and promotes tumor cell anchorage-independent growth." Molecular Cancer 9: 11.

Zhang, Y., H. Lu, P. Dazin and Y. Kapila (2004). "Squamous cell carcinoma cell aggregates escape suspension-induced, p53-mediated anoikis - Fibronectin and integrin alpha(v) mediate survival signals through focal adhesion kinase." Journal of Biological Chemistry 279(46): 48342-48349.

Zimerman, B., T. Volberg and B. Geiger (2004). "Early molecular events in the assembly of the focal adhesion-stress fiber complex during fibroblast spreading." Cell Motil Cytoskeleton 58(3): 143-159.

CHAPTER 2. DIFFERENCES IN ADHESION AND PROTRUSION PROPERTIES CORRELATE WITH DIFFERENCES IN MIGRATION SPEED UNDER EGF STIMULATION

This chapter was modified from the paper published in *BMC Biophysics* 2012, 5:8.

Yue Hou, Sarah Hedberg and Ian C. Schneider

Cell migration plays an essential role in many biological processes, such as cancer metastasis, wound healing and immune response. Cell migration is mediated through protrusion and focal adhesion (FA) assembly, maturation and disassembly. Epidermal growth factor (EGF) is known to enhance migration rate in many cell types; however it is not known how FA maturation, FA dynamics and protrusion dynamics are regulated during EGF-induced migration. Here I used total internal reflection fluorescence (TIRF) microscopy and image analysis to quantify FA properties and protrusion dynamics under different doses of EGF stimulation. EGF was found to broaden the distribution of cell migration rates, generating more fast and slow cells. Furthermore, groups based on EGF stimulation condition or cell migration speed were marked by characteristic signatures. When data was binned based on EGF stimulation conditions, FA intensity and FA number per cell showed the largest difference among stimulation groups. FA intensity decreased with increasing EGF concentration and FA number per cell was highest under intermediate stimulation conditions. No difference in protrusion behavior was observed. However, when data were binned based on cell migration speed, FA intensity and not FA number per cell showed the largest difference among groups. FA intensity was lower for fast migrating cells. Additionally, waves of protrusion tended to correlate with fast migrating cells. Only a portion of the FA properties and protrusion dynamics that correlate with migration speed, correlate with EGF stimulation condition. Those that do not correlate with EGF stimulation

condition constitute the most sensitive output for identifying why cells respond differently to EGF. The idea that EGF can both increase and decrease the migration speed of individual cells in a population has particular relevance to cancer metastasis where the microenvironment can select subpopulations based on some adhesion and protrusion characteristics, leading to a more invasive phenotype as would be seen if all cells responded like an average cell.

2.1 Introduction

Cell migration plays an important role in tumor progression (Friedl and Wolf 2010). During invasion and metastasis, migration is driven by soluble extracellular cues like EGF. EGF is a well-known chemoattractant (Segall, Tyerech et al. 1996, Sawyer, Sturge et al. 2003, Wang, Saadi et al. 2004); however, uniform doses also stimulate chemokinetic responses. EGF′s control of cell motility originates from its regulation of adhesion and protrusion (Bailly, Condeelis et al. 1998, Hinz, Alt et al. 1999, Harms, Bassi et al. 2005). This occurs through altering adhesive attachments called focal adhesions (Xie, Pallero et al. 1998, Katz, Amit et al. 2007, Schneider, Hays et al. 2009) as well as actin cytoskeleton organization (Rijken, Hage et al. 1991, Chan, Raft et al. 1998, Schneider, Hays et al. 2009). The response to EGF at the level of cell migration is dose dependent, but there exists a range of maximal stimulation concentrations. Often migration saturates at 2-10 nM EGF (Ando and Jensen 1993, Segall, Tyerech et al. 1996, Li, Fan et al. 2006), but some of the studies showed an inhibition of migration at EGF concentrations >2-10 nM (Hinz, Alt et al. 1999, Price, Tiganis et al. 1999). This is in agreement with other work demonstrating that in certain contexts, EGF can inhibit migration (Maheshwari, Wells et al. 1999, Maheshwari, Wiley et al. 2001). Within each study there is wide diversity in migration behavior, even among cells observed during the same experiment (Ando and Jensen 1993). Interestingly, the distribution in migration speed and persistence time appears to be dependent on EGF stimulation (Ware, Wells et al. 1998), suggesting that EGF controls not only the mean response, but also the distribution in responses through cell-to-cell variability.

Cell-to-cell variability has been widely observed, and has drawn much attention due to its influence on physiology (Monine and Haugh 2008), pathology (Anderson, Weaver et al. 2006)

and pharmacology (Niepel, Spencer et al. 2009). Cell-to-cell variability arises from noise in intracellular processes (Rao, Wolf et al. 2002, Raj and van Oudenaarden 2008). This noise can be traced to heterogeneity in protein level (Rinott, Jaimovich et al. , Yuan, Wulf et al. 2011), membrane organization (Wieser, Weghuber et al. 2009) as well as cytoskeleton organization (Lacayo, Pincus et al. 2007) and this heterogeneity can be enhanced through extracellular stimuli (Colman-Lerner, Gordon et al. 2005). Consequently, cell-to-cell variability has also begun to permeate mathematical models (Anderson, Weaver et al. 2006, Monine and Haugh 2008), where even small changes in the distribution of protein concentrations yield enhanced wound healing or metastasis due to the selection of an optimal subpopulation. However, while protein concentration differences among cells can result in different behavior, differences in the distribution and dynamics of macromolecular complexes might also play a large role in driving cell-to-cell variability. FAs and cytoskeleton structures regulating adhesion and protrusion dynamics constitute two examples of how macromolecular complexes regulate cell behavior and their diversity in behavior directly impacts cell migration.

FAs are dynamic, macromolecular structures that serve as both mechanical linkages and centers of intracellular signal transduction (Gardel, Schneider et al. 2010, Parsons, Horwitz et al. 2010, Zaidel-Bar and Geiger 2010). They assemble as nascent adhesions, mature into focal complexes, focal adhesions and fibrillar adhesions and disassemble (Parsons, Horwitz et al. 2010). Consequently, FAs exhibit different morphological maturation states throughout their lifetime and this is thought to regulate their behavior. For example, small, nascent FAs, transmit strong forces and serve as traction points for propulsive forces to move the cell body forward (Beningo, Dembo et al. 2001, Gardel, Sabass et al. 2008). They also generate signals for protrusion by activating actin accessory proteins (DeMali, Barlow et al. 2002, Zaidel-Bar, Ballestrem et al. 2003, Valles, Beuvin et al. 2004, Nayal, Webb et al. 2006, Serrels, Serrels et al. 2007). Under tension, these small FAs can mature into larger focal complexes, focal adhesions and fibrillar complexes with different force transmission characteristics and propensities for protrusion signaling (Geiger, Zamir et al. 1999, Balaban, Schwarz et al. 2001, Stricker, Aratyn-Schaus et al. 2011). Several morphological characteristics have been used to describe maturation states including FA size and elongation. Immature FAs that resist propulsive forces

and signal for protrusion have small areas and are minimally elongated (Parsons, Horwitz et al. 2010, Zaidel-Bar and Geiger 2010). Additionally, FA protein density, sliding speed and number have been used to predict the magnitude of force transmission to the surroundings (Balaban, Schwarz et al. 2001, Beningo, Dembo et al. 2001, Stricker, Aratyn-Schaus et al. 2011) and migration rate (Smilenov, Mikhailov et al. 1999). Characteristics that drive the maturation and turnover of FAs have begun to be quantitatively measured (Berginski, Vitriol et al. 2011, Wurflinger, Gamper et al. 2011) and the distributions properly quantified (Welf, Ogunnaike et al. 2009). However, their direct correlation to migratory states as well as their response to extracellular cues like EGF is unknown.

Protrusion is mediated by actin polymerization, whereas retraction is driven through myosin II activity and actin depolymerization (Pollard and Borisy 2003, Small 2011). Protrusion and retraction can either occur continuously in spatially confined regions as in keratocyte migration or it can occur in cycles or waves of protrusion that move laterally along the edge (Machacek and Danuser 2006, Barnhart, Lee et al. 2011). This has been characterized in several cell types when cells are either spreading (Giannone, Dubin-Thaler et al. 2004) or migrating (Machacek and Danuser 2006, Barnhart, Lee et al. 2011). In fact a recent paper has shown that slower migrating keratocytes employ lateral protrusion waves (Barnhart, Lee et al. 2011). While the timing of the cycles and the propagation of the waves is dependent on intracellular pathways, very little work has been done to examine how protrusion is quantitatively altered in response to extracellular stimuli like EGF.

In order to understand the relationship between EGF-stimulated cell migration, FA maturation and turn over and protrusion and retraction dynamics, I imaged metastatic (MTLn3) and non-metastatic (MTC) cell lines. I analyzed the cell migration speed and persistence under various EGF stimulation conditions and found that EGF moderately increased the median migration rates and persistence of MTLn3 cells, whereas it had no significant effect on the speed and persistence of MTC cells. Interestingly, higher concentrations of EGF broadened the distributions and increased the coefficient of variation of both the migration rate and persistence of MTLn3 cells, but not MTC cells. In the same manner FA characteristics and protrusion velocities did not seem to differ dramatically between EGF concentrations. However, when

cells were binned based on speed, there were differences in the distributions of FA characteristics and the qualitative behavior of protrusion, suggesting certain signatures for fast migrating cells. Finally, increasing doses of EGF regulated some characteristics differently in fast migrating cells than in slow migrating cells, suggesting that these FA and protrusion characteristics are not solely tied to migration rate. The idea that EGF can both increase and decrease the migration speed of individual cells in a population has particular relevance to cancer metastasis where the microenvironment can select subpopulations based on some adhesion and protrusion characteristics, leading to a more invasive phenotype as would be seen if all cells responded like an average cell.

2.2 Materials and Methods

Materials

Cell culture media was α-MEM medium with L-glutamine (Invitrogen) containing 5% fetal bovine serum (Invitrogen) and 1% penicillin-streptomycin (Invitrogen). Collagen and poly-L-lysine (PLL) solution contained 1.8 μg/ml of rat tail collagen I (Invitrogen) and 2 μg/ml of PLL hydrochloride (Sigma), dissolved in 0.5 M acetic acid (Fisher) and sterilized under ultraviolet light for 30 minutes. Serum free imaging media was α-MEM medium without phenol red (Invitrogen) containing 1 mg/ml bovine serum albumin (Sigma), 12 mM HEPES (Fisher), and 1% penicillin-streptomycin (Invitrogen), adjusted to pH 7.4 and filtered through 0.22 μm pore size filter (Millipore, Fisher).

Cell culture

Rat mammary adenocarcinoma cell lines (metastatic MTLn3 and non-metastatic MTC) were obtained from Dr. Jeffrey E. Segall (Albert Einstein college of Medicine). Cell lines were derived from the 13762NF rat mammary adenocarcinoma tumor (Neri, Welch et al. 1982). Cells were maintained in cell culture media at 37°C in 5% CO_2 and were passed every 2 or 3 days. Collagen and PLL solution was incubated on 22 $\times$ 22 mm squeaky cleaned coverslips (Corning, Fisher) at room temperature for 1 hour. Cells were seeded on coverslips with collagen and PLL and incubated for 24 - 48 hours at 37°C in 5% CO_2 (50,000 - 100,000 cells/coverslip).

Cell migration assay

MTLn3 and MTC cells were incubated on coverslips with collagen and PLL for 48 hours and were switched to serum free imaging media for 2 hours. Coverslips were mounted onto glass slide chambers in serum free imaging media with different concentrations of EGF (0, 0.01, 0.1, 1, 10 and 100 nM). Chambers were maintained at 37°C for 2 hours and then imaged on a heated stage every 2 minutes for 8 hours. Phase contrast time-lapse images were captured at 20× (NA 0.50, Nikon) with a charge-coupled device (CoolSNAP HQ2, Photometrics) attached to an inverted microscope (Eclipse Ti, Nikon). Cell centroids were identified and tracked manually by MTrackJ plugins of ImageJ. Single cell instantaneous speed, S, and directional persistence time, P, were obtained by fitting these to the persistent random walk equation 2.1 (Othmer, Dunbar et al. 1988):

$$< d^2(t) >= 2S^2P[t - P(1 - e^{-t/P)}], \tag{2.1}$$

using a non-linear least squares regression analysis. The sampling time is every two minutes for 6-8 hours. The instantaneous speed decreased when the time lags increased from 0 to 200 minutes. I fit the model over a 30 minute time lag. To quantify protrusion rate I used a constrained optimization program to measure the protrusion and retraction rates from masked images as done previously (Machacek and Danuser 2006). The cell edge was segmented into 100 sectors. The average protrusion rate in these sectors was calculated over time.

Fluorescence imaging

MTLn3 cells were incubated on coverslips with collagen and PLL for 24 hours and transfected with paxillin-EGFP and Fugene 6 (Roche) according to the manufacturers protocol (6 μl of Fugene 6 and 3 μg of paxillin -EGFP). After one hour transfection, the media was changed to cell culture media and the transfected cells were maintained at 37°C in 5% CO_2 for 23 hours. Then the cells were switched to serum free imaging media for 2 hours. Coverslips were mounted onto glass slide chambers in serum free imaging media with different concentrations of EGF (0, 0.01, 0.1, 1, 10 and 100 nM). Chambers were maintained at 37°C for 2 hours and then imaged on a heated stage every 10 seconds for 40 - 60 minutes. TIRF images were captured at 60× oil objective (NA 1.49, Nikon) equipped with a TIRF illuminator and fiber optic-coupled laser illumination. The 488 nm laser line of an air-cooled tunable Argon laser (Omnichrome Model 543-AP-A01, MellesGriot) was reflected off a dichroic mirror (89000 ET-QUAD, Chroma).

Camera and shutter were controlled by μManager 1.3. An automated segmentation and tracking algorithm was utilized for large-scale analysis of FA dynamics (Wurflinger, Gamper et al. 2011). FAs smaller than 0.05 μm^2 and larger than 10 μm^2 were excluded from the analysis because they represent either FAs consisting of less than three pixels or several FAs clustered together. FA fluorescence intensities were calibrated to the standard condition of 1 mW laser power with a 300 ms exposure time, so FA intensity should be directly proportional to protein level across all samples. FA numbers of individual cells were counted at each frame and then all the FA numbers/frame for 240 - 360 frames were included in the histogram and the mean value calculation. For other FA properties, such as intensity, speed, lifetime, size and elongation, properties of each FA were first averaged over 240 - 360 frames, and then all the averaged values of FA properties were included in the histogram and mean value calculation.

Statistical analysis

All graphs and statistical analyses were done using JMP and MATLAB software. To determine the statistical differences between the conditions under various EGF stimulations, a one-way analysis of variance (ANOVA) was applied to the data. To determine the statistical differences of the distributions between slow and fast migrating cells, a MATLAB function `kstest2` was used. This function is a two-sample Kolmogorov-Smirnov test to determine whether the data in the two groups are from the same continuous distribution. To determine the statistical differences of the mean values between slow and fast migrating cells, a students t-test was utilized. The significant level is 99% for p-value = 0.01.

2.3 Results

EGF stimulation broadens the distributions of migration rate and persistence of MTLn3 cells.

In many cell types EGF has been reported to enhance the mean migration rate. EGF is also a known chemoattractant for rat adenocarcinoma cells, stimulating acute protrusion. However, the long term migration response of individual cells after challenge with EGF in this model system is not known. Consequently, I examined cell migration under various doses of EGF in both adenocarcinoma cells (MTLn3) and non-metastatic cells taken from the same

tumor (MTC) (Fig. 2.1). *In vivo*, EGF concentrations in serum can be between 0.1-2 nM, with local tissue concentrations as high as 20 nM (Li, Fan et al. 2006). Consequently, MTLn3 and MTC cell lines were stimulated with a wide range of EGF concentrations (from 0-100 nM). Some typical migration trajectories under different EGF concentrations were shown in Fig. 2.2. Contrary to previous reports in other cell lines, EGF stimulation only increased the median speed and decreased the median persistence slightly in MTLn3 cells and acted more like an on-off switch between no EGF stimulation and EGF stimulation (Fig. 2.1A and B). In addition, there was no dose response in either median speed or persistence of MTC cells (Fig. 2.1A and B). Cell persistence decreased somewhat with increasing cell speed in MTLn3 cells, but MTC cells showed no such correlation, populating a much lower range of migration speeds (Fig. 2.1C) with roughly the same range of persistence times. Interestingly, differences in the distribution of migration speed of MTLn3 cells were more robust, showing that at higher EGF concentrations, there were some cells that both migrated faster and slower than those at lower EGF concentrations (Fig. 2.1A). Similarly, at higher EGF concentrations, there were some cells that had a much longer persistence time than those at lower EGF concentrations (Fig. 2.1B). On the other hand, MTC cells did not show this same behavior (Fig. 2.1A and B). The coefficient of variation (standard deviation/mean) increased in a dose dependent manner for both cell speed and persistence in MTLn3 cells (Fig. 2.1D and E).

Given that the variability in cell migration speed and persistence seems to be the dominant feature over the median (or mean) migration speed and persistence, I decided to group cells based on cell migration speed rather than EGF concentration. A k-means clustering algorithm for a cluster number equal to two was applied to the migration speeds of all cells under different EGF concentrations. The cutoff speed between slow and fast migrating cells was found to be 42 μm/hr. Thus, I assigned cells with speeds of greater than 42 μm/hr to the fast migrating group and cells with speeds of less than 42 μm/hr to the slow migrating group. Having grouped cells in this manner I wanted to examine intracellular processes that regulate migration such as FA characteristics and protrusion dynamics to see if certain signatures were exhibited by fast moving cells.

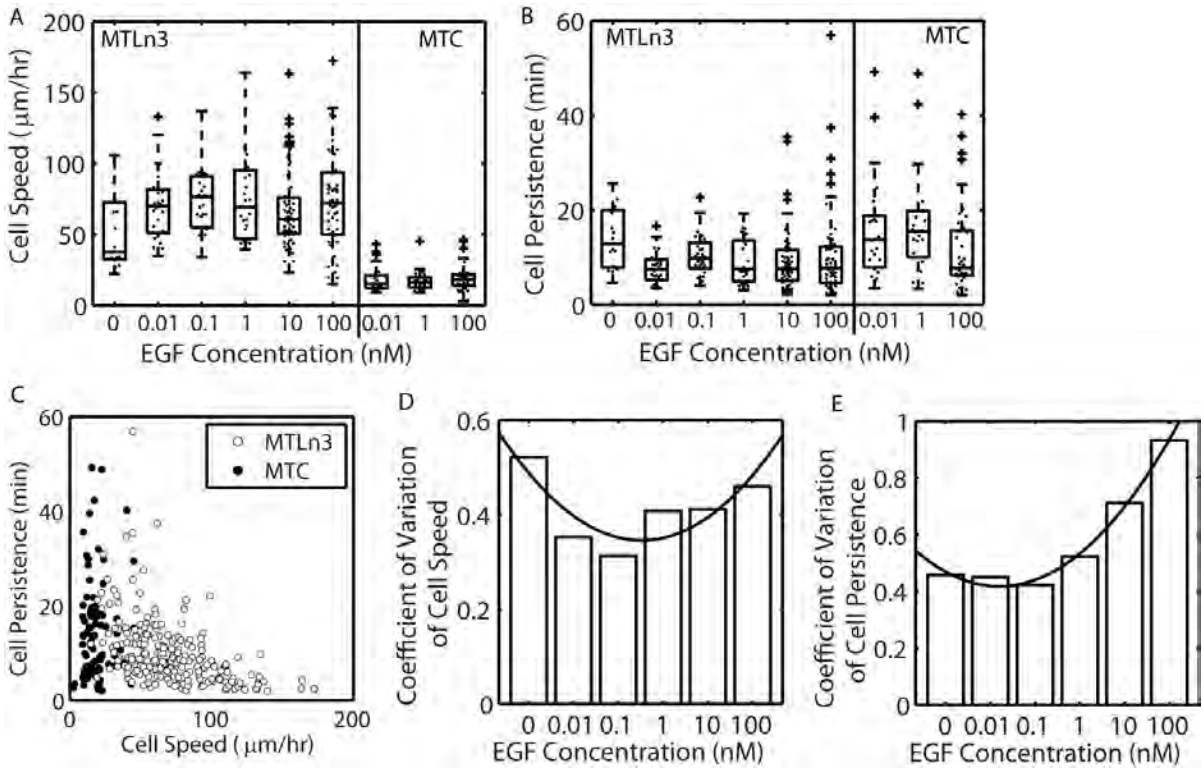

Figure 2.1 **Increasing EGF broadens the distribution of both cell speed and persistence of MTLn3 cells while not changing MTC cell migration.** A. Cell speed of MTLn3 (left) and MTC (right) under different EGF concentrations. B. Cell persistence time of MTLn3 (left) and MTC (right) under different EGF concentrations. On each box, the central marker is the median; the edges of the box are the 25^{th} and 75^{th} percentiles; the whiskers extend to the most extreme data points not considered outliers, and outliers are plotted individually as +. (For MTLn3, $N_0 = 16$, $N_{0.01}= 24$, $N_{0.1} = 30$, $N_1 = 26$, $N_{10} = 65$, $N_{100} = 60$; For MTC, $N_{0.01} = 26$, $N_1 = 24$, $N_{100} = 41$.) C. Correlation between cell speed and persistence for MTLn3 cells (white circles, $N = 221$) and MTC cells (black circles, $N = 91$). D. Coefficient of variation of speed of MTLn3 cells as a function of EGF concentration. E. Coefficient of variation of persistence of MTLn3 cells as a function of EGF concentration. Curves were fitted to a 2^{nd} order polynomial and meant only to guide the eyes.

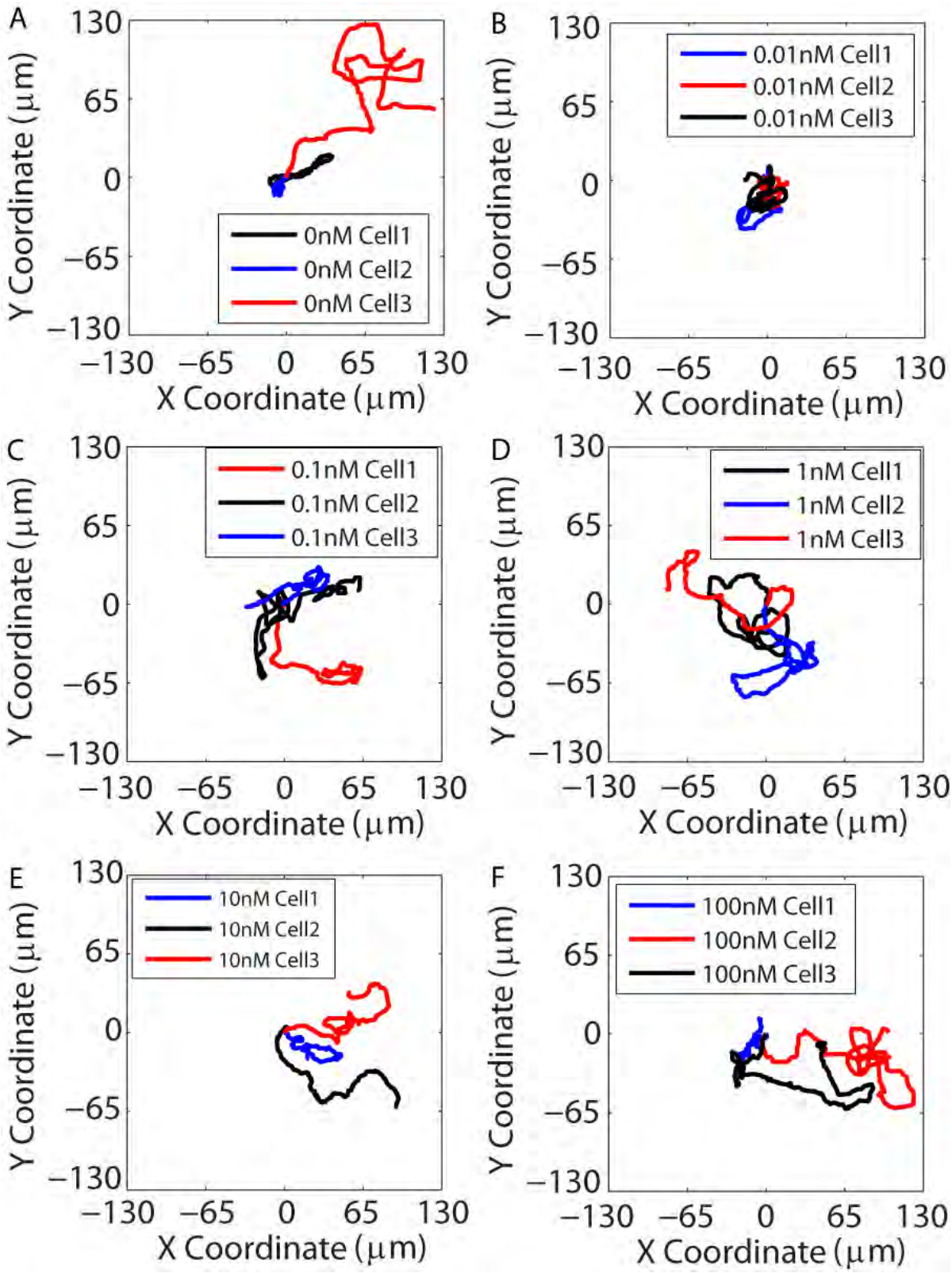

Figure 2.2 **Migration trajectories of typical cells under different EGF concentrations.** Three cell tracks were chosen randomly under each EGF concentrations and labeled with different colors. All trajectories were aligned to the starting point (0, 0).

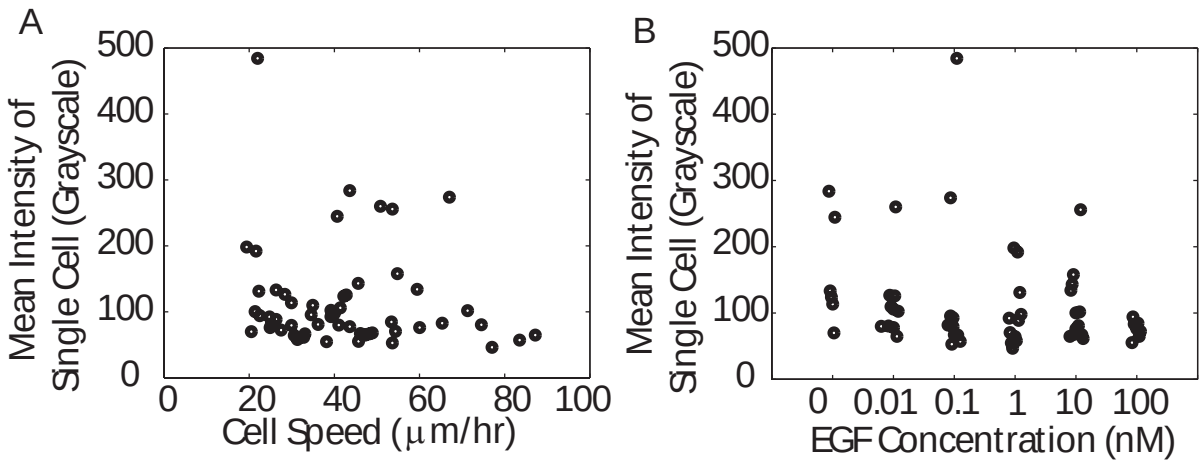

Figure 2.3 **Paxillin-EGFP expression levels for cells with different cell speeds and under different EGF stimulation conditions.** Mean intensity of individual cells as a function of A. cell speed, and B. EGF concentrations. $N_{cell} = 56$.

The distribution of FA characteristics differs between fast and slow migrating cells.

Cell migration depends on FA maturation, traction and turnover. These properties can be quantified using several characteristics such as FA size, intensity, elongation, number per frame, speed and lifetime. In order to measure these FA characteristics, I used TIRF microscopy to observe FAs within a single cell transfected with paxillin-EGFP, a component that marks FAs throughout their entire lifetime. Expression of paxillin-EGFP did not seem to alter the migration speed, nor was the expression dependent on EGF stimulation (Fig. 2.3). In MTLn3 cells, many FAs assembled, matured and disassembled over several minutes, so images were taken every 10 s (Fig. 2.4A), with little influence of photobleaching (Fig. 2.5). A segmentation and tracking algorithm was used to quantify FA characteristics (Fig. 2.4B-D) and time-resolved data of FA characteristics (Fig. 2.6) (Wurflinger, Gamper et al. 2011). I categorized by eye the FA tracking results of different EGF concentrations and scored them as poor, good and excellent. The example shown in Fig. 2.4 was scored as good. Most tracks at each EGF condition resulted in more than 70% that were either good or excellent (Table 2.1).

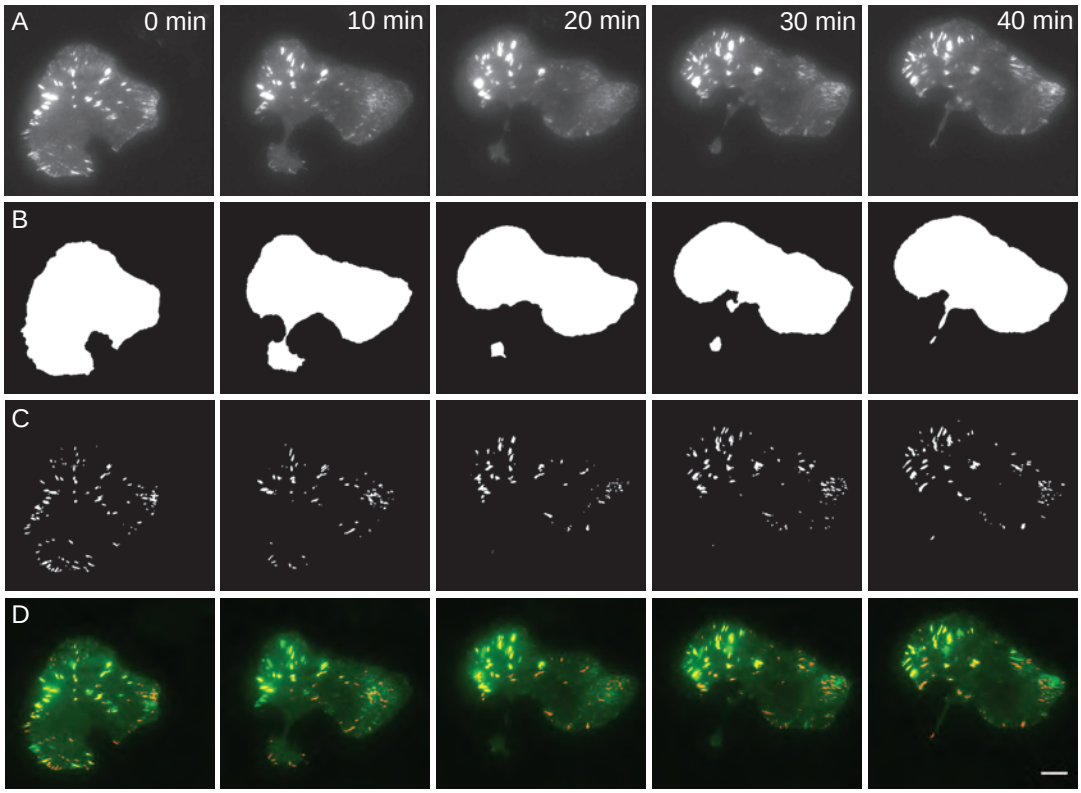

Figure 2.4 **Time-lapse series of FA dynamics in MTLn3 cells.** MTLn3 cell expressing paxillin-EGFP and stimulated with 0.01 nM EGF is shown. Images were taken at 0, 10, 20, 30 and 40 min. A. Original total internal reflection fluorescence (TIRF) images of cells with FAs. B. Binary images of whole cell masks after segmentation. C. Binary images of FA masks after segmentation. D. Composite images of tracked FAs within the cell, where green represents original images and red represents the segmented FA masks. The scale bar is 10 μm.

Table 2.1 **Qualitative assessment of tracking results.** Percentages of poor, good or excellent FA tracking results under different EGF concentrations are shown. An example of a cell that was rated as good is shown in Fig. 2.4.

EGF (nM)	CELL NUMBER	POOR	GOOD	EXCELLENT
0	5	0	60%	40%
0.01	10	20%	70%	10%
0.1	10	50%	20%	30%
1	10	10%	20%	70%
10	12	17%	33%	50%
100	8	25%	50%	25%
Total	55	22%	40%	38%

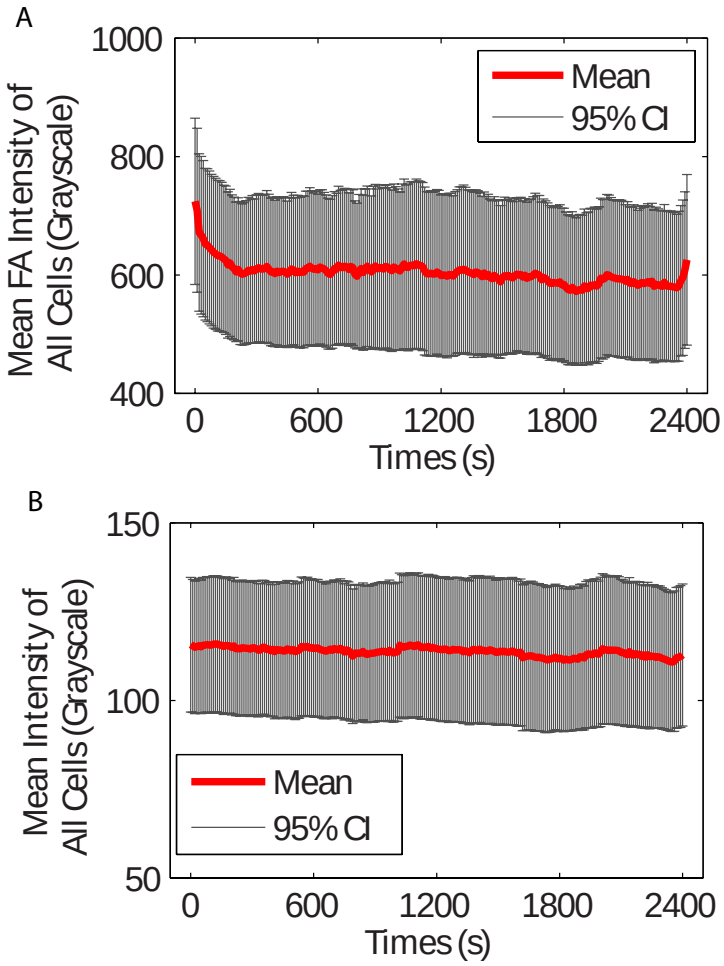

Figure 2.5 **Average paxillin-EGFP intensity in cells as a function of time.** A. Mean FA intensity and B. mean intensity of the whole cell for all cells as a function of time. Mean FA Intensity: $N_{cell} = 55$. Mean Intensity $N_{cell} = 53$.

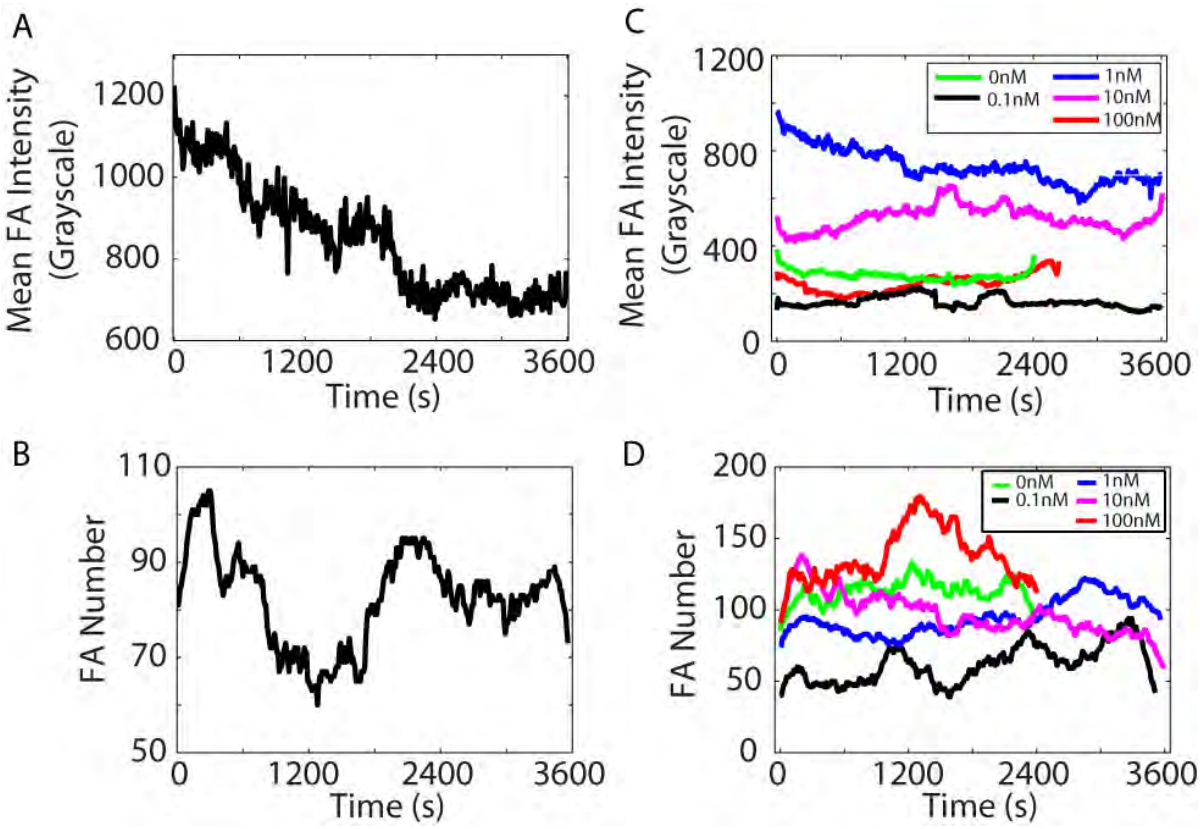

Figure 2.6 **Time-resolved data of mean FA intensity and FA number per cell.** A. Mean FA intensity and B. FA number per cell for the cell shown in Fig. 2.4 under 0.01 nM EGF stimulation as a function of time. C. FA mean intensity and D. number per cell of five typical cells under different EGF concentrations as a function of time.

Table 2.2 **Summary of FA characteristics in fast migrating cells and those stimulated with low and high EGF concentrations.** The ranges indicates areas of higher probability of fast migrating cells compared to slow migrating cells, cells stimulated with low concentrations of EGF compared to those exposed to no EGF and cells stimulated with high concentrations of EGF compared to those exposed to no EGF. The ranges were determined by calculating crossover points between the fit distributions. N/A means no crossover points.

Properties	Fast Migrating Cells	Low EGF	High EGF
FA Number	> 110	> 86	> 97
FA Size (μm^2)	0.30 - 3.0	0.18 - 3.0	0.24 - 3.0
FA Sliding Speed (μm/hr)	> 12	> 12	> 12
FA Lifetime (s)	0 - 440	160 - 530	160 - 620
FA Intensity (grayscale)	$< 22{,}000$	$<25{,}000$	$<25{,}000$
FA Elongation	N/A	1.3 - 2.1	1.3 - 2.2

FA characteristics can be ordered based on the magnitude in the difference between either the no, low and high EGF stimulation conditions or between slow and fast migrating cells. This magnitude was quantified by the Kolmogorov-Smirnov statistic (Fig. 2.7). When this statistic is large, it is more likely that there is a difference in distributions between groups. FA intensity and number per cell showed the largest values, so I decided to focus on these characteristics. Distributions of all other FA characteristics are shown as Fig. 2.8 and Fig. 2.9 and a summary of relevant ranges of these FA characteristics under different conditions is shown in Table 2.2. Most FA characteristics fit best to either lognormal or Weibull probability distribution functions. As EGF concentration increased from no to low to high, FA intensity decreased (Fig. 2.10). FA number per cell on the other hand showed highest numbers at low concentrations of EGF. Both FA intensity and number per cell showed strong differences between EGF concentration groups (Fig. 2.7). When cells were grouped based on migration speed, FA intensity was lower for fast migrating cells (Fig. 2.11). However, K-S statistic for FA number per cell was now much less, indicating that this characteristic shows poorer correlation with migration speed (Fig. 2.7). Having identified some FA characteristics that correlate with either EGF stimulation conditions or cell speed, I was interested if any protrusion characteristics showed difference among groups.

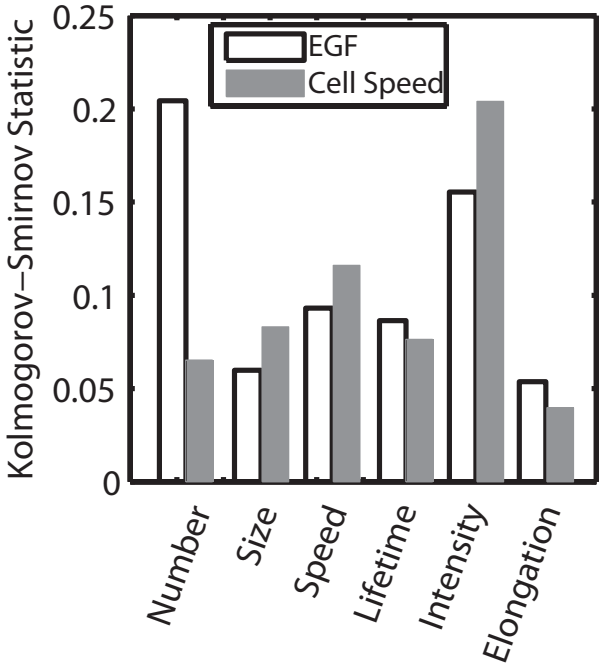

Figure 2.7 **Quantification of the difference between experimental distributions of FA properties.** Cells were binned based on EGF concentration (no (0 nM), low (0.1 and 0.01 nM) and high (100, 10 and 1 nM)) or cell speed (low (< 42 μm/hr) or high (> 42 μm/hr)). The Kolmogorov-Smirnov statistic was the average of three pair-wise comparisons (EGF) or simply the pair-wise comparison (cell speed). A larger value for the Kolmogorov-Smirnov statistic signifies a higher probability that there are differences between groups

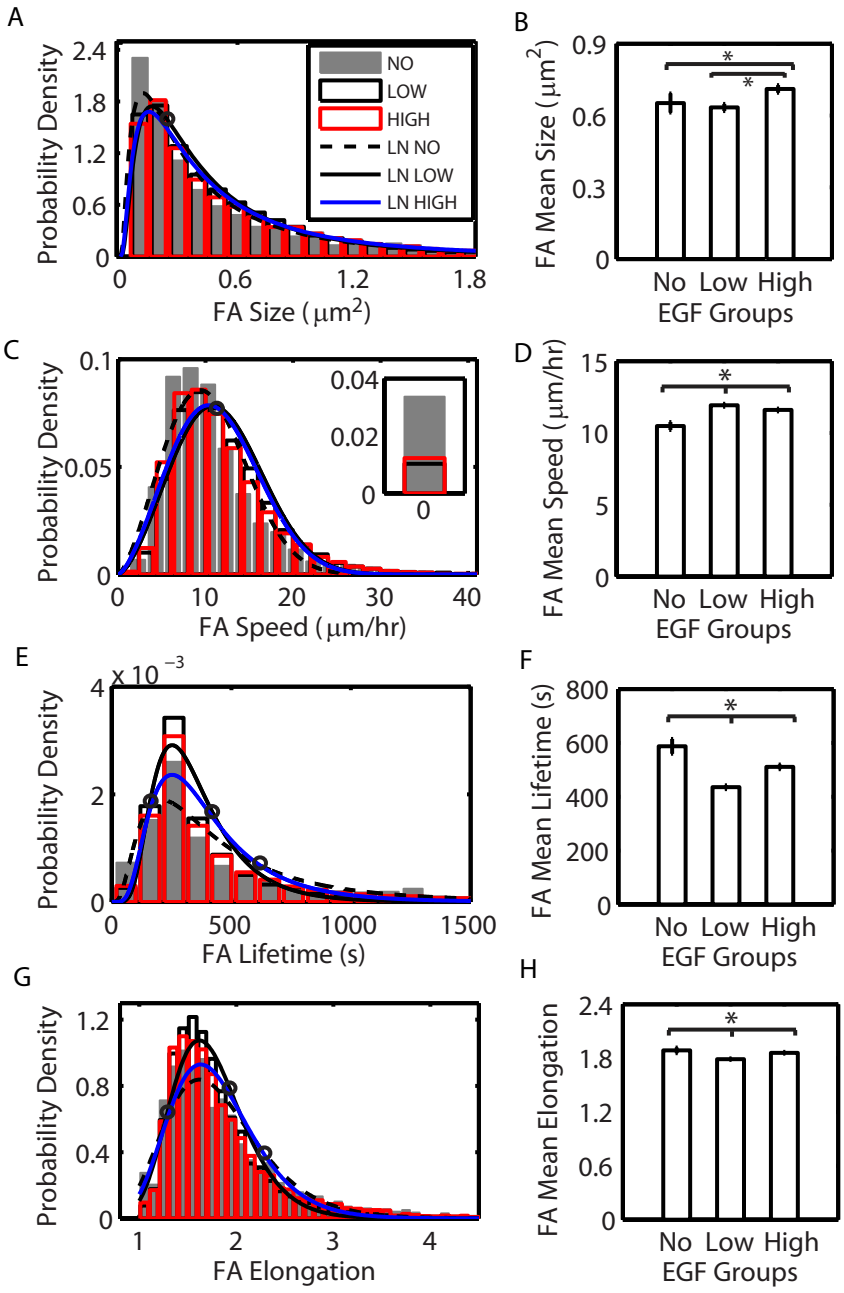

Figure 2.8 **Distributions of FA size, speed, lifetime and elongation for different EGF stimulation conditions.** Histograms of FA size A.-C., speed E.-G., lifetime I.-K. and size M.-O. were generated by dividing cells into three EGF stimulation groups (A., E., I. and M., no EGF (0 nM), B., F., J. and N. low EGF (0.01 and 0.1 nM) and C., G.,K. and O. high EGF (1, 10 and 100 nM)). Histograms were fitted with lognormal probability distributions except for speed, which was fitted with a Weibull probability distribution. The mean values of FA D. size, H. speed, L. lifetime and P. elongation are also shown. The number of measurements of FA properties is the product of the average FA number and the cell number. Size, speed, lifetime and elongation: $N_{cell,no} = 5$, $N_{FA,no} = 1963$, $N_{cell,low} = 20$, $N_{FA,low} = 13{,}024$, $N_{cell,high} = 30$, $N_{FA,high} = 14{,}648$. Error bars are 95% confidence intervals and asterisks denote $p < 0.01$.

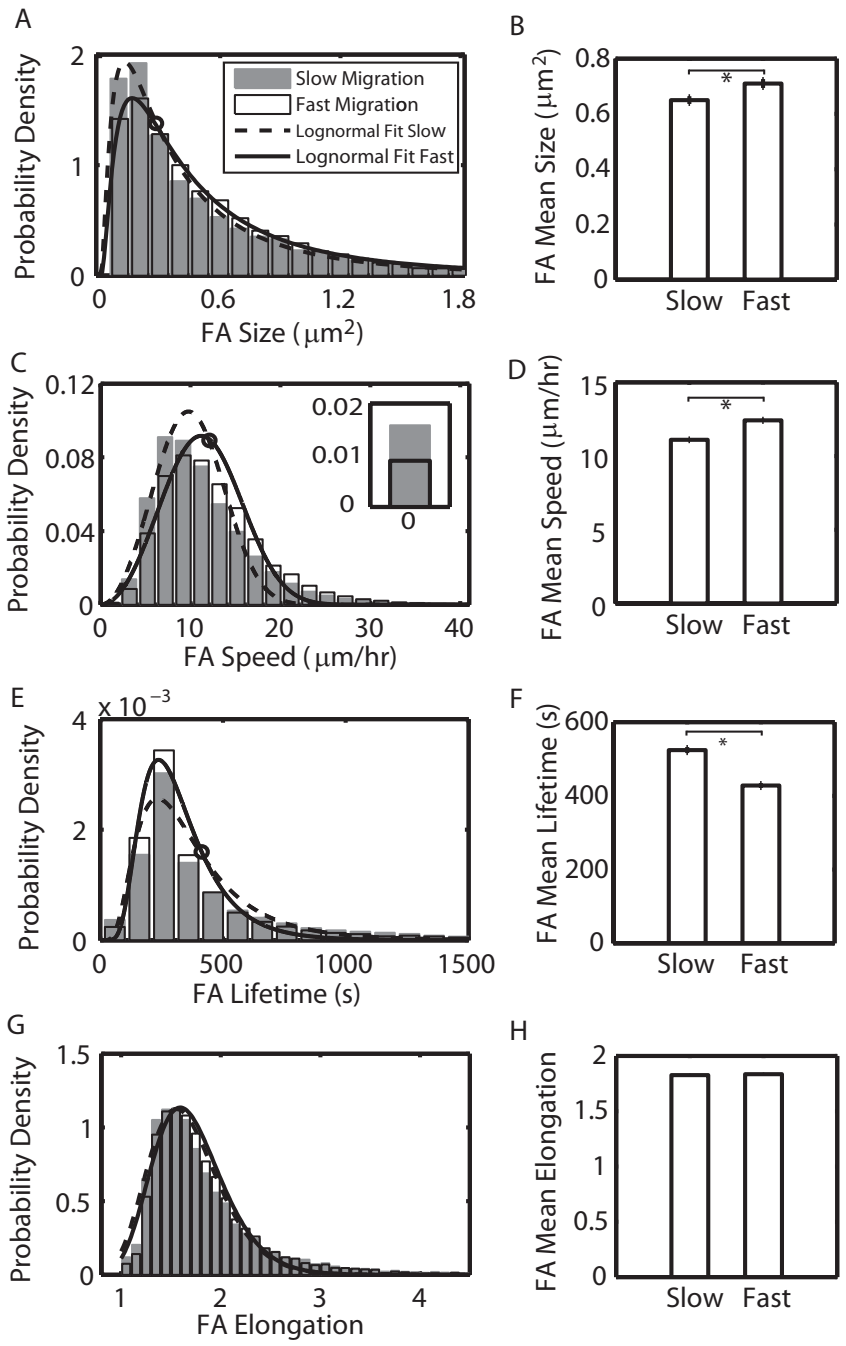

Figure 2.9 **Distributions of FA size, speed, lifetime and elongation for slow and fast migrating cells.** Histograms of FA size A.-B., speed D.-E., lifetime G.-H. and size J.-K. were generated by dividing cells into slow and fast migrating groups (A., D., G. and J. slow migrating cells and B., E., H. and K. fast migrating cells). Histograms were fitted with lognormal probability distributions except for speed, which was fitted with a Weibull probability distribution. The mean values of FA C. size, F. speed, I. lifetime and L. elongation are also shown. The number of measurements of FA properties is the product of the average FA number and the cell number. Size, speed, lifetime and elongation: $N_{cell,slow} = 21$, $N_{FA,slow} =$ 12,773, $N_{cell,fast} = 34$, $N_{FA,fast} = 16{,}862$. Error bars are 95% confidence intervals and asterisks denote $p < 0.01$.

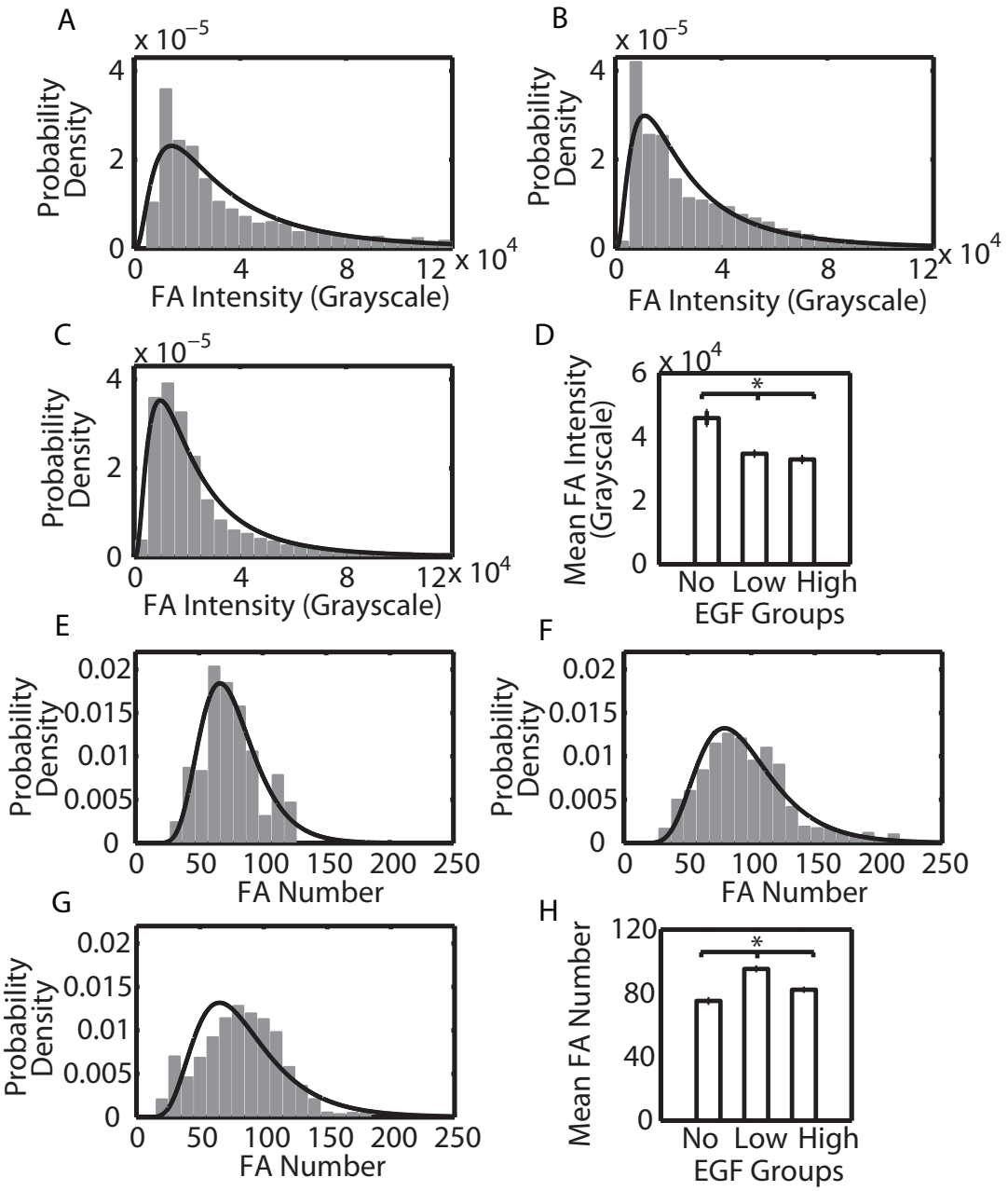

Figure 2.10 **FA intensity decreases with increasing EGF concentration and number per cell is maximal at intermediate EGF concentrations.** Histograms of FA intensity A.-C. and number per cell E.-G. were generated by dividing cells into three EGF stimulation groups (A., E. no EGF (0 nM), B., F. low EGF (0.01 and 0.1 nM) and C., G. high EGF (1, 10 and 100 nM)). Histograms were fitted with lognormal probability distributions. The mean values of FA D. intensity and H. number per cell are also shown. The number of measurements of FA number per cell is the product of the average number of frames and the cell number. The number of measurements of FA properties is the product of the average FA number and the cell number. Intensity: $N_{cell,no} = 5$, $N_{FA,no} = 1963$, $N_{cell,low} = 20$, $N_{FA,low} = 13{,}024$, $N_{cell,high} = 30$, $N_{FA,high} = 14{,}648$. Number per cell: $N_{cell,no} = 5$, $N_{FA,no} = 1545$, $N_{cell,low} = 20$, $N_{FA,low} = 5909$, $N_{cell,high} = 30$, $N_{FA,high} = 8937$. Error bars are 95% confidence intervals and asterisks denote $p < 0.01$.

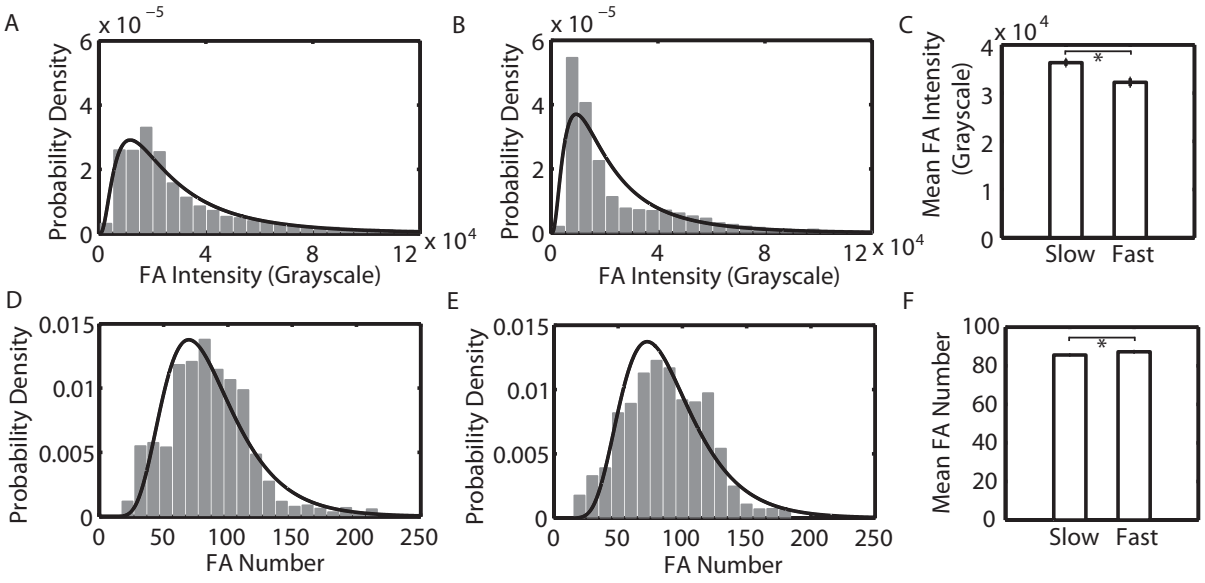

Figure 2.11 **FA intensity is lower in fast migrating cells and FA number per cell is slightly higher in fast migrating cells.** Histograms of FA intensity A.-B. and FA number per cell D.-E. were generated by dividing cells into two cell migration speed groups (A., D. slow (<42 μm/hr) and B., E. fast (>42 μm/hr)). Histograms were fit with lognormal probability distributions. The mean values of FA C. intensity and F. number per cell are also shown. The number of measurements of FA number per cell is the product of the average number of frames and the cell number. The number of measurements of FA properties is the product of the average FA number and the cell number. Intensity: $N_{cell,slow} = 21$, $N_{FA,slow} = 12{,}773$, $N_{cell,fast} = 34$, $N_{FA,fast} = 16{,}862$. Number per cell: $N_{cell,slow} = 21$, $N_{FA,slow} = 6146$, $N_{cell,fast} = 34$, $N_{FA,fast} = 10{,}245$. Error bars are 95% confidence intervals and asterisks denote $p < 0.01$.

Unique spatial organization of protrusion and retraction is exhibited in fast migrating cells.

I assessed differences in protrusion and retraction behavior under different EGF stimulation conditions and between the slow and fast migrating cells. The cell-average protrusion and retraction velocities would be faster in the fast migrating cells resulting in the increased migration rate; however different patterns of protrusion could lead to the same average value, so I analyzed local protrusion behavior. One prominent feature that I observed was traveling waves of protrusion along the edge of the cell. This traveling wave behavior had the effect of broadening of the protrusion velocity distribution. Upon qualitative examination, traveling waves did not seem to be linked to EGF stimulation conditions. Additionally, slow migrating cells usually showed large quiescent areas (green) and random, disorganized protrusion and retraction behavior (Fig. 2.12A). Only fast migrating cells showed traveling waves of protrusion (Fig. 2.12B). I examined the difference in protrusion velocity distributions in the same way that I examined distributions of FA properties (Fig. 2.7). The Kolmogorov-Smirnov statistic was smaller when comparing EGF stimulation conditions than it was when comparing cell migration speeds (Fig. 2.12C). This suggested that waves as described by a wide protrusion velocity distribution correlate with differences in migration speed and not EGF concentration. I computed the fraction of cells with waves and measured the standard deviation of the protrusion velocity distribution in slow and fast migrating cells. Both waves and high standard deviations were features of fast migrating cells (Fig. 2.12D, E and F). Consequently, fast cells tend to organize their protrusion in a qualitatively different way than slow migrating cells and this does not necessarily correlate with EGF stimulation.

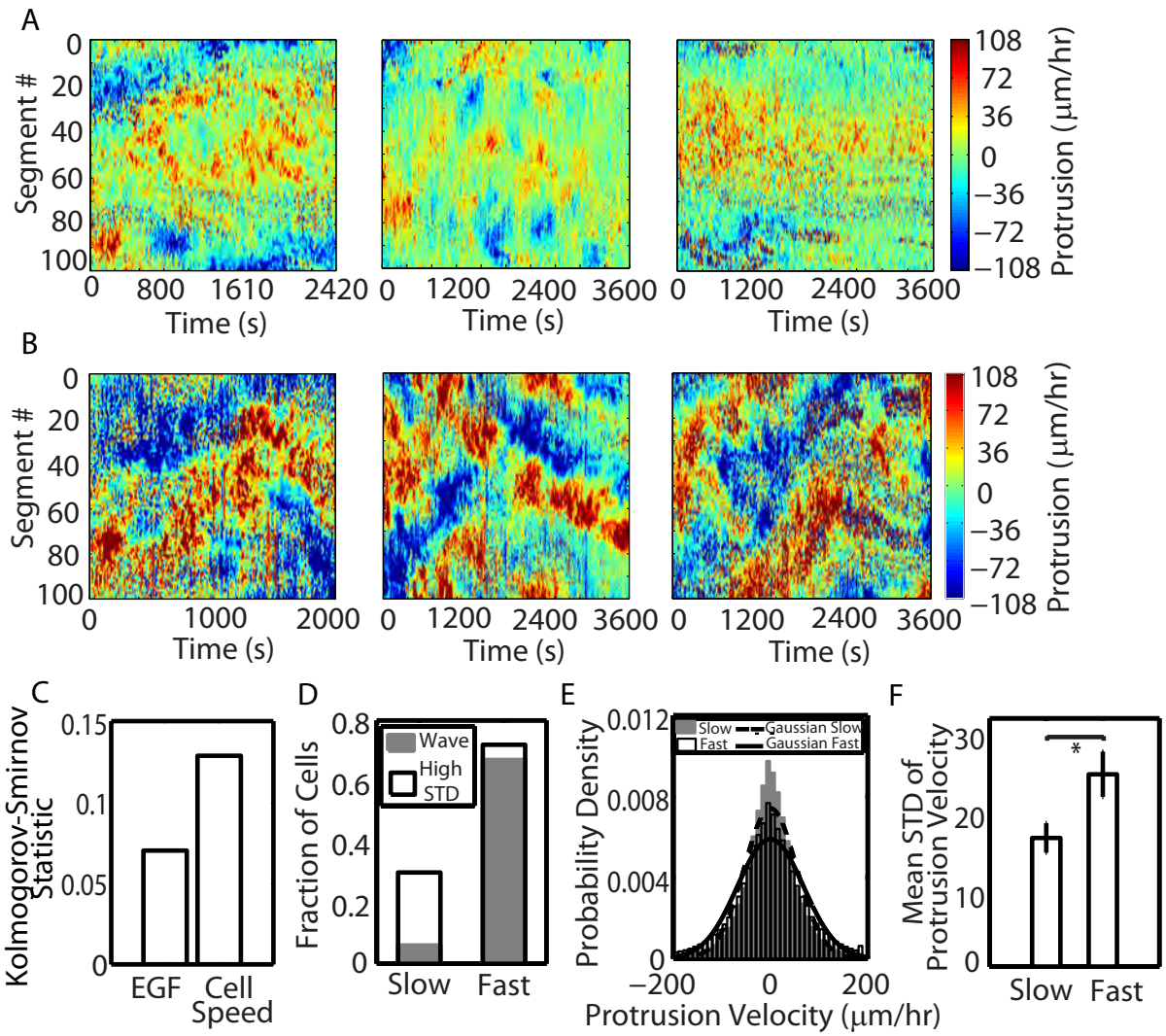

Figure 2.12 **The spatial control of protrusion differs between slow and fast migrating cells.** A. Protrusion velocity map for slow migrating cells at 0.01, 1, and 100 nM EGF from left to right. B. Protrusion velocity map for fast migrating cells at 0.01, 1, and 100 nM EGF from left to right. The cell edge was divided into 100 segments and the average protrusion rate in each segment was determined over time. Red represents fast protrusion, green represents quiescence and blue represents fast retraction. C. The Kolmogorov-Smirnov statistic was the average of three pair-wise comparisons (EGF) or simply the pair-wise comparison (cell speed). A larger value for the Kolmogorov-Smirnov statistic signifies a higher probability that there are differences between groups. D. The fraction of cells with lateral waves (gray bars) or high standard deviation (STD) of protrusion velocity (white bars) between slow and fast migrating cells. E. Histograms of protrusion/retraction velocity between slow migrating cells (gray bars) and fast migrating cells (white bars). Histograms of slow (dot lines) and fast migrating cells (solid lines) were fit with Gaussian distribution. F. The mean values of standard deviation (STD) of protrusion velocity between slow and fast migrating cells were also shown. $N_{slow} = 34$, $N_{fast} = 24$. Error bars are 95% confidence intervals and asterisks denote $p < 0.01$.

2.4 Discussion

Variability in cell response to environmental cues is becoming a more appreciated phenomenon that can drive how populations of cells respond to their environment. Cell-to-cell variability arises from heterogeneity in protein level (Rinott, Jaimovich et al. , Yuan, Wulf et al. 2011) or organization of cellular structures such as the membrane (Wieser, Weghuber et al. 2009) or the cytoskeleton (Lacayo, Pincus et al. 2007). Interestingly, this variability can be enhanced by extracellular stimuli (Colman-Lerner, Gordon et al. 2005). The idea that variability can be enhanced under certain conditions sets up the interesting possibility that the mean response is a relatively poor statistical metric. Rather, the distribution itself or the standard deviation or another parameter that characterizes the distribution may be more appropriate. The obvious result of this dependence on the distribution is a sensitizing of a subpopulation of cells to particular environments. This is acutely evident in pathologies such as cancer metastasis, where subpopulations of cells are selected based on different responses to the tumor microenvironment. Therefore, the fastest cells most likely drive metastasis, whereas the average cell migration rate might be less important. I showed that the distribution of cell migration speed and persistence is very much regulated under EGF stimulation, even though the average response differs marginally. Indeed, this has been demonstrated previously (Ware, Wells et al. 1998). Ware et al. generated distributions of migration rate in response to no EGF or high EGF concentration. However, the focus of that paper was primarily on the changes in the average migration response and the widening of the distribution in response to EGF was evident, but not discussed. What causes this widening? Heterogeneity in the local ECM concentration might play a role. I have examined collagen coverage and it tends to be fairly homogeneous at the resolution of the light microscope (about 100 nm) and I observed cells in close proximity that varied greatly with respect to their migration speed. However, ECM inhomogeneity cannot be fully dismissed as a possible cause for the cell-to-cell variability. Another cause of the cell-to-cell variability might be autocrine or paracrine signaling. MTLn3 cells are known to secrete other EGF receptor ligands, namely TGF-α (Goswami, Sahai et al. 2005). However, I did not observe clustering of migration speeds around sources. Often cells in the

same clusters showed distinct behavior. A third possibility is that concentrations of signaling, adhesion or cytoskeletal regulatory proteins might contribute to the heterogeneity. This might be the most probable cause of the cell-to-cell variability; however determining which specific components might contribute to this is the subject of further investigation.

EGF does seem to regulate some FA characteristics, namely FA intensity and number per cell (Fig. 2.13). FA intensity decreases as EGF stimulation increases. FA number per cell is highest at low EGF concentrations, suggesting that either the assembly is maximized or disassembly is minimized at this point. EGF is known to alter actin cytoskeleton dynamics, perhaps resulting in enhanced assembly dynamics. Alternatively, EGF is also known to up-regulate calpain, a protease involved in disassembly, which might be activated highly at high EGF concentrations. Interestingly, FA number per cell does not seem to affect cell migration rate. Rather, low FA intensity seems to correlate with fast migrating cells. This might be the direct link between EGF stimulation and cell migration speed regulation. Zaidel-Bar et al. observed that the localization of paxillin in large FAs did not affect the rate of protrusion of the nearby lamellapodia. However, paxillin association with focal complexes was inversely correlated with the rate of local protrusion. Thus, focal complexes containing relatively low levels of paxillin were found in fast protrusions (Zaidel-Bar, Ballestrem et al. 2003). While seemingly less important as measured by the Kolmogorov-Smirnov statistic, I also found that fast migrating cells contain FAs with intermediate sizes, intermediate sliding speeds and short lifetimes (Table 2.2 and Fig. 2.9). The fact that fast migrating requires intermediate sized FAs (0.3 - 3 μm^2) is not surprising. Focal complexes, small FAs are traditionally thought to occupy this range of areas (Gardel, Schneider et al. 2010). These smaller FAs are usually located near the leading edge and transmit strong propulsive traction forces needed during fast migration. Larger, mature FAs exert weaker forces (Beningo, Dembo et al. 2001) and supermature fibrillar adhesions (Goffin, Pittet et al. 2006) are involved in ECM remodeling, both processes that are typically seen in slower migrating cells. Fast migrating cells also contained FAs with intermediate speed. FA speed affects cell speed in complicated ways due to its spatial regulation. For example, Smilenov et al. found that fibroblasts with stationary FAs tend to transmit large forces and result in migratory cells (Smilenov, Mikhailov et al. 1999). However, Diener et al.

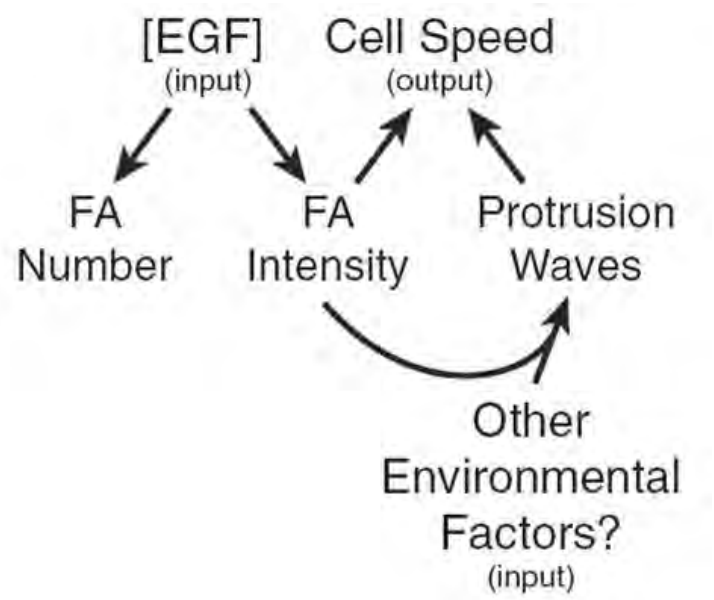

Figure 2.13 **Different adhesion and protrusion characteristics correlate with EGF stimulation and cell speed.** Cells can either be grouped based on EGF concentration or cell speed. EGF concentration is considered an input that acts to regulate adhesion and protrusion characteristics, whereas cell speed is an output that acts to integrate information determined by inputs such as EGF concentration. Both FA intensity and number per cell correlate with EGF concentration, whereas FA intensity and the presence or absence of protrusion waves correlate with cell speed. Cell speed could be regulated by EGF through changes in FA intensity, but other inputs are most likely needed to regulate the presence of protrusion waves, since EGF concentration correlates poorly with the presence or absence of protrusion waves.

found that FAs moved with a sliding speed of 4 μm/hr in migrating human osteosarcoma cells on collagen-coated coverslips (Diener, Nebe et al. 2005) and FAs at the trailing edge are pulled forward at rates of $>$ 5 - 10 μm/hr (Palecek, Schmidt et al. 1996). Lifetime was minimal in fast migrating cells. Others have shown that FAs with short lifetimes correlate with fast migrating cells, in line with what I observe (Nayal, Webb et al. 2006).

Given that local protrusion is linked to FA intensity and that FA intensity was lowest in fast migrating cells, I examined the protrusion dynamics under different stimulation conditions. These cells are known to respond acutely to EGF stimulation with two peaks of barbed end formation resulting in a robust protrusion response (Mouneimne, Soon et al. 2004). However, cells are often not exposed to these acute signals *in vivo* and so how protrusion changes under

chronic EGF stimulation? I found that while EGF stimulation condition correlated poorly with lateral waves generated in cells, fast migrating cells usually generated lateral waves of protrusion as has been seen elsewhere (Machacek and Danuser 2006, Barnhart, Lee et al. 2011). The existence of lateral protrusion waves suggests locally activated feedback loops that travel laterally along the edge of the cell (Enculescu, Sabouri-Ghomi et al. 2010, Barnhart, Lee et al. 2011). This positive feedback loop operates through adhesion signaling for protrusion and protrusion resulting in more adhesions (Cirit, Krajcovic et al. 2010). How does this behavior relate to migration rate? Barnhart et al. noticed that keratocytes migrating on more adhesive substrates generated these lateral waves and migrated with a slower speed (Barnhart, Lee et al. 2011). I see an opposite relationship, where high speeds result in lateral waves of protrusion. This difference may be related to the differences in cytoskeleton organization and morphology between these cells. Keratocytes adopt highly regular persistent cytoskeleton structure and cellular morphology resulting in extremely fast migration speeds ($500 - 600$ μm/hr). MTLn3 cells on the other hand have a varied cytoskeleton structure and cellular morphology and are much slower (< 100 μm/hr). Consequently, highly organized, persistent protrusion that is seen in keratocytes results in the fastest migrating cells. Less efficient, but somewhat organized lateral protrusion seen in both keratocytes and MTLn3 cells results in intermediate speeds. Poorly organized protrusion seen in MTLn3 cells results in slow speeds. Local differences in ECM in our system might explain why EGF is not a primary driver for fast migrating cells or lateral protrusion waves, leading high cell-to-cell variability.

2.5 Conclusions

EGF was found to broaden the distribution of cell migration rates, generating both faster and slower cells, but not dramatically affecting the average response. Several different adhesion and protrusion characteristics correlated with EGF stimulation and cell migration speed, however there is a hierarchy of these correlations. FA intensity and number per cell correlate with EGF stimulation conditions. FA intensity decreases with increasing EGF stimulation and FA number per cell is highest at low EGF stimulation conditions. In contrast, FA intensity and protrusion waves rather than number per cell correlate with cell speed. Fast cells are marked

by low FA intensity and protrusion waves. Consequently, while EGF stimulation could regulate FA intensity to modulate cell speed directly or by partially activating protrusion waves, other factors such as contractility most likely lead to protrusion waves. Adhesion and protrusion characteristics that do not correlate with EGF stimulation condition but do correlate with cell migration speed constitute the most sensitive outputs for identifying why cells respond differently to EGF. The idea that EGF can both increase and decrease the migration speed of individual cells in a population has particular relevance to cancer metastasis where the microenvironment can select subpopulations based on some adhesion and protrusion characteristics, leading to a more invasive phenotype as would be seen if all cells responded like an average cell.

Since metastasis is mainly caused by those fast migrating cells invading surrounding tissue and migrating to secondary tumor sites, it is especially important to study the adhesion, protrusion and migration behavior of fast migrating cells. In the next chapter, I will describe a simple and high throughput method to mark or isolate fast migrating cells in order to determine if differences in protein expression level can explain the cell-to-cell variability. Additionally, in order to determine the cause of protrusion waves as well as the effects of other factors on migration, I will examine how substrate adhesion and contraction regulate migration, protrusion waves and FA properties. This will be discussed in chapter 4.

2.6 Acknowledgements

I thank Dr. Ian C. Schneider for his guidance, patience and revision throughout this chapter; Sarah Hedberg for help with the experiments; Dr. Antonio Sechi and Thomas Wurflinger for help with the FA analysis; Dr. Gaudenz Danuser and Shann-Ching Chen for help with the protrusion analysis and Nick Romsey for his help with the cell migration analysis.

2.7 References

Anderson, A. R. A., A. M. Weaver, P. T. Cummings and V. Quaranta (2006). "Tumor morphology and phenotypic evolution driven by selective pressure from the microenvironment." Cell 127(5): 905-915.

Ando, Y. and P. J. Jensen (1993). "Epidermal Growth-factor and Insulin-like Growth Factor-I Enhance Keratinocyte Migration." Journal of Investigative Dermatology 100(5): 633-639.

Ashkenazy, Y. and H. Gildor (2011). "On the probability and spatial distribution of ocean surface currents." Journal of Physical Oceanography.

Bailly, M., J. S. Condeelis and J. E. Segall (1998). "Chemoattractant-induced lamellipod extension." Microscopy Research and Technique 43(5): 433-443.

Balaban, N. Q., U. S. Schwarz, D. Riveline, P. Goichberg, G. Tzur, I. Sabanay, D. Mahalu, S. Safran, A. Bershadsky, L. Addadi and B. Geiger (2001). "Force and focal adhesion assembly: a close relationship studied using elastic micropatterned substrates." Nature Cell Biology 3(5): 466-472.

Barnhart, E. L., K. C. Lee, K. Keren, A. Mogilner and J. A. Theriot (2011). "An Adhesion-Dependent Switch between Mechanisms That Determine Motile Cell Shape." Plos Biology 9(5): 19.

Beningo, K. A., M. Dembo, I. Kaverina, J. V. Small and Y.-l. Wang (2001). "Nascent Focal Adhesions Are Responsible for the Generation of Strong Propulsive Forces in Migrating Fibroblasts." The Journal of Cell Biology 153(4): 881-888.

Berginski, M. E., E. A. Vitriol, K. M. Hahn and S. M. Gomez (2011). "High-Resolution Quantification of Focal Adhesion Spatiotemporal Dynamics in Living Cells." Plos One 6(7): 13.

Burzynski, T. and M. Papini (2011). "Measurement of the particle spatial and velocity distributions in micro-abrasive jets." Measurement Science and Technology 22(2).

Chan, A. Y., S. Raft, M. Bailly, J. B. Wyckoff, J. E. Segall and J. S. Condeelis (1998). "EGF stimulates an increase in actin nucleation and filament number at the leading edge of

the lamellipod in mammary adenocarcinoma cells." Journal of Cell Science 111: 199-211.

Cirit, M., M. Krajcovic, C. K. Choi, E. S. Welf, A. F. Horwitz and J. M. Haugh (2010). "Stochastic Model of Integrin-Mediated Signaling and Adhesion Dynamics at the Leading Edges of Migrating Cells." Plos Computational Biology 6(2): -.

Colman-Lerner, A., A. Gordon, E. Serra, T. Chin, O. Resnekov, D. Endy, C. Gustavo Pesce and R. Brent (2005). "Regulated cell-to-cell variation in a cell-fate decision system." Nature 437(7059): 699-706.

DeMali, K. A., C. A. Barlow and K. Burridge (2002). "Recruitment of the Arp2/3 complex to vinculin: coupling membrane protrusion to matrix adhesion." Journal of Cell Biology 159(5): 881-891.

Diener, A., B. Nebe, F. Luthen, P. Becker, U. Beck, H. G. Neumann and J. Rychly (2005). "Control of focal adhesion dynamics by material surface characteristics." Biomaterials 26(4): 383-392.

Enculescu, M., M. Sabouri-Ghomi, G. Danuser and M. Falcke (2010). "Modeling of Protrusion Phenotypes Driven by the Actin-Membrane Interaction." Biophysical Journal 98(8): 1571-1581.

Friedl, P. and K. Wolf (2010). "Plasticity of cell migration: a multiscale tuning model." J Cell Biol 188(1): 11-19. Gardel, M. L., B. Sabass, L. Ji, G. Danuser, U. S. Schwarz and C. M. Waterman (2008). "Traction stress in focal adhesions correlates biphasically with actin retrograde flow speed." J Cell Biol 183(6): 999-1005.

Gardel, M. L., I. C. Schneider, Y. Aratyn-Schaus and C. M. Waterman (2010). Mechanical Integration of Actin and Adhesion Dynamics in Cell Migration. Annual Review of Cell and Developmental Biology, Vol 26. R. Schekman, L. Goldstein and R. Lehmann. Palo Alto, Annual Reviews. 26: 315-333.

Geiger, B., E. Zamir, B. Z. Katz, S. Aota, K. M. Yamada and Z. Kam (1999). "Molecular diversity of cell-matrix adhesions." Journal of Cell Science 112(11): 1655-1669.

Giannone, G., B. J. Dubin-Thaler, H. G. Dobereiner, N. Kieffer, A. R. Bresnick and M. P. Sheetz (2004). "Periodic lamellipodial contractions correlate with rearward actin waves." Cell 116(3): 431-443.

Goffin, J. r. m. M., P. Pittet, G. Csucs, J. W. Lussi, J.-J. Meister and B. Hinz (2006). "Focal adhesion size controls tension-dependent recruitment of -smooth muscle actin to stress fibers." The Journal of Cell Biology 172(2): 259-268.

Goswami, S., E. Sahai, J. B. Wyckoff, N. Cammer, D. Cox, F. J. Pixley, E. R. Stanley, J. E. Segall and J. S. Condeelis (2005). "Macrophages promote the invasion of breast carcinoma cells via a colony-stimulating factor-1/epidermal growth factor paracrine loop." Cancer Research 65(12): 5278-5283.

Harms, B. D., G. M. Bassi, A. R. Horwitz and D. A. Lauffenburger (2005). "Directional Persistence of EGF-Induced Cell Migration Is Associated with Stabilization of Lamellipodial Protrusions." Biophysical Journal 88(2): 1479-1488.

Hinz, B., W. Alt, C. Johnen, V. Herzog and H.-W. Kaiser (1999). "Quantifying Lamella Dynamics of Cultured Cells by SACED, a New Computer-Assisted Motion Analysis." Experimental Cell Research 251(1): 234-243.

Janmey, P. A. (1998). "The cytoskeleton and cell signaling: Component localization and mechanical coupling." Physiological Reviews 78(3): 763-781.

Joslin, E. J., L. K. Opresko, A. Wells, H. S. Wiley and D. A. Lauffenburger (2007). "EGF-receptor-mediated mammary epithelial cell migration is driven by sustained ERK signaling from autocrine stimulation." Journal of Cell Science 120(20): 3688-3699.

Katz, M., I. Amit, A. Citri, T. Shay, S. Carvalho, S. Lavi, F. Milanezi, L. Lyass, N. Amariglio, J. Jacob-Hirsch, N. Ben-Chetrit, G. Tarcic, M. Lindzen, R. Avraham, Y.-C. Liao, P. Trusk, A. Lyass, G. Rechavi, N. L. Spector, S. H. Lo, F. Schmitt, S. S. Bacus and Y. Yarden (2007). "A reciprocal tensin-3-cten switch mediates EGF-driven mammary cell migration." Nat Cell Biol 9(8): 961-969.

Lacayo, C. I., Z. Pincus, M. M. VanDuijn, C. A. Wilson, D. A. Fletcher, F. B. Gertler, A. Mogilner and J. A. Theriot (2007). "Emergence of Large-Scale Cell Morphology and Movement from Local Actin Filament Growth Dynamics." PLoS Biol 5(9): e233.

Li, Y., J. Fan, M. Chen, W. Li and D. T. Woodley (2006). "Transforming Growth Factor-Alpha: A Major Human Serum Factor that Promotes Human Keratinocyte Migration." J Invest Dermatol 126(9): 2096-2105.

Machacek, M. and G. Danuser (2006). "Morphodynamic profiling of protrusion phenotypes." Biophysical Journal 90(4): 1439-1452.

Maheshwari, G., A. Wells, L. G. Griffith and D. A. Lauffenburger (1999). "Biophysical integration of effects of epidermal growth factor and fibronectin on fibroblast migration." Biophysical Journal 76(5): 2814-2823.

Maheshwari, G., H. S. Wiley and D. A. Lauffenburger (2001). "Autocrine epidermal growth factor signaling stimulates directionally persistent mammary epithelial cell migration." Journal of Cell Biology 155(7): 1123-1128.

Miyamoto, S., H. Teramoto, J. S. Gutkind and K. M. Yamada (1996). "Integrins can collaborate with growth factors for phosphorylation of receptor tyrosine kinases and MAP kinase activation: Roles of integrin aggregation and occupancy of receptors." Journal of Cell Biology 135(6): 1633-1642.

Monine, M. I. and J. M. Haugh (2008). "Cell population-based model of dermal wound invasion with heterogeneous intracellular signaling properties." Cell Adh Migr 2(2): 137-146.

Mouneimne, G., L. Soon, V. DesMarais, M. Sidani, X. Y. Song, S. C. Yip, M. Ghosh, R. Eddy, J. M. Backer and J. Condeelis (2004). "Phospholipase C and cofilin are required for carcinoma cell directionality in response to EGF stimulation." Journal of Cell Biology 166(5): 697-708.

Nayal, A., D. J. Webb, C. M. Brown, E. M. Schaefer, M. Vicente-Manzanares and A. R. Horwitz (2006). "Paxillin phosphorylation at Ser273 localizes a GIT1-PIX-PAK complex and regulates adhesion and protrusion dynamics." The Journal of Cell Biology 173(4): 587-589.

Neri, A., D. Welch, T. Kawaguchi and G. L. Nicolson (1982). "Development and Biologic Properties of Malignant-Cell Sublines and Clones of a Spontaneously Metastasizing Rat Mammary Adenocarcinoma." Journal of the National Cancer Institute 68(3): 507-517.

Niepel, M., S. L. Spencer and P. K. Sorger (2009). "Non-genetic cell-to-cell variability and the consequences for pharmacology." Current Opinion in Chemical Biology 13(5-6): 556-561.

Othmer, H. G., S. R. Dunbar and W. Alt (1988). "Models of dispersal in biological systems." J Math Biol 26(3): 263-298.

Palecek, S. P., C. E. Schmidt, D. A. Lauffenburger and A. F. Horwitz (1996). "Integrin

dynamics on the tail region of migrating fibroblasts." Journal of Cell Science 109: 941-952.

Parsons, J. T., A. R. Horwitz and M. A. Schwartz (2010). "Cell adhesion: integrating cytoskeletal dynamics and cellular tension." Nature Reviews Molecular Cell Biology 11(9): 633-643.

Pollard, T. D. and G. G. Borisy (2003). "Cellular motility driven by assembly and disassembly of actin filaments." Cell 112(4): 453-465.

Price, J. T., T. Tiganis, A. Agarwal, D. Djakiew and E. W. Thompson (1999). "Epidermal Growth Factor Promotes MDA-MB-231 Breast Cancer Cell Migration through a Phosphatidylinositol 3-Kinase and Phospholipase C-dependent Mechanism." Cancer Research 59(21): 5475-5478.

Raj, A. and A. van Oudenaarden (2008). "Nature, Nurture, or Chance: Stochastic Gene Expression and Its Consequences." Cell 135(2): 216-226.

Rao, C. V., D. M. Wolf and A. P. Arkin (2002). "Control, exploitation and tolerance of intracellular noise." Nature 420(6912): 231-237.

Rijken, P. J., W. J. Hage, P. Henegouwen, A. J. Verkleij and J. Boonstra (1991). "Epidermal Growth-fator Induces Rapid Reorganization of the Actin Microfilament System in Human A431 Cells." Journal of Cell Science 100: 491-499.

Rinott, R., A. Jaimovich and N. Friedman "Exploring transcription regulation through cell-to-cell variability." Proceedings of the National Academy of Sciences 108(15): 6329-6334.

Sawyer, C., J. Sturge, D. C. Bennett, M. J. O'Hare, W. E. Allen, J. Bain, G. E. Jones and B. Vanhaesebroeck (2003). "Regulation of breast cancer cell chemotaxis by the phosphoinositide 3-kinase p110 delta." Cancer Research 63(7): 1667-1675.

Schneider, I. C., C. K. Hays and C. M. Waterman (2009). "Epidermal Growth Factor-induced Contraction Regulates Paxillin Phosphorylation to Temporally Separate Traction Generation from De-adhesion." Molecular Biology of the Cell 20(13): 3155-3167.

Segall, J. E., S. Tyerech, L. Boselli, S. Masseling, J. Helft, A. Chan, J. Jones and J. Condeelis (1996). "EGF stimulates lamellipod extension in metastatic mammary adenocarcinoma cells by an actin-dependent mechanism." Clinical and Experimental Metastasis 14(1): 61-72.

Serrels, B., A. Serrels, V. G. Brunton, M. Holt, G. W. McLean, C. H. Gray, G. E. Jones and

M. C. Frame (2007). "Focal adhesion kinase controls actin assembly via a FERM-mediated interaction with the Arp2/3 complex." Nature Cell Biology 9(9): 1046-U1015.

Small, J. V. (2011). "Dicing with dogma: de-branching the lamellipodium." Trends in Cell Biology 20(11): 628-633. Smilenov, L. B., A. Mikhailov, R. J. Pelham, E. E. Marcantonio and G. G. Gundersen (1999). "Focal adhesion motility revealed in stationary fibroblasts." Science 286(5442): 1172-1174.

Stricker, J., Y. Aratyn-Schaus, P. W. Oakes and M. L. Gardel (2011). "Spatiotemporal Constraints on the Force-Dependent Growth of Focal Adhesions." Biophysical Journal 100(12): 2883-2893.

Valles, A. M., M. Beuvin and B. Boyer (2004). "Activation of Rac1 by paxillin-Crk-DOCK180 signaling complex is antagonized by Rap1 in migrating NBT-II cells." Journal of Biological Chemistry 279(43): 44490-44496.

Wang, S. J., W. Saadi, F. Lin, C. M. C. Nguyen and N. L. Jeon (2004). "Differential effects of EGF gradient profiles on MDA-MB-231 breast cancer cell chemotaxis." Experimental Cell Research 300(1): 180-189.

Ware, M. F., A. Wells and D. A. Lauffenburger (1998). "Epidermal growth factor alters fibroblast migration speed and directional persistence reciprocally and in a matrix-dependent manner." Journal of Cell Science 111: 2423-2432.

Welf, E. S., B. A. Ogunnaike and U. P. Naik (2009). "Quantitative statistical description of integrin clusters in adherent cells." Iet Systems Biology 3(5): 307-316.

Wieser, S., J. Weghuber, M. Sams, H. Stockinger and G. J. Schutz (2009). "Cell-to-cell variability in the diffusion constants of the plasma membrane proteins CD59 and CD147." Soft Matter 5(17): 3287-3294.

Wurflinger, T., I. Gamper, T. Aach and A. S. Sechi (2011). "Automated segmentation and tracking for large-scale analysis of focal adhesion dynamics." Journal of Microscopy 241(1): 37-53.

Xie, H., M. A. Pallero, K. Gupta, P. Chang, M. F. Ware, W. Witke, D. J. Kwiatkowski, D. A. Lauffenburger, J. E. Murphy-Ullrich and A. Wells (1998). "EGF receptor regulation of cell motility: EGF induces disassembly of focal adhesions independently of the motility-associated

PLC gamma signaling pathway." Journal of Cell Science 111: 615-624.

Yuan, T. L., G. Wulf, L. Burga and L. C. Cantley (2011). "Cell-to-Cell Variability in PI3K Protein Level Regulates PI3K-AKT Pathway Activity in Cell Populations." Current Biology 21(3): 173-183.

Zaidel-Bar, R., C. Ballestrem, Z. Kam and B. Geiger (2003). "Early molecular events in the assembly of matrix adhesions at the leading edge of migrating cells." Journal of Cell Science 116(22): 4605-4613.

Zaidel-Bar, R. and B. Geiger (2010). "The switchable integrin adhesome." Journal of Cell Science 123(9): 1385-1388.

CHAPTER 3. COMBINATION OF QD-BASED PHAGOKINETIC ASSAY AND FLOW CYTOMETRY TO ASSESS CELL-TO-CELL VARIABILITY IN MIGRATION

Cancer metastasis is often driven by fast moving cells. Consequently, simple and high-throughput methods by which to mark or isolate fast moving cells are needed. I constructed a homogeneous quantum dot (QD) coating on collagen substrates with 200 nM aminopropanediol-QDs in cell culture medium. After incubation on QD substrates, cells could uptake fluorescent QDs through phagocytosis. I hypothesized that the fast migrating cells uptake more QDs and are brighter due to the longer distances over which they migrated in comparison to slow migrating cells. Therefore, I compared the migration distance and the fluorescent intensities of tumor cells (MTLn3) and non-tumor cells mouse embryonic fibroblast (MEF) using the combination of phagokinetic assay and flow cytometry. While cell migration speed was the largest contributor to the QD uptake, cell area affects the uptake, too. Consequently, fluorescence was normalized based on cell area, so that a dependence of fluorescence intensity on cell migration speed could be seen. There is a positive but weak correlation between QD uptake and cell speed, especially after long time migration for MTLn3 cells. Therefore, the combination of QD-based phagokinetic assay and flow cytometry is a reasonable approach to analyze cell-to-cell variability in migration.

3.1 Introduction

Cell adhesion and migration play essential roles in cancer development. Metastases, rather than primary tumors, are responsible for most cancer deaths. During metastasis, cancer cells detach from the primary tumor, invade surrounding connective tissue and blood vessels, are

transported in the bloodstream and invade other organs after extravasation (Chambers, Groom et al. 2002). The ability of tumor cells to invade surrounding tissue and to metastasize to different sites in the body is known to be related to the motility of the cells. Aggressive metastasis requires fast migration. Therefore, it is important to study the migration behavior of those fast migrating cells and understand why those invasive cells migrate fast. It is also important to have a simple, robust and quantitative method that can separate fast migrating cells from other cells and can be employed widely in a clinical setting as a diagnostic tool.

Albrecht-Buehler introduced a method called the phagokinetic assay to indirectly measure cell migration behavior (Albrecht-Buehler 1977; Guenter 1977; Guenter 1977). He coated cell culture substrates with nanoparticles and seeded cells on the nanoparticles. Upon migration along the surface, cells internalized the nanoparticles and thus left clear tracks which represented a blueprint of their motility. Compared to particles dissolved in solution the uptake of nanoparticles adsorbed to a surface is more efficient, because solution uptake is limited by diffusional transport (Pellegrino, Kudera et al. 2005). Originally gold colloids were used as nanoparticles, and they were visualized by dark-field microscopy or by transmission electron microscopy (Guenter 1977). This method has been improved over time (Scott, McCool et al. 2000) and has been used for a variety of migration studies on a wide spectrum of cell types, including fibroblasts (Guenter 1977), neutrophils (Igarashi, Kawa et al. 1997), keratinocytes (Ando and Jensen 1993; Chen, Helmold et al. 1994) and endothelial cells (Mcauslan and Reilly 1980).

The gold particles originally used in phagokinetic assays were quite inhomogeneous and large, up to a few hundred nanometers in diameter (Parak, Gerion et al. 2003). Since the typical size of a cell is of the order of a few tens of microns, the gold particles are relatively large for the cells to internalize. Therefore, the use of small CdSe/ZnS quantum dots (QD) is advantageous (Alivisatos, Parak et al. 2002; Larabell, Pellegrino et al. 2003). QDs also have other advantages. For example, the uptake of QDs has minimal impact on the morphology and migration behavior of cells (Alivisatos, Parak et al. 2002). Fluorescence is an easier measurement to quantify than scattering. QDs are good fluorescent probes for multicolor cell structure labeling because of their high quantum yields (Sha, Han et al. 2009), high molecular

excitation coefficients (Beuthan, Dressler et al. 2004), strong resistance to photobleaching (Le Gac, Vermes et al. 2006) and chemical degradation (Park, Weng et al. 2008), broad excitation spectra (Van Orden, Willard et al. 2001), narrow emission spectra (Han and Huang 2010), large stokes shift (Avidan and Oron 2008) and long fluorescence lifetimes (Li, Mueller et al. 2010). Because QDs have smaller sizes and are more homogeneous than colloidal gold, improved spatial resolution can be achieved. The use of QDs also facilitates monitoring live cells, both before and after perturbations, such as potential chemotherapeutic agents (Alivisatos, Gu et al. 2005). Furthermore, tracks can be observed in stacked layers with different color of fluorescence, which would allow for analyzing migration behavior in three dimensional cultures (Parak, Pellegrino et al. 2005).

This ability to determine migration rate from QD-based phagokinetic assay has led those to propose to use it in determining the invasiveness of cancer cells. Teresa et al. provided a rapid, robust and quantitative *in vitro* measurement of metastatic potential by utilizing the the phagokinetic assay to distinguish between non-invasive and invasive cancer cell lines (Larabell, Pellegrino et al. 2003). They used 8 nm and 16 nm diameter QDs and incubated cells for 24 hrs or longer. They found tumor cells MDA-MB-231 had larger ratio of A_{track}/A_{cell} (area of the track/area of the cell) than non-tumor cells MCF-10A. Although phagokinetic assays are powerful tools for cell motility studies and can be highly automated, the analysis has revolved around the cell tracks rather than the cells themselves. However, the fluorescence of the cell can be correlated with the migration speed.

Flow cytometry is a convenient method for the analysis of multiple parameters of individual cells in a population. In addition, cells can be sorted using fluorescence assisted cell sorting. The cell samples containing internalized fluorescent QDs can be introduced into a carrier fluid, called a sheath fluid, which forces the cells into the center of the flow chamber so that only one cell can be detected at a time. The light source, which is typically one or more lasers, is focused onto the cell stream at a specific point by specialized optics. The light scattered by cells or emitted from fluorescent QDs associated with the cells triggers a photomultiplier tube (PMT), which enhances the light signal and converts it into a digital signal. Bandpass filters are used in conjunction with PMTs so that the emission from a specific fluorophore can be

measured. The output of each of the PMTs is recorded for each cell, and the data is stored on a computer. Cell sorting relies on droplet deflection instruments. In these instruments the stream is broken up into drops by means of a vibrator that operates at nearly 100 kHz. Under most conditions, the drops that are formed will contain only a single cell. As the sheath fluid typically contains phosphate-buffered saline, a charge can be applied to a droplet that contains a cell of interest, such as the cell with high fluorescent intensity, and the charged droplet will be deflected into a collection tube by a charged plate. Today′s high-speed droplet deflection sorters, such as the Becton-Dickinson FACS-Aria or the Dako MoFlo, can sort up to 90,000 cells per second (Link, Jeong et al. 2007). Therefore, fast migrating cells which take up more QDs and thus have higher fluorescent intensities, could be stained for different proteins and a correlation between migration speed (QD fluorescence) and protein expression can be drawn. Additionally, cells might be able to be separated based on migration speed (QD fluorescence) using cell sorting techniques. Consequently, I began to optimize the phagokinetic assay using QDs and determine if flow cytometry could be used.

I first tried different coating conditions including three types of QDs, different concentrations of and buffers for the QDs to find the most homogeneous QD substrates. I found that 200 nM aminopropanediol-QDs in cell culture medium showed a more homogeneous surface distribution of QDs than other conditions. I hypothesized that the fast migrating cells would uptake more QDs and be brighter due to the longer distances over which they migrated in comparison to slow migrating cells. Then I compared the phagokinetic tracks and the fluorescent intensities of tumor cells (MTLn3) and non-tumor cells mouse embryonic fibroblast (MEF) using the phagokinetic assay and flow cytometry. However, the slower moving MEF cells were brighter and had larger and clearer phagokinetic tracks than fast moving MTLn3 cells. This is probably because MEF cells have much larger area than MTLn3 cells. While cell migration speed was the largest contributor to the QD uptake, cell area affects the uptake, too. I also compared the effects of different densities of collagen and different incubation times on the cell migration behavior and found that the cells incubated on 300 μg/ml of collagen (300COL) had larger tracks and were brighter than the cells on 3 μg/ml of collagen (3COL). The cells incubated for 24 hours had larger tracks and were brighter than the cells incubated for 6 hours. However,

if I focused my attention on brighter cells more predictable results were seen. MTLn3 cells incubated on 3COL and for 24 hours (a condition that produces fast migrating cells) were brighter than MTLn3 cells incubated on 300COL and for 24 hours (a condition that produces slow cells). These results suggested that the combination of the phagokinetic assays and flow cytometry might be a simple method to mark and isolate cells according to their migration rates, however, optimization was not fully realized. Additionally, large changes in uptake efficiency among cells migrating at different speeds might also affect the correlation between fluorescence and migration speed. Cells with higher QD internalization might be better models for further studies.

3.2 Materials and Methods

Cell Culture

Mouse embryonic fibroblasts (MEF) were obtained from Dr. Clare Waterman (NIH NHLBI) and were maintained in Dulbecco's Modified Eagle Medium (DMEM, from Invitrogen) containing 10% fetal bovine serum (FBS, from Invitrogen), 2% glutamax (Invitrogen) and 1% penicillin-streptomycin at 37°C in 5% CO_2 incubator. Rat mammary adenocarcinoma cells (MTLn3) were obtained from Dr. Jeffrey E. Segall (Albert Einstein College of Medicine) and maintained in α-MEM media with L-glutamine, containing 5% FBS and 1% penicillin-streptomycin at 37°C in 5% CO_2 incubator. Cells were passed at 80% confluence every 2 or 3 days until passage 20. Cells were seeded on QD-coated coverslips at 50,000-100,000 cells/coverslip density and incubated from 6 hours to 5 days at 37°C in 5% CO_2 incubator.

QD substrate coating

3 μg/ml of rat tail collagen I (Invitrogen) and 2 μg/ml poly-L-lysine hydrochloride (PLL, from Sigma) was dissolved in 0.5 M acetic acid (Fisher) for coating on coverslips. A 150 μl drop of this solution was placed on the center of each 35 mm cell culture dish (Fisher) and then a 22 mm $\times$ 22 mm squeaky clean coverslip (Corning, Fisher) was placed on top of the collagen solution. The collagen was allowed to incubate under aluminum foil for at least 1 hour for every experiment. An alternate concentration used was 300 μg/ml of collagen without PLL. Cysteine, lysine and aminopropanediol-QDs were prepared at various concentrations depend-

ing on the specific experiment (from 10 nM to 200 nM). QD solutions were either nanopure water or α-MEM medium with L-glutamine (Invitrogen) containing 1% penicillin-streptomycin (Invitrogen) and 1 mg/ml bovine serum albumin (BSA, from Sigma). Method 1 of coating QDs includes directly adding 150-200 μl of QD solution on top of the coverslips with collagen and PLL and then allowing the solution to dry continues were sterilized under Ultra-Violet (UV) light for 15 minutes. Method 2 of coating QDs includes treating the QD solution similarly to collagen coating. A 150 μl drop of QD solution was placed on a new cell culture dish and the collagen-coated coverslip was placed on top of the QD solution, with the collagen-coated side facing downward. The coverslips were incubated in the refrigerator for overnight and dried and sterilized under UV light for 15 minutes.

Microscopy

Coverslips were mounted onto glass slide chambers in cell culture media without phenol red. Chambers were maintained at 37°C on a heated stage. Phase contrast images were captured at 20× (NA 0.50, Nikon) with a charged-coupled device (CoolSNAP HQ2, Photometrics) attached to an inverted microscope (Eclipse Ti, Nikon). Fluorescent images were captured at 20× with the microscope connected to a fluorescence illumination system (Lumen200PRO, Prior). Camera and shutter were controlled by μManager 1.3. To detect the cysteine-QDs, an excitation filter 555/25 and an emission filter 605/52 were used. For lysine and aminopropanediol-QDs, an excitation filter ET 645/30*times* and an emission filter ET 705/72m were used. Exposure times of either 50 ms or 2000 ms were used. NOTE: The epi-illumination mercury arc lamp was changed during our research period, so absolute fluorescence may vary slightly.

Flow cytometry

Cells were incubated on QD substrates for 6 hours or 24 hours and then detached from the coverslips using 0.25% (w/v) trypsin (Invitrogen). Cell culture media was added to neutralized the trypsin and the cells in neutralized solution were centrifuged at 1500 RCF for 5 minutes at 4°C. The supernatant was aspirated and 100 μl of 1% cold paraformaldehyde (PFA, Fisher) was added. The cells in fix solution was transferred into a 12 × 75 mm, 5 ml polystyrene round bottom test tube (BD Falcon) and then taken to the flow cytometry facility (Iowa State University) for analysis. To detect the QDs, an emission wavelength of 555 nm for cysteine-QDs

and an emission wavelength of 605 nm for lysine and aminopropanediol-QDs were used.

Cell migration assay

Cells were incubated on QD substrates for 24 hours and then made into glass slide chambers in cell culture media without phenol red. Chambers were maintained at 37°C on an automated heated stage (Warner). Phase contrast time-lapse images were captured every 2 minutes for 12 hours at 20× with the charged-coupled device attached to the inverted microscope. Cell centroids were identified and tracked manually by MTrackJ plugins of ImageJ. Single cell speed, S, and directional persistence time, P, were obtained by fitting these to the persistent random walk equation 3.1 (Dunn 1983; Othmer, Dunbar et al. 1988; Ware, Wells et al. 1998):

$$< d^2(t) >= 2S^2P[t - P(1 - e^{-t/P)}], \tag{3.1}$$

where t is the time interval, using a non-linear least squares regression analysis.

Statistical analysis

All graphs and statistical analyses were done using MATLAB and JMP software. To determine the statistical differences of mean values between pairs under different conditions, a Turkey HSD test was applied to the data.

3.3 Results

Optimizing QD coating conditions

I tested three types of QDs containing differently charged ligands: neutral aminopropanediol (AP), negatively charged cysteine (Cys) and positively charged lysine (Lys) ligands. By imaging these three types of QDs on collagen and poly-L-lysine (PLL) substrates, I found that only AP-QDs could be seen under 50 ms exposure time, while Cys and Lys-QDs were hardly visible (Fig. 3.1). Although AP-QDs easily aggregate, I chose AP-QDs as the candidate QD. However, a 50 ms exposure time is too short to properly excite QDs. Experiments at a longer exposure times were used to properly visualize the QDs. I compared three types of QDs and measured the mean values and standard deviation to decide which conditions resulted in the brightest and most homogenously distributed.

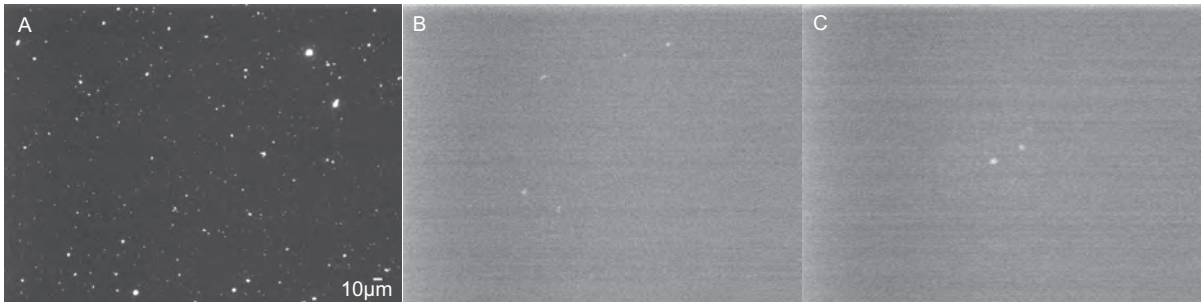

Figure 3.1 **Aminopropanediol-QDs are the brightest among three types of QDs.** 10 nM of A. aminopropanediol, B. cysteine, C. lysine-QDs on collagen and poly-L-lysine substrates under 50 ms exposure time. Scale bar is 10 μm. Number of images for different types of QDs is: $N_{AP} = 6$, $N_{Cys} = 3$, $N_{Lys} = 6$.

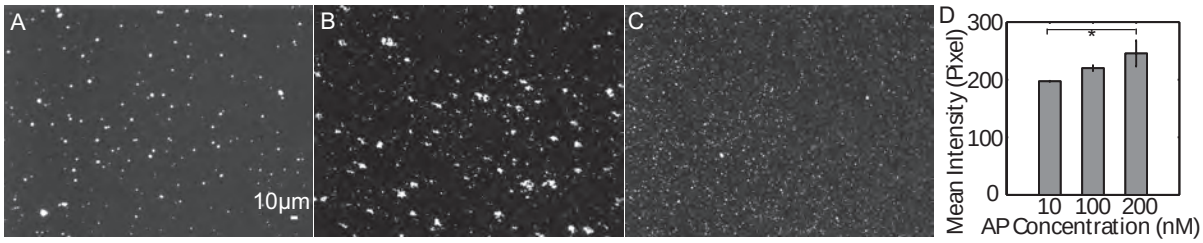

Figure 3.2 **Different concentrations of AP-QDs on collagen and poly-L-lysine substrates.** A. 10 nM, B. 100 nM, C. 200 nM of AP-QDs under 50 ms exposure time. Scale bar is 10 μm. D. The mean values of QD intensity under various concentrations of AP. Error bars are 95% confidence interval and asterisk denotes $p < 0.01$. Number of images under different concentrations of AP-QDs is: $N_{10nM} = 21$, $N_{100nM} = 19$, $N_{200nM} = 23$.

I coated different concentrations of AP-QDs on the substrates, as shown in Fig. 3.2. AP-QDs aggregated at 10 nM and 100 nM. However, they seemed to be homogeneously distributed at 200 nM. In addition, 200 nM AP-QDs had the highest mean intensity among three concentrations (Fig. 3.2D). For these two reasons I chose 200 nM AP-QDs for further study. Different buffers and coating methods also affect QD aggregation (Zhang, Haage et al. 2012). Consequently, I dissolved 200 nM AP-QDs in either nano-pure water or DMEM with BSA solution and then coated them on substrates by either method 1 or method 2. Method 1 includes adding QD solution on top of the substrates and allowing them to dry. Method 2 includes adding QD solution on cell culture dishes and then covering the substrate coverslips

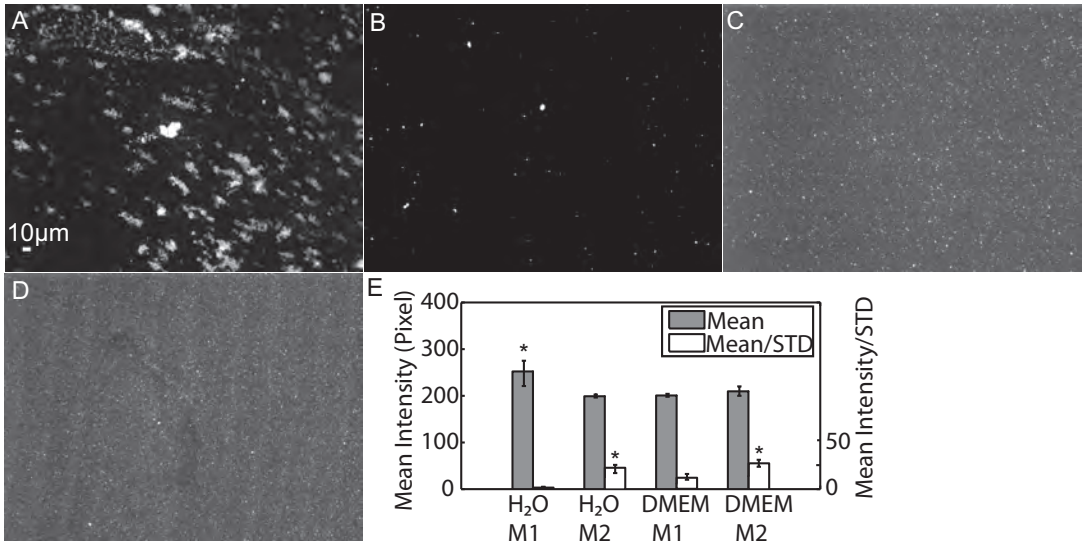

Figure 3.3 **AP in DMEM media with method 2 had brighter and more homogenous distribution.** Images of 200 nM AP-QDs in A. water with method 1, B. water with method 2, C. DMEM + BSA with method 1, D. DMEM + BSA with method 2, under 50 ms exposure time. Scale bar is 10 μm. E. The mean values of QD intensity (gray bars) and mean intensity/standard deviation (white bars) treated by different methods. Error bars are 95% confidence intervals. The data with asterisks is significantly different with the data without asterisks. Number of images treated by different method is: $N_{H2O-M1} = 10$, $N_{H2O-M2} = 14$, $N_{DMEM-M1} = 15$, $N_{DMEM-M2} = 11$.

on top of the QD solution overnight. By observing QD images in different buffers and treating with different methods, I found that QDs in DMEM solution had smaller size than QDs in water (Fig. 3.3A-D), which indicated that DMEM caused less aggregation than water buffer. I also measured the inverse of coefficient of variation (CV^{-1}) for QD distribution, which is defined as the mean intensity over the standard deviation (STD). Either brighter QDs (larger mean intensity) or more homogeneous QDs (smaller STD) or both result in higher CV^{-1}. It is obvious that method 2 had higher CV^{-1} than method 1 (Fig. 3.3E). Therefore, I decided to use 200 nM AP-QDs in DMEM+BSA solution with method 2 for the following phagokinetic experiments.

Phagokinetic assays

After determining the optimal QD coating method, I began to compare the QD uptake behavior and phagokinetic tracks between two types of cells, rat mammary adenocarcinoma cells (MTLn3) and mouse embryonic fibroblast cells (MEF). The MTLn3 cell line was derived from a lung metastasis and is highly metastatic. The MEF cell line was derived from mouse embryos and migrate relatively slowly compared to MTLn3 cells. It has been shown that cells are able to phagocytose QDs in a nonspecific way as they migrate on a homogenous layer of QDs, leaving behind a dark phagokinetic track absent of fluorescent particles (Alivisatos, Parak et al. 2002). I hypothesized that the fast migrating cells would uptake more QDs due to the longer distances over which they migrated compared to slow migrating cells. If this is true, I would be able to detect the fast migrating cells using flow cytometry.

I absorbed 200 nM AP-QDs in DMEM+BSA media on either 3 μg/ml of collagen (3COL) or 300 μg/ml of collagen (300COL) substrates and then incubated MTLn3 and MEF cells on homogenous QD substrates for different time periods, from 6 hours to 5 days. From the phase contrast images, I observed that MEF cells were more elongated and had larger areas than MTLn3 cells (Fig. 3.4A and D). The cells on 300COL were larger than those on 3COL substrates and this trend was more apparent for MEF cells compared to MTLn3 cells (Fig. 3.4A, D, G and J). After incubating for a long time (5 days), MTLn3 cells were more likely to cluster together than MEF cells (Fig. 3.4M and P). From the fluorescent and composite images, I found that MEF cells were brighter and had larger and clearer phagokinetic tracks than MTLn3 cells (Fig. 3.4B, C, E and F). However, there were almost no tracks for the cells incubated for 5 days (Fig. 3.4N, O, Q and R), indicating that the cells migrated over the entire substrate, phagocytosing almost all of the AP-QDs or that the QD dissociated from the surface.

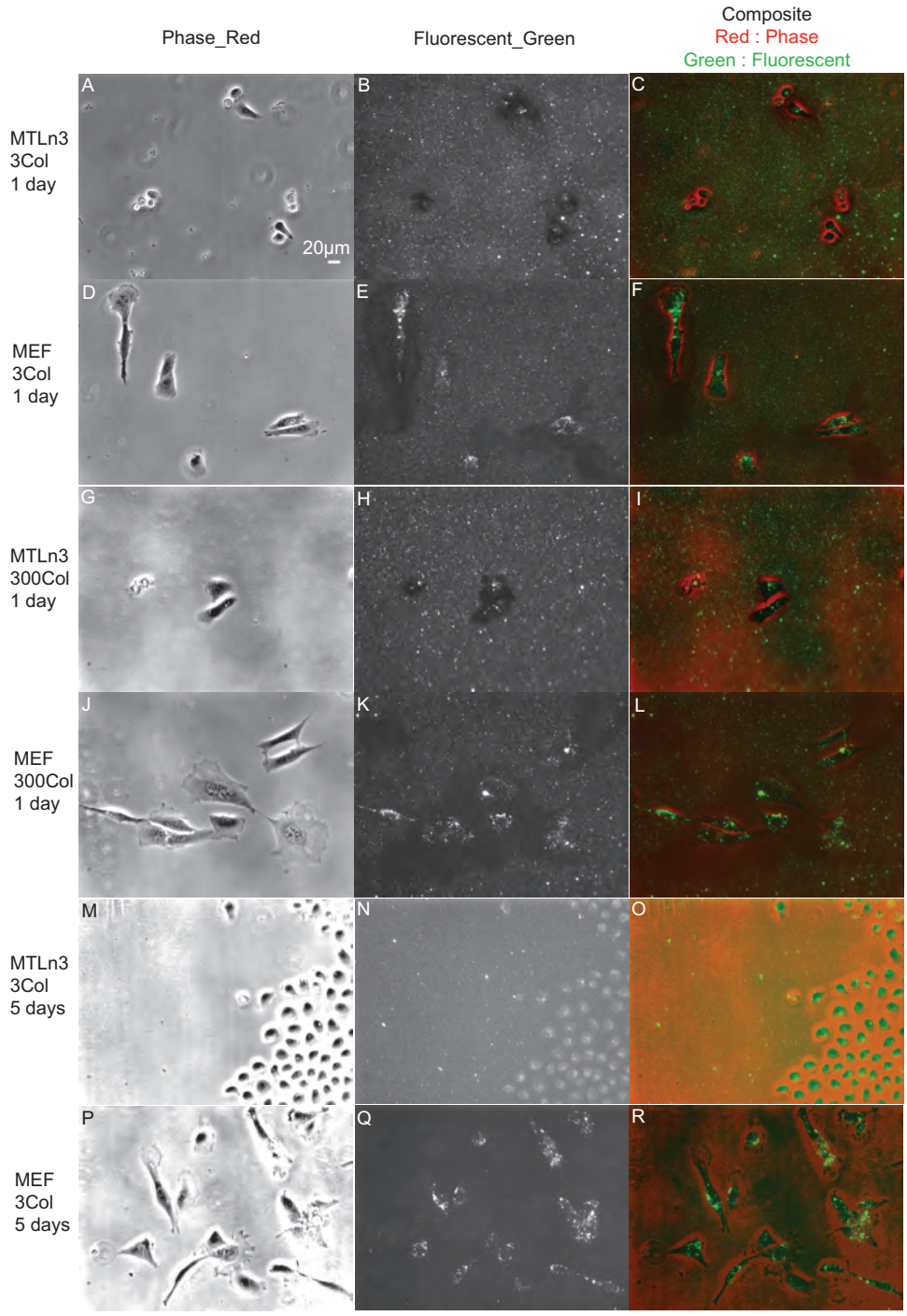

Figure 3.4 **Phagokinetic assays of MTLn3 and MEF cells on different substrates incubated for different days.** MTLn3 cells on 3 μg/ml collagen for 1 day (A-C) or 5 days (M-O) incubation. MTLn3 cells on 300 μg/ml collagen for 1 day incubation (G-I). MEF cells on 3 μg/ml collagen for 1 day (D-F) or 5 days (P-R) incubation. MEF cells on 300 μg/ml collagen for 1 day incubation (J-L). Left columns are phase contrast images of the cells. Middle columns are fluorescent images of the cells and QDs. Right columns are composite images, where red is phase and green is fluorescent image. Scale bar is 20 μm.

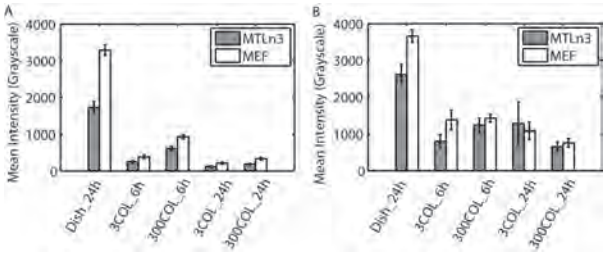

Figure 3.5 **Different substrates and incubation time affect the phagokinetic migration of MTLn3 and MEF cells.** Mean intensity of MTLn3 (gray bars) and MEF (white bars) for A. all cells or B. cells with mean intensity higher than 300 pixels analyzed by flow cytometry. 200 nM of AP-QDs were coated on cell culture dishes (Dish), 3 μg/ml of collagen (3COL) or 300 μg/ml of collagen (300COL) substrates and cells were incubated on different AP-QDs substrates for either 6 hours (6h) or 24 hours (24h). Error bars represent 95% confidence interval.

Flow cytometry quantification of AP-QD uptake

To quantify the amount of AP-QDs phagocytosed by the cells, I used flow cytometry to measure the intensity of individual cells under different conditions. Under the same condition, MEF cells always had higher mean intensity than MTLn3 cells (Fig. 3.5A), either due to faster migration, larger area or more efficient phagocytosis. Cells on 300COL had higher mean intensity than those on 3COL (Fig. 3.5A), which might due to larger area of cells on 300COL. The cells on cell culture plastic dishes had the highest intensity, however, the volume of AP-QDs on the dish was 3 times larger than on the collagen substrates. Cells on the dish phagocytosed AP-QDs with higher efficiency. The cells incubated for 24 hours had lower mean intensity than those incubated for 6 hours (Fig. 3.5A). However, these cells have doubling times of roughly 24 hours, so a fraction of those cells at 24 hours might have undergone division, effectively halving the fluorescence signal of the AP-QDs. Interestingly, if I only analyzed those cells with mean intensity higher than 300 pixels, which should have indicated fast migrating cells, I observed that MTLn3 cells on 300COL had lower mean intensity than those on 3COL substrates for 24 hours incubation (Fig. 3.5B). This is reasonable, given that MTLn3 cells adhere more tightly to the 300COL substrate, resulting in a slower migration speed and shorter migration tracks.

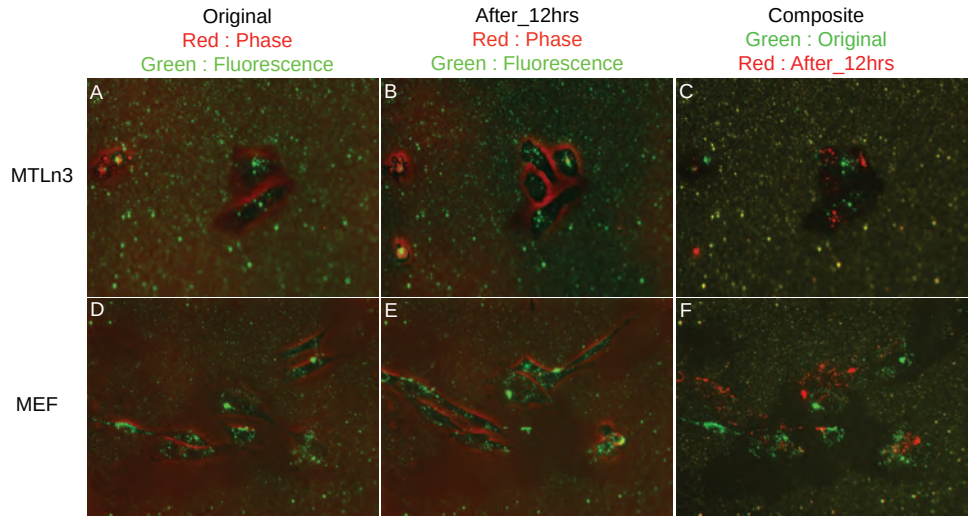

Figure 3.6 **12 hours phagokinetic assay of MTLn3 and MEF cells on 300COL substrates incubated for 1 day.** Merged images of MTLn3 cells A. before 12 hours and B. after 12 hours migration and merged images of MEF cells D. before 12 hours and E. after 12 hours migration. Phase images are in red and fluorescent images are in green for A, B, D and E. Composite images of C. MTLn3 and F. MEF cells before and after 12 hours migration. Original images are in green and after 12hrs images are in red.

Correlation between AP-QD uptake and cell speed via cell migration assays

To further confirm the hypothesis that fast migrating cells might phagocytose more AP-QDs and thus be brighter than slow migrating cells, I took a 12 hour time-lapse series of MTLn3 and MEF cells on 300COL substrates incubated for 1 day and also compared the fluorescent images of AP-QDs before and after the 12 hours migration (Fig. 3.6). I measured the cell migration rate and quantified the AP-QDs uptake amount in individual cells in Fig. 3.6. The R^2 before 12 hours was very low, indicating there is no correlation between AP-QD uptake and cell speed. However, after 12 hours, R^2 value became higher, indicating there is a positive but weak correlation between AP-QD uptake and cell speed (Fig. 3.7). The slope of the data after 12 hours was steeper than the slope before 12 hours, which means after 12 hours migration, the coupling between AP-QD uptake and cell speed was more dominant than the coupling before 12 hours. Additionally, the values of mean intensity/area of MTLn3 cells were higher than the values of MEF cells with the same migration speed, which indicates that MTLn3 cells are more sensitive to the phagokinetic assay than MEF cells.

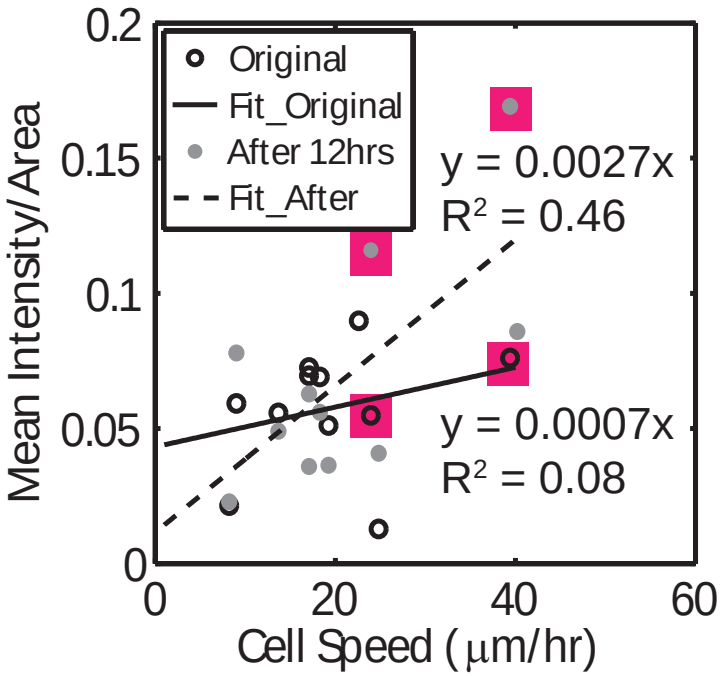

Figure 3.7 **AP-QDs uptake amount was affected by cell speed.** Correlations between mean intensity/area for individual cells and cell speed were fit with linear relationship. Cells in original images of Fig. 3.6 are white circles and were fit in black line. Cells in after 12hrs images of Fig. 3.6 are gray circles and were fit in dash line. Cells with pink background are MTLn3 cells and the others are MEF cells. The correlation curve is based on MEF and MTLn3 Cells combined.

3.4 Discussion

Invasive cancer cells have been studied most frequently in populations, not as individual cells. However, single-cell assays revealed that genetically identical cells in identical environments can display variability in drug sensitivity, cellular response and phenotype (Sorger, Niepel et al. 2009). Since cancer metastasis is caused by those fast migrating tumor cells, it is important to understand why those cells migrate faster than other cells and how this cell-to-cell variability can be predicted for future treatment of cancer metastasis. My objective was to optimize an easy way to mark or isolate the fast migrating tumor cells from other cells and then study the migration behavior of those cells. Previous research showed that the QD-based phagokinetic assay is simple and effective in discriminating between non-invasive and invasive cancer cell lines (Larabell, Pellegrino et al. 2003). After incubating on a homogenous layer of fluorescent QDs for a certain time, motile cells phagocytose enough QDs to leave behind tracks void of fluorescence. I hypothesized that the fast migrating cells phagocytose more QDs than slow migrating cells. Furthermore, I hypothesized that flow cytometry could detect fluorescence differences between fast and slow migrating cells. Several experiments were designed to test this hypothesis. However, direct results from the flow cytometry data didn′t match the hypothesis well (Fig. 3.5). While cell migration speed was the largest contributor to the QD uptake, cell area affects the uptake, too. Consequently, fluorescence must be normalized based on cell area. When this was done, a dependence of fluorescence intensity on cell migration speed could be seen, especially after long time migration for MTLn3 cells (Fig. 3.4, 3.6 and 3.7).

In order to optimize the QD uptake efficiency, it is important to select the type of QDs based on the homogeneity of the substrates. Due to the negatively charged collagen substrates and the generally negatively charged cell membranes, positively charged Lys-QDs might be better for the coating collagen and interacting with cells through electrostatic interaction. However, it is well known that negatively charged particles could also be taken up into cells through ATP-dependent pathways (Park, Nam et al. 2010). In fact many cell labeling experiments with QDs have been carried out with negatively charged particles (Parak, Pellegrino et al.

2005). I selected AP-QDs based on fluorescence intensity, however, longer excitation times could make other QDs more attractive. Therefore, a longer exposure time should be used for future experiments geared at optimizing this system. As described above conditions that generate bright and homogeneous fields should be chosen. In addition, different buffers should be more thoroughly assessed as others in the lab have shown this to dramatically affect QD aggregate size (Zhang, Haage et al. 2012). For instance, Lys and AP-QDs had the smallest size in DMEM + BSA solution, while Cys had the least aggregation in water or PBS + FBS solution. The best QD coating technique found may not be the best condition due to the limited number of experiments conducted.

From the phagokinetic trackings and the flow cytometry quantification data of MTLn3 and MEF cells, I did observe fast migrating cells with longer phagokinetic trails and higher fluorescence intensities using flow cytometry indicating higher QD uptake. However, I was not sure whether QD uptake was constant. Albrecht-Buehler studied the phagokinetic tracks of 3T3 cells using gold particles and he found that the removed particles are partly ingested, partly accumulate on the dorsal cell surface in big clumps which can be released once in a while (Guenter 1977). There is still uncertainty associated with the mechanism of uptake. This might dramatically affect the ability to correlate migration speed with QD intensity.

From the cell migration assay, I found that there is a correlation between QD uptake and cell speed. However, the relationship was not strong enough to make a solid statement. In addition, by observing the migration paths of MEF cells, I found one cell migrated very fast but didn′t leave any phagokinetic track behind it (Fig. 3.8). This might occur because the QDs adhere too tightly to the collagen substrates that the cells were not able to pull them off the surface or that they adhere too loosely and passively deadhere. Alternatively, cells might reach a point at which they are saturated with QDs and cannot phagocytose additional QDs. Consequently, the degree of QD uptake may only marginally reflect the migratory behavior of the cells. However, if this approach can be optimized in the future, cells might be sorted based on fluorescence. Then long time migration assay should be used to measure their migration rates. If the higher intensity subpopulation of cells migrated faster than the lower intensity group, the hypothesis is confirmed. Additionally, subpopulations of cells could be sorted for several

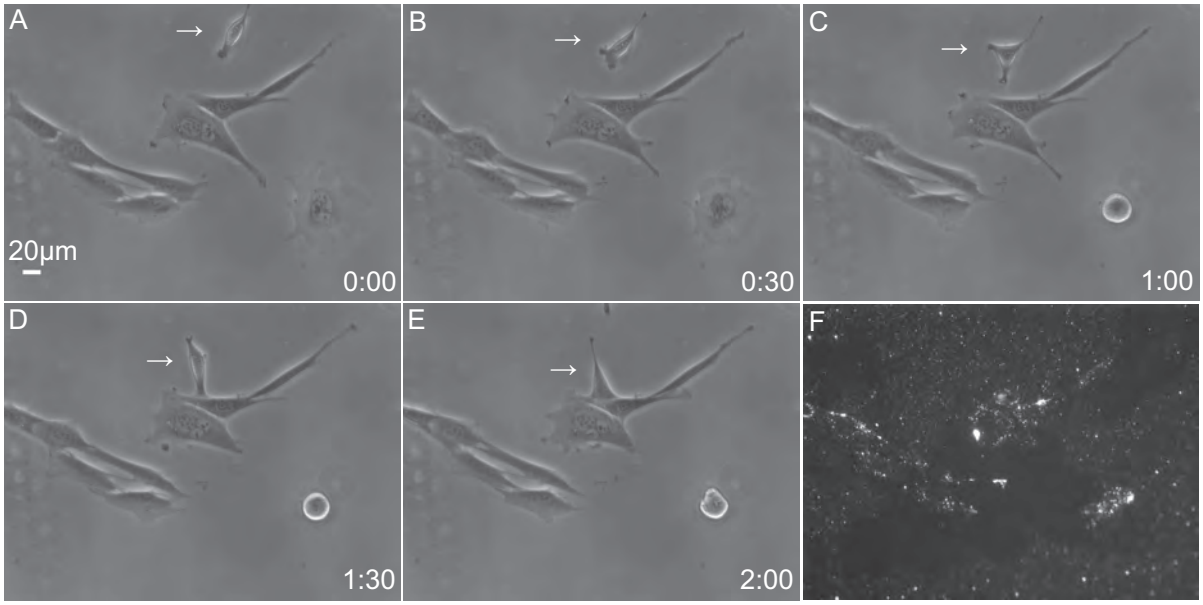

Figure 3.8 **Timelapse images of MEF cells migrating on 300COL substrates.** A-E. Time-lapse series and F. phagokinetic tracks of MEF cells migrating on 300COL substrates incubated for 1 day. Scale bar is 20μm. The time on the lower-right corner indicates hours:minutes. White arrow points to one fast migrating cell without any phagokinetic track.

generations and the speed and persistence of each subpopulation of cells could be measured. If they still exhibit large variability, then the variability comes from microenvironment factors. If the variability diminishes after separation and the genetics are stable over several generations, then the variability is controlled translationally.

3.5 Conclusions

I began to optimize a QD-based phagokinetic assay and flow cytometry as a high throughput approach to study the cell-to-cell variability in migration. By comparing different types, concentrations, buffers and coating methods of QDs, I found that 200 nM AP-QDs in DMEM with a sandwich-like incubation method was the best condition for highest intensity and most homogeneous distribution. I then studied the phagokinetic tracks of both tumor cells (MTLn3) and fibroblast cells (MEF) as well as the fluorescent intensity of each individual cell by flow cytometry. While cell migration speed was the largest contributor to the QD uptake, cell area

affects the uptake, too. Consequently, fluorescence was normalized based on cell area, so that a dependence of fluorescence intensity on cell migration speed could be seen, especially after long time migration for MTLn3 cells. Therefore, this combination of QD-based phagokinetic assay and flow cytometry is a reasonable approach to analyze cell-to-cell variability in migration, but needs more optimization.

3.6 Acknowledgements

I thank Dr. Ian C. Schneider for his guidance, patience and revision throughout this chapter; I thank Dr. Clare Waterman and Dr. Jeff Segall for providing me MEF and MTLn3 cells; Dr. Yanjie Zhang for providing me the QDs. Victor Wang and Michael Zimmerman for their help with the experiments.

3.7 References

Albrecht-Buehler, G. (1977). "Daughter 3T3 cells. Are they mirror images of each other?" The Journal of Cell Biology 72(3): 595-603.

Alivisatos, A. P., W. W. Gu, et al. (2005). Quantum dots as cellular probes. Annual Review of Biomedical Engineering. 7: 55-76.

Alivisatos, A. P., W. J. Parak, et al. (2002). "Cell motility and metastatic potential studies based on quantum dot imaging of phagokinetic tracks." Advanced Materials 14(12): 882-885.

Ando, Y. and P. J. Jensen (1993). "Epidermal growth-factor and insulin-like growth factor-I enhance keratinocyte migration." Journal of Investigative Dermatology 100(5): 633-639.

Avidan, A. and D. Oron (2008). "Large blue shift of the biexciton state in tellurium doped CdSe colloidal quantum dots." Nano Letters 8(8): 2384-2387.

Beuthan, J., C. Dressler, et al. (2004). "Laser-induced fluorescence detection of quantum dots redistributed in thermally stressed tumor cells." Laser Physics 14(2): 213-219.

Chambers, A. F., A. C. Groom, et al. (2002). "Dissemination and growth of cancer cells in metastatic sites." Nature Reviews Cancer 2(8): 563-572.

Chen, J. D., M. Helmold, et al. (1994). "Human Keratinocytes Make Uniquely Linear Phagokinetic Tracks." Dermatology 188(1): 6-12.

Dunn, G. A. (1983). "Characterising a kinesis response: time averaged measures of cell speed and directional persistence." Agents Actions Suppl 12: 14-33.

Guenter, A.-B. (1977). "The phagokinetic tracks of 3T3 cells." Cell 11(2): 395-404.

Guenter, A.-B. (1977). "Phagokinetic tracks of 3T3 cells: Parallels between the orientation of track segments and of cellular structures which contain actin or tubulin." Cell 12(2): 333-339.

Han, H. Y. and L. Huang (2010). "One-step synthesis of water-soluble ZnSe quantum dots via microwave irradiation." Materials Letters 64(9): 1099-1101.

Igarashi, Y., S. Kawa, et al. (1997). "Inhibition of chemotactic motility and trans-endothelial migration of human neutrophils by sphingosine 1-phosphate." Febs Letters 420(2-3): 196-200.

Larabell, C. A., T. Pellegrino, et al. (2003). "Quantum dot-based cell motility assay."

Differentiation 71(9-10): 542-548.

Le Gac, S. v., I. Vermes, et al. (2006). "Quantum Dots Based Probes Conjugated to Annexin V for Photostable Apoptosis Detection and Imaging." Nano Letters 6(9): 1863-1869.

Li, L. S., M. L. Mueller, et al. (2010). "Triplet States and Electronic Relaxation in Photoexcited Graphene Quantum Dots." Nano Letters 10(7): 2679-2682.

Link, A. J., K. J. Jeong, et al. (2007). "Beyond toothpicks: new methods for isolating mutant bacteria." Nat Rev Micro 5(9): 680-688.

Mcauslan, B. R. and W. Reilly (1980). "Endothelial-Cell Phagokinesis in Response to Specific Metal-Ions." Experimental Cell Research 130(1): 147-157.

Othmer, H. G., S. R. Dunbar, et al. (1988). "Models of dispersal in biological systems." J Math Biol 26(3): 263-98.

Parak, W. J., D. Gerion, et al. (2003). "Biological applications of colloidal nanocrystals." Nanotechnology 14(7): R15-R27.

Parak, W. J., T. Pellegrino, et al. (2005). "Labelling of cells with quantum dots." Nanotechnology 16(2): R9-R25.

Park, J., J. Nam, et al. (2010) "Compact and Stable Quantum Dots with Positive, Negative, or Zwitterionic Surface: Specific Cell Interactions and Non-Specific Adsorptions by the Surface Charges." Advanced Functional Materials 21(9): 1558-1566.

Park, J. W., K. C. Weng, et al. (2008). "Targeted tumor cell internalization and imaging of multifunctional quantum dot-conjugated immunoliposomes in vitro and in vivo." Nano Letters 8(9): 2851-2857.

Pellegrino, T., S. Kudera, et al. (2005). "On the development of colloidal nanoparticles towards multifunctional structures and their possible use for biological applications." Small 1(1): 48-63.

Reuning, U., S. Sperl, et al. (2003). "Urokinase-type plasminogen activator (uPA) and its receptor (uPAR): development of antagonists of uPA/uPAR interaction and their effects in vitro and in vivo." Curr Pharm Des 9(19): 1529-43.

Scott, W. N., K. McCool, et al. (2000). "Improved method for the production of gold colloid monolayers for use in the phagokinetic track assay for cell motility." Analytical Biochemistry

287(2): 343-344.

Sha, Y. L., R. C. Han, et al. (2009). "A Facile Synthesis of Small-Sized, Highly Photoluminescent, and Monodisperse CdSeS QD/SiO(2) for Live Cell Imaging." Langmuir 25(20): 12250-12255.

Sorger, P. K., M. Niepel, et al. (2009). "Non-genetic cell-to-cell variability and the consequences for pharmacology." Current Opinion in Chemical Biology 13(5-6): 556-561.

Van Orden, A., D. M. Willard, et al. (2001). "CdSe-ZnS quantum dots as resonance energy transfer donors in a model protein-protein binding assay." Nano Letters 1(9): 469-474.

Ware, M. F., A. Wells, et al. (1998). "Epidermal growth factor alters fibroblast migration speed and directional persistence reciprocally and in a matrix-dependent manner." Journal of Cell Science 111: 2423-2432.

Zhang, Y. J., A. Haage, E. M. Whitley, I. C. Schneider and A. R. Clapp (2012). "Mixed-surface, lipid-tethered quantum dots for targeting cells and tissues." Colloids and Surfaces B-Biointerfaces 94: 27-35.

CHAPTER 4. EGF, ADHESIVITY AND CONTRACTILITY INTEGRALLY MODULATE CELL MIGRATION THROUGH PROTRUSION AND FOCAL ADHESION DYNAMICS

It is well known that EGF affects the cyclic processes of migration, such as protrusion and adhesion. However, these properties are also regulated by the ability of cells to adhere to the surroundings and generate contractile force. In addition, some work indicates that down regulating adhesion might have the same effect as down regulating contractility. Consequently, adhesion and contraction can potentially modulate EGF-stimulated migration. However, it is not clear whether adhesion and contraction modulates migration through the same mechanism. Therefore, I measured EGF-stimulated cell migration speed and persistence as well as protrusion and FA properties under conditions where adhesion and contraction were altered. I found that increasing non-specific adhesion or decreasing ROCK-mediated contractility have the same effect of EGF-mediated migration. Both resulted in a decrease in migration speed, but the dose response remained biphasic. Do these perturbations affect protrusion dynamics and FA properties similarly? The answer seems no. While protrusion waves were originally thought to correlate with cell migration speed, here they do not. Increasing non-specific adhesion decreases migration speed, but dramatically increases protrusion waves, whereas decreasing contractility by blocking ROCK seems to block protrusion waves. Consequently, ROCK may be the causative agent in generating protrusion waves. Instead, FA characteristics seem to regulate migration speed as both increasing adhesion and decreasing contractility lead to more and smaller focal adhesions with longer lifetimes. Consequently, the disassembly rate, which is dependent on the FA number and is exhibited by the lifetime, might be leading to a decrease in migration speed. This shows that while perturbations might affect migration speed similarly, the regulation of subcellular properties is distinct.

4.1 Introduction

EGF stimulation is a widely used model to induce cell migration in wound healing (Segall, Tyerech et al. 1996, Wells, Gupta et al. 1998) and tumor progression (Xie, Turner et al. 1995, Turnert, Chen et al. 1996, Arteaga 2002, Wells, Kassis et al. 2002, Herbst 2004). The migration speed response to EGF is dose dependent. For example, phagokinetic assay of keratinocyte migration induced by EGF indicated that there was a 2.5 - 4.5 fold increase of migration in a log-linear manner, with a maximum concentration at 1.6 - 8 nM EGF (Ando and Jensen 1993). Joslin et al. found that the average speed of human mammary epithelial cells increased with increasing concentrations of exogenous EGF, from 0.2 to 2 nM (Joslin, Opresko et al. 2007). In other types of cells, EGF stimulation has a negative relationship with cell migration (Maheshwari, Wells et al. 1999, Maheshwari, Wiley et al. 2001). A low concentration of EGF (1.6 nM) has a stimulatory effect on trophoblast migration, whereas high concentrations of EGF (16 nM) shows an inhibitory effect (Han, Li et al.). Interestingly, EGF stimulation can also be biphasic. For example, MDA-MB-231 cells demonstrated a characteristic bell-shaped chemomigratory curve toward EGF (0.16 - 16 nM), with an optimal concentration of 1.6 nM (Price, Tiganis et al. 1999). Maheshwari et al. found that EGF can either decrease or increase fibroblast speed depending on the concentration of fibronectin surface (Maheshwari, Wells et al. 1999). Furthermore, the distribution in migration speed and persistence time appears to be dependent on EGF stimulation (Ware, Wells et al. 1998), suggesting that EGF controls not only the mean response, but also the cell-to-cell variability in response. The diversity in response to EGF at the level of cell migration speed indicates that other characteristics that define a particular cell state might modulate the response to EGF. Two of these characteristics include adhesion to the substrate, whether specific or non-specific, and contractile force generated by the cell. These regulate protrusion and focal adhesion dynamics which are determining factors that lead to migration.

Cell motility relies on underlying biophysical processes, including membrane protrusion and retraction (Zhang, Yang et al. , Chinkers, McKanna et al. 1979, Hinz, Alt et al. 1999, Maheshwari, Wells et al. 1999), as well as formation and disruption of FA organization (Han,

Li et al. , Peppelenbosch, Tertoolen et al. 1993, Segall, Tyerech et al. 1996, Harms, Bassi et al. 2005, Katz, Amit et al. 2007). Dynamics of protrusion and FAs are in turn affected by the cells ability to adhere to the surroundings and generate contractile force. The effect of EGF on protrusion is context dependent and might depend on the ECM concentration, where fractional membrane protrusion and retraction activity vary with surface fibronectin concentration in the presence of EGF but not in its absence (Maheshwari, Wells et al. 1999). The effect of EGF on FA dynamics also depends on adhesion on substrates. For example, there is a dose dependency of FA disassembly in response to decreased adhesiveness of substrates under EGF stimulation, which is mediated by Erk through calpain to promote proteolysis of FA proteins and thus drive adhesion disassembly (Xie, Pallero et al. 1998). Contraction couples adhesion and protrusion, too. Myosin II-mediated contraction drives the retrograde flow of F-actin filaments, which is a major inhibitor of protrusion (Lim, Sabouri-Ghomi et al. 2010). Myosin II-mediated periodic contraction also correlates with regeneration of lamellipodial actin, causing initiation of new adhesion sites (Giannone, Dubin-Thaler et al. 2007). Rho activates contractility through its effector, Rho kinase (ROCK), leading to subsequent phosphorylation of the regulatory chain of myosin and myosin-actin mediated contraction (Totsukawa, Yamakita et al. 2000). This Rho/ROCK-mediated contractility is involved in FA dynamics, including both the formation (Kaibuchi, Kuroda et al. 1999) and the disassembly of FAs (Lauffenburger and Horwitz 1996).

While it seems that adhesion and contraction are two sides to the same coin, is this always true? Gupton et al. found that when turning adhesion up or contraction down, both the cell migration speed and the subcellular signatures such as FA size decreased. They recapitulated fast migration of the intermediate ECM density at a higher ECM density by activating myosin II. However, they didn′t recapitulate fast migration at a lower ECM density by inhibiting myosin II activity (Gupton and Waterman-Storer 2006). Therefore, the mechanism by which changes in adhesion and contraction result in the same change in migration. In order to investigate whether adhesivity and contractility modulate EGF-mediated cell migration by the same mechanism, protrusion and adhesion dynamics were examined under those perturbations. I measured EGF-stimulated cell migration speed and persistence as well as protrusion and FA characteristics under conditions where adhesion and contraction were altered. I found that

increasing non-specific adhesion or decreasing ROCK mediated contractility have the same effect on EGF-mediated migration. Both resulted in a decrease in migration speed, but the dose response remained biphasic. While protrusion waves were originally thought to correlate with cell migration speed, here they do not. Increasing non-specific adhesion decreases migration speed, but dramatically increases protrusion waves, whereas decreasing contractility by blocking ROCK seems to block protrusion waves. Consequently, ROCK may be the causative agent in generating protrusion waves. Instead, FA characteristics seem to regulate migration speed as both increasing adhesion and decreasing contractility lead to more and smaller focal adhesions with longer lifetimes. Consequently, the disassembly rate, which is dependent on the FA number and is exhibited by the lifetime, might be leading to a decrease in migration speed.

4.2 Materials and Methods

Materials.

Cell culture media was α-MEM medium with L-glutamine (Invitrogen) containing 5% fetal bovine serum (Invitrogen) and 1% penicillin-streptomycin (Invitrogen). Collagen and poly-L-lysine (PLL) solution contained 0.3 or 3 μg/ml of rat tail collagen I (Invitrogen) and 2 μg/ml of PLL hydrochloride (Sigma), dissolved in 0.5 M acetic acid (Fisher) and sterilized under ultraviolet light for 30 minutes. Serum free imaging media was α-MEM medium without phenol red (Invitrogen) containing 1 mg/ml bovine serum albumin (Sigma), 12 mM HEPES (Fisher), and 1% penicillin-streptomycin (Invitrogen), adjusted to pH 7.4 and filtered through 0.22 μm pore size filter (Millipore, Fisher). An EGF solution containing 0.1 or 100 nM of EGF with or without 10 μM Rho kinase (ROCK) inhibitor Y-27632 (Calbiochem) was dissolved in serum free imaging media.

Cell culture.

Rat mammary adenocarcinoma cell line (metastatic MTLn3) was obtained from Dr. Jeffrey E. Segall (Albert Einstein college of Medicine). The cell line was derived from the 13762NF rat mammary adenocarcinoma tumor (Neri, Welch et al. 1982). Cells were maintained in cell culture media at 37°C in 5% CO_2 and were passed every 2 or 3 days. Collagen and PLL solution was incubated on 22 $\times$ 22 mm squeaky cleaned coverslips (Corning, Fisher) at room

temperature for 1 hour. Cells were seeded on coverslips with three types of coatings: 0.3 μg/ml of collagen (0.3COL), 3 μg/ml of collagen (3COL) and 3 μg/ml of collagen with 2 μg/ml of PLL (3COL+PLL). 50,000 - 100,000 cells per coverslip were seeded and incubated for 24 - 48 hours at 37°C in 5% CO_2.

Cell migration assay.

MTLn3 cells were incubated on coverslips with three types of substrates (0.3COL, 3COL and 3COL+PLL) for 48 hours and were switched to serum free imaging media for 2 hours. Coverslips were mounted onto glass slide chambers in serum free imaging media with different concentrations of EGF (0, 0.1and 100nM) with or without Y-27632. Chambers were maintained at 37°C for 2 hours and then imaged on a heated stage every 2 minutes for 8 hours. Phase contrast time-lapse images were captured at 10× (NA 0.30, Nikon) with a charge-coupled device (CoolSNAP HQ2, Photometrics) attached to an inverted microscope (Eclipse Ti, Nikon). Cell centroids were identified and tracked manually by MTrackJ plugins of ImageJ. Single cell instantaneous speed, S, and directional persistence time, P, were obtained by fitting these to the persistent random walk equation 4.1 (Othmer, Dunbar et al. 1988):

$$< d^2(t) >= 2S^2P[t - P(1 - e^{-t/P)}], \tag{4.1}$$

using a non-linear least squares regression analysis. The sampling time is every two minutes for 6 - 8 hours. The instantaneous speed decreased when the time lags increased from 0 to 200 minutes. I fit the model over a 30 minute time lag. To quantify protrusion rate we used a constrained optimization program to measure the protrusion and retraction rates from masked images as done previously (Machacek and Danuser 2006). The cell edge was segmented into 100 sectors. The average protrusion rate in these sectors was calculated over time.

Fluorescence imaging.

MTLn3 cells were incubated on coverslips with two types of substrates (3COL and 3COL+PLL) for 24 hours and transfected with paxillin-EGFP and Fugene 6 (Roche) according to the manufacturers protocol (6 μl of Fugene 6 and 3 μg of EGFP-paxillin). After one hour transfection, the media was changed to cell culture media and the transfected cells were maintained at 37°C in 5% CO_2 for 23 hours. Then the cells were switched to serum free imaging media for 2 hours.

Coverslips were mounted onto glass slide chambers in serum free imaging media with different concentrations of EGF (0, 0.1 and 100 nM EGF) with or without Y-27632. Chambers were maintained at 37°C for 2 hours and then imaged on a heated stage every 10 seconds for 40 - 60 minutes. TIRF images were captured at 60× oil objective (NA 1.49, Nikon) equipped with a TIRF illuminator and fiber optic-coupled laser illumination. The 488nm laser line of an air-cooled tunable Argon laser (Omnichrome Model 543-AP-A01, MellesGriot) was reflected off a dichroic mirror (89000 ET-QUAD, Chroma). Camera and shutter were controlled by μManager 1.3. An automated segmentation and tracking algorithm was utilized for large-scale analysis of FA dynamics (Wurflinger, Gamper et al. 2011). FAs smaller than 0.05 μm^2 and larger than 10 μm^2 were excluded from our analysis because they represent either FAs consisting of less than three pixels or several FAs clustered together. FA fluorescence intensities were calibrated to the standard condition of 1 mW laser power with a 300 ms exposure time, so FA intensity should be directly proportional to protein level across all samples. FA numbers of individual cells were counted at each frame and then all the FA numbers/frame for 240 - 360 frames were included in the histogram and mean value calculation. For other FA properties, such as intensity, speed, lifetime, size and elongation, properties of each FA were first averaged over 240 - 360 frames, and then all the averaged values of FA properties were included in the histogram and mean value calculation.

Statistical analysis.

To determine the statistical differences between the conditions under various EGF stimulations, a one-way analysis of variance (ANOVA) was applied to the data. The significant level is 99% for p-value = 0.01.

4.3 Results

Adhesivity and contractility modulate cell speed in response to EGF.

Cell migration plays an important role in tumor progression and I as well as others have shown that migration is altered through EGF stimulation. Along with migration speed, protrusion and focal adhesion characteristics can be altered as well. Because adhesion to the substrate and intracellular contractility represent two important processes during cell migration, I was interested in determining if altering adhesion and contraction potentiated the response to EGF. As mentioned above there is much evidence indicating that adhesion and contraction are interconnected, so it is plausible that decreasing either adhesion or contraction would have the same effect on cell migration, protrusion characteristics and focal adhesion (FA) characterics. As decribed in my previous work, the migration speed of rat adenocarcinoma cell line (MTLn3) is a biphasic function of EGF concentration, so I picked three EGF concentrations that could illustrate this behavior (0, 0.1 and 100 nM). Cells plated on substrates with optimal collagen concentration (3 μg/ml) showed a characteristic biphasic migrational response to EGF. However, when plated on substrates with less specific adhesivity, i.e. less collagen (0.3 μg/ml), the migration speed increased monotonically with EGF concentration (the blue line in Fig. 4.1A). In order to further investigate the adhesivity influence on migration response to EGF, I added a non-specific adhesive component poly-L-lysine onto the 3 μg/ml of collagen substrate and found that the biphasic response was preserved, but the migration speed decreased significantly under all conditions of EGF (the green line in Fig. 4.1A). Given that adhesivity and contractility are often interrelated, I wondered whether contractility had similar effects on migration response. I used 10 μM of Rho kinase (ROCK) inhibitor Y-27632 to inhibit Rho-mediated contractility of the MTLn3 cells on 3 μg/ml of collagen substrate. Amazingly, I found that decreasing contractility had the same response as increasing non-specific adhesion with PLL (the orange line in Fig. 4.1A). Finally, in order to see if the speed modulation by adhesion and contractility was saturated, I examined migration on the high non-specific adhesion substrate (3COL+PLL) under contractility inhibition (10 μM Y-27632). The response was similar to what was seen at lower collagen concentrations, speeds at the intermediate EGF concentrations decreased,

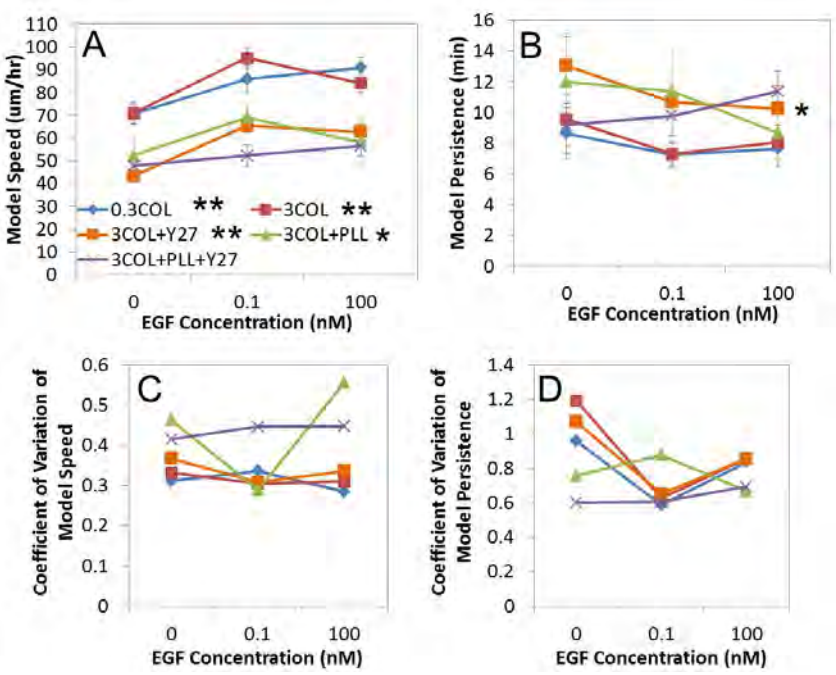

Figure 4.1 **Adhesivity and contractility modulate cell migration speed in response to EGF.** A. Speed, B. persistence time, C. coefficient of variation (CV) of speed and D. CV of persistence time for MTLn3 cells on different substrates in response to 0, 0.1 and 100 nM EGF. Blue line represents 0.3 μg/ml of collagen; red line represents 3 μg/ml of collagen; orange line represents 3 μg/ml of collagen with Y-27632; green line represents 3 μg/ml of collagen with PLL; purple line represents 3 μg/ml of collagen with PLL and Y-27632. Error bars are 95% confidence intervals. Asterisks indicate significant differences between different EGF concentrations ($**$: $p < 0.01$; $*$: $p < 0.05$). Cell numbers for 0.3COL: $N_0 = 92$, $N_{0.1} = 92$, $N_{100} = 113$; for 3COL: $N_0 = 99$, $N_{0.1} = 164$, $N_{100} = 146$; for 3COL+Y27: $N_0 = 208$, $N_{0.1} = 203$, $N_{100} = 132$; for 3COL+PLL: $N_0 = 32$, $N_{0.1} = 44$, $N_{100} = 42$; for 3COL+PLL+Y27: $N_0 = 59$, $N_{0.1} = 86$, $N_{100} = 133$.

resulting in a monotonic response (the purple line in Fig. 4.1A). Although adhesivity and contractility affected the migration speed dramatically, they had a much smaller impact on persistence. As shown in Fig. 4.1B, persistence seemed to increase when speed decreased and vice versa, however, there was no significant difference in persistence at no EGF and high concentrations of EGF. In addition, unlike what I saw previously, no changes in the cell-to-cell variability in migration speed among EGF concentrations were observed when altering either the adhesion or contraction (Fig. 4.1C and D).

Protrusion waves do not necessarily correlate with fast migration speed, but are dependent on Rho kinase.

Given that non-specific adhesion and contractility act in similar ways to alter migrational responses to EGF, I was interested in determining if this could be explained by altering a previously determined signature of fast migrating cells, protrusion waves. I assessed differences in protrusion and retraction velocities in response to EGF under four different conditions, 3 μg/ml of collagen (3COL) and 3 μg/ml of collagen adding PLL (3COL+PLL), either with (3COL+Y27 and 3COL+PLL+Y27) or without ROCK inhibitor Y-27632. By qualitatively observing the lateral protrusion/retraction waves under different treatment, it is hard to tell any difference (Fig. 4.2), so I quantified the fraction of cells with waves in response to EGF under different adhesion and contractility conditions. I found that without EGF stimulation, there were almost no waves for all substrates, whereas increasing EGF concentration often times increased the fraction of cells exhibiting wave behavior (Fig. 4.3A). Interestingly, the previous marker for fast migration, protrusion waves, seemed to not be as good of a signature as originally hypothesized. Conditions with fast migration (3 μg/mL collagen) seemed only to produce an intermediate fraction of cells with waves, whereas increasing the adhesion with PLL increased the fraction with waves and decreasing the contractility with Y-27632 decreased the faction with waves (Fig. 4.3A and B), even though both decreased the migration speed. Consequently, contractility through ROCK might be important for wave formation, but wave formation itself is not an indicator of fast migration. Furthermore, a Kolmogorov-Smirnov statistic test was used to determine which type of perturbation causes the largest difference between the distribution of protrusion velocities in response to EGF. When this statistic is large, it is more likely that there is a difference in distributions of protrusion velocities under the perturbation. On original 3COL substrate, increasing adhesivity caused larger difference than decreasing contractility and the largest difference appeared when both increasing adhesivity and decreasing contractility together (Fig. 4.3C). However, on more adhesive substrates (3COL+PLL), decreasing contractility had a more significant effect on protrusion distribution than on the original 3COL substrates (Fig. 4.3C). This data indicated that on less adhesive substrates, adhesivity plays an important role in altering protrusion dynamics, whereas on ad-

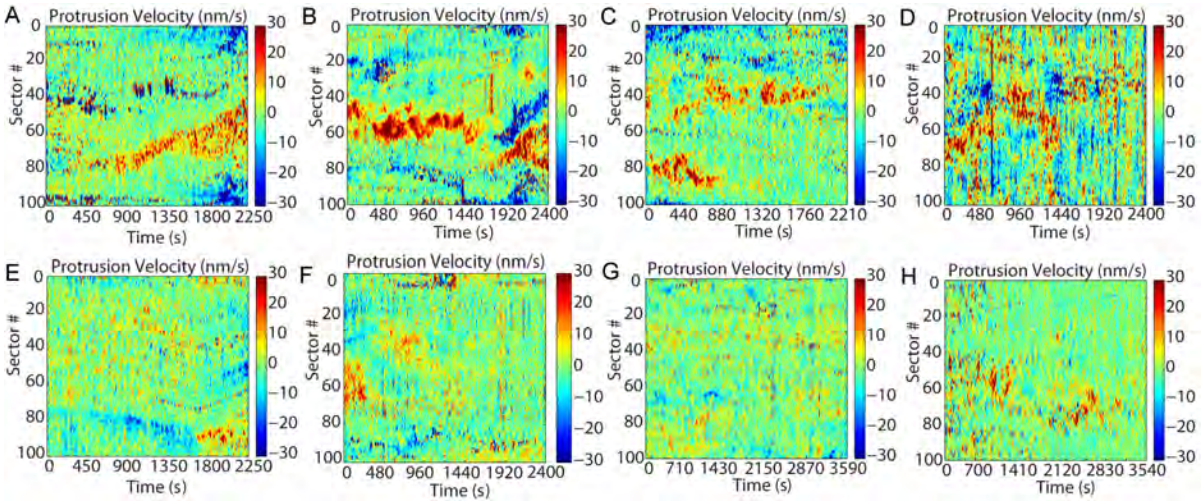

Figure 4.2 **Protrusion velocity maps of MTLn3 cells on different substrates under 0.1 nM EGF stimulation.** Protrusion with lateral waves on A. 3COL, B. 3COL+PLL, C. 3COL+Y27, D. 3COL+PLL+Y27 and protrusion without lateral waves on E. 3COL, F. 3COL+PLL, G. 3COL+Y27, H. 3COL+PLL+Y27. The cell edge was divided into 100 segments and the average protrusion rate in each segment was determined over time. Red represents fast protrusion, green represents quiescence and blue represents fast retraction.

hesive substrates, contractility has an larger impact on protrusion dynamics. EGF was also required to affect protrusion velocity because under EGF stimulation, the KS statistic values for conditions with EGF were always larger than those without EGF stimulation under both perturbations (Fig. 4.3C).

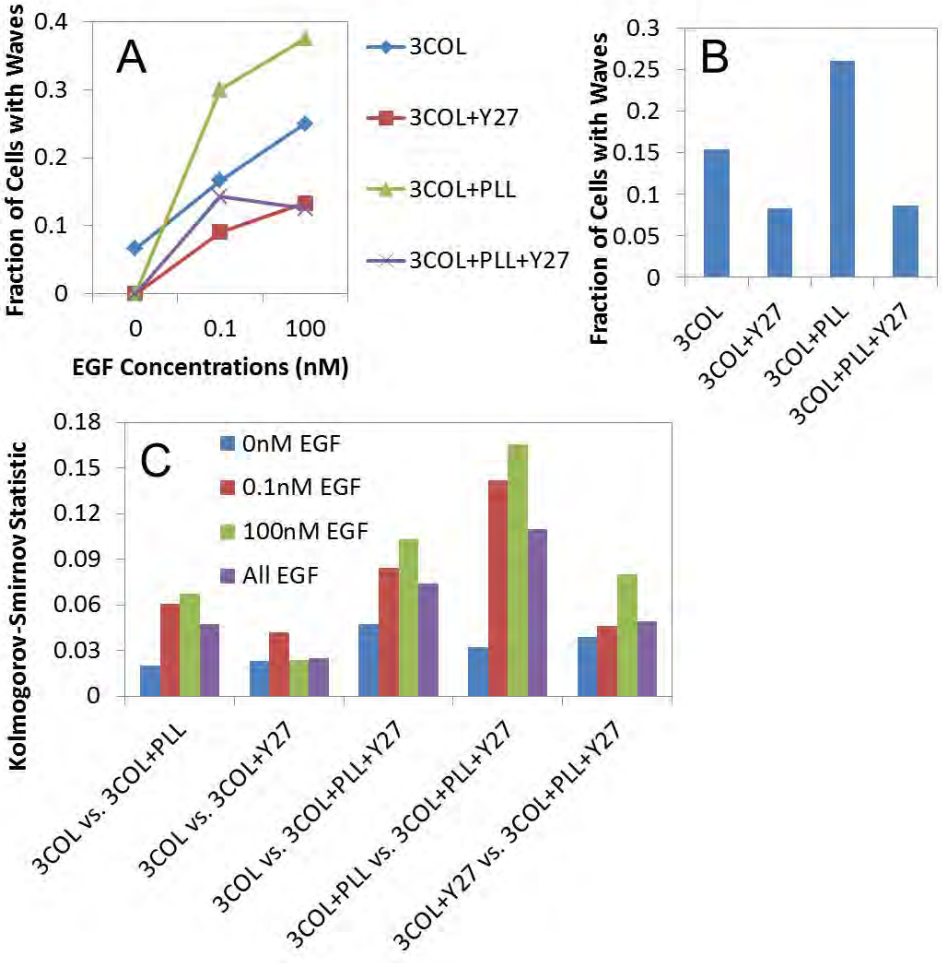

Figure 4.3 **Adhesivity and contractility affected protrusion waves differently.** A. Fraction of cells with protrusion waves on different substrates in response to EGF. Blue line represents 3 μg/ml of collagen; red line represents 3 μg/ml of collagen with Y-27632; green line represents 3 μg/ml of collagen with PLL; purple line represents 3 μg/ml of collagen with PLL and Y-27632. B. Fraction of cells with waves on different substrates under all concentrations of EGF. C. Kolmogorov-Smirnov statistic test of protrusion velocity distribution between various pertubations under different concentrations of EGF. Number of cells for different substrates: $N_{3COL,0EGF} = 15$; $N_{3COL,0.1EGF} = 12$; $N_{3COL,100EGF} = 12$; $N_{3COL+Y27,0EGF} = 10$; $N_{3COL+Y27,0.1EGF} = 11$; $N_{3COL+Y27,100EGF} = 15$; $N_{3COL+PLL,0EGF} = 5$; $N_{3COL+PLL,0.1EGF} = 10$; $N_{3COL+PLL,100EGF} = 8$; $N_{3COL+PLL+Y27,0EGF} = 8$; $N_{3COL+PLL+Y27,0.1EGF} = 7$; $N_{3COL+PLL+Y27,100EGF} = 8$.

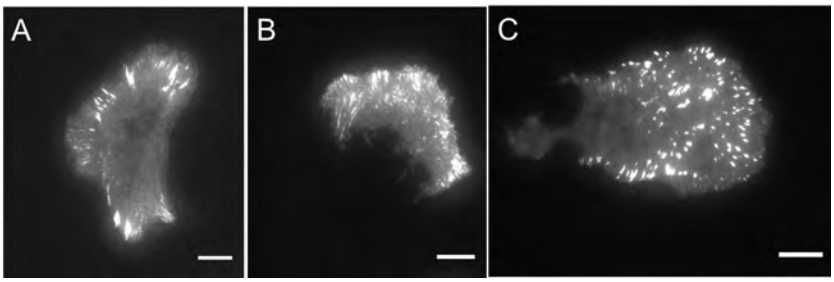

Figure 4.4 **FA morphology of MTLn3 cells on different substrates under 0.1 nM EGF.** A. 3COL, B. 3COL+PLL and C. 3COL+PLL+Y27. Scale bar is 10 μm.

Adhesivity and contractility modulate EGF-induced migration through different focal adhesion dynamics.

Given that adhesivity and contractility affected the presence of protrusion waves differently, I was interested in determining if these two perturbations affected focal adhesion (FA) characteristics differently. FA assembly, maturation and disassembly process can be quantified using several FA properties, such as FA number, size, intensity, lifetime, elongation and speed. By qualitatively observing the FA morphology under three different conditions (3COL, 3COL+PLL and 3COL+PLL+Y27) under 0.1 nM EGF stimulation, I found that increasing adhesivity and decreasing contractility increased FA number and decreased FA size (Fig. 4.4).

FA characteristics can be ordered based on the magnitude in the difference between two perturbations: increasing adhesion (3COL vs. 3COL+PLL) and decreasing contractility (3COL+PLL vs. 3COL+PLL+Y27). This magnitude was quantified by the Kolmogorov-Smirnov statistic, which is the pair-wise comparisons between 3COL and 3COL+PLL or between 3COL+PLL and 3COL+PLL+Y27 (Fig. 4.5). When this statistic is large, it is more likely that there is a difference in distributions of FA properties under the perturbation. Similar to previous results in chapter 2, FA number per cell and intensity showed the largest values for both increasing adhesion and decreasing contractility. However, adhesivity and contractility affected the FA distribution in response to EGF differently. FA number per cell and intensity showed the biphasic response to EGF when the substrate adhesivity was increased, whereas they showed the monotonic response to EGF when the contractility was decreased (Fig. 4.5). Cells on 3COL+PLL had more FAs than on 3COL substrates for all levels of EGF and cells with Y-

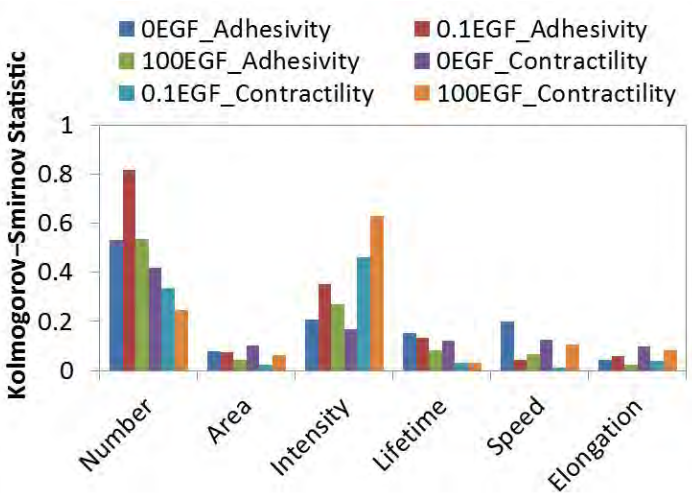

Figure 4.5 **Adhesivity and contractility modulate the distribution of FA properties in response to EGF differently.** Quantification of the distribution difference of FA properties between adhesivity and contractility perturbations under different EGF concentrations. The Kolmogorov-Smirnov statistic was the pair–wise comparisons between 3COL and 3COL+PLL (adhesivity perturbation) or between 3COL+PLL and 3COL+PLL+Y27 substrates (contractility perturbation). A larger value for the Kolmogorov-Smirnov statistic signifies a higher probability that there are differences between groups.

27632 had more FAs than without Y-27632 under EGF stimulation (Fig. 4.6A). Inhibition of contractility significantly increased FA intensity under EGF stimulation. Adhesivity affected FA intensity was more complexity. When increasing adhesivity under no and low EGF concentrations, FA intensity increased, while intensity decreased under high EGF concentration (Fig. 4.6B). In addition, both increasing adhesivity and decreasing contractility decreased FA area under EGF stimulation (Fig. 4.6C). Decreasing contractility also resulted in FAs with longer lifetime and smaller elongation (Fig. 4.6 D and F). Therefore, adhesivity and contractility also affected FA properties differently. Although both increasing adhesion and decreasing contractility generated more and smaller FAs, contraction additionally increases the FA intensity and lifetime and decreased FA elongation under EGF stimulation.

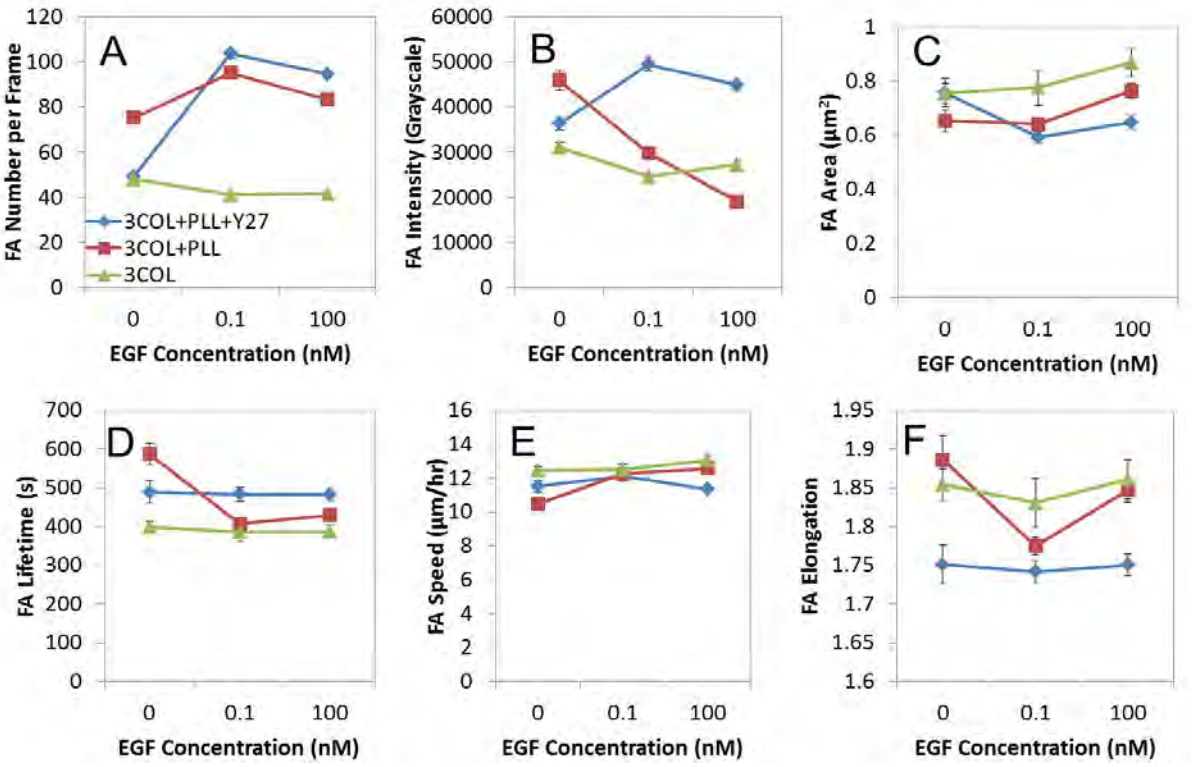

Figure 4.6 **Adhesivity and contractility modulate focal adhesion dynamics in response to EGF differently.** FA A. number per frame, B. intensity, C. area, D. lifetime, E. speed and F. elongation on different substrates under 0, 0.1 and 100 nM EGF stimulation. Blue line represents 3 μg/ml of collagen with PLL and Y-27632; red line represents 3 μg/ml of collagen with PLL; green line represents 3 μg/ml of collagen. Error bars are 95% confidence interval. Cell number for 3COL: $N_0 = 8$, $N_{0.1} = 3$, $N_{100} = 6$; for 3COL+PLL: $N_0 = 5$, $N_{0.1} = 10$, $N_{100} = 8$; for 3COL+PLL+Y27: $N_0 = 4$, $N_{0.1} = 6$, $N_{100} = 7$. FA number for number per cell on 3COL: $N_0 = 2881$, $N_{0.1} = 1309$, $N_{100} = 2049$; on 3COL+PLL: $N_0 = 1545$, $N_{0.1} = 2987$, $N_{100} = 2473$; on 3COL+PLL+Y27: $N_0 = 1434$, $N_{0.1} = 1912$, $N_{100} = 2465$. FA number for other FA properties on 3COL: $N_0 = 3386$, $N_{0.1} = 1596$, $N_{100} = 2132$; on 3COL+PLL: $N_0 = 1963$, $N_{0.1} = 7009$, $N_{100} = 4919$; on 3COL+PLL+Y27: $N_0 = 1423$, $N_{0.1} = 4067$, $N_{100} = 4795$.

4.4 Discussion

An optimal organization of actin filaments, myosin II and FAs is required for fast migration, indicating that actin filament assembly, myosin II-mediated contractile force generation and FA dynamics are interdependent functions (Gupton and Waterman-Storer 2006). The forces driving protrusion waves are generated by actin polymerization at the cell front (Pollard and Borisy 2003), while myosin II-mediated contractility causes the entire actin network to flow back and depolymerizes (Vallotton, Gupton et al. 2004). Therefore, contractility might indirectly affect protrusion through modulating the depolymerization rates of actin. For example, Myosin II-mediated contraction promotes the F-actin retrograde flow, which is a major inhibitor of protrusion (Lim, Sabouri-Ghomi et al. 2010). Evidence has been shown that both oscillating rates of actin polymerization and depolymerizaiton produce periodic contractions of the leading edge (Giannone, Dubin-Thaler et al. 2004). When inhibiting contractility through downregulation of the Rho-ROCK pathway, actin depolymerization might be inhibited, decreasing the production of free actin monomers for the generation of new actin filaments. The results showed that increasing EGF concentration often increased the fraction of cells with protrusion waves. This result seems to contradict the previous findings in chapter 2, whereas EGF stimulation had little effect upon protrusion waves. However, in chapter 2, EGF concentrations were grouped into thirds instead of two (no EGF vs. EGF). By reexamining the fraction of cells with waves between no EGF and EGF stimulation in chapter 2, the result indicated that EGF stimulation did increase the fraction of cells with protrusion waves and this enhancement was even larger than the conditions in this chapter (Fig. 4.7). Upon EGF stimulation, activated EGF receptors near the edges of the cell promote a local increase in actin polymerization sites. The new actin filaments pushes the membrane out along the substratum, resulting in the protrusion waves (Bailly, Condeelis et al. 1998). Adhesion to substrate is another promoter of protrusion waves according to my results. When increasing substrate adhesivity, there is a higher fraction of cells with protrusion waves and more FAs (Fig. 4.3 and 4.6A). These FAs might play a role in stabilizing the protrusion as well as in the control of its final shape and amplitude. However, Bailly et al. has found that EGF-stimulated lamellipods still extended

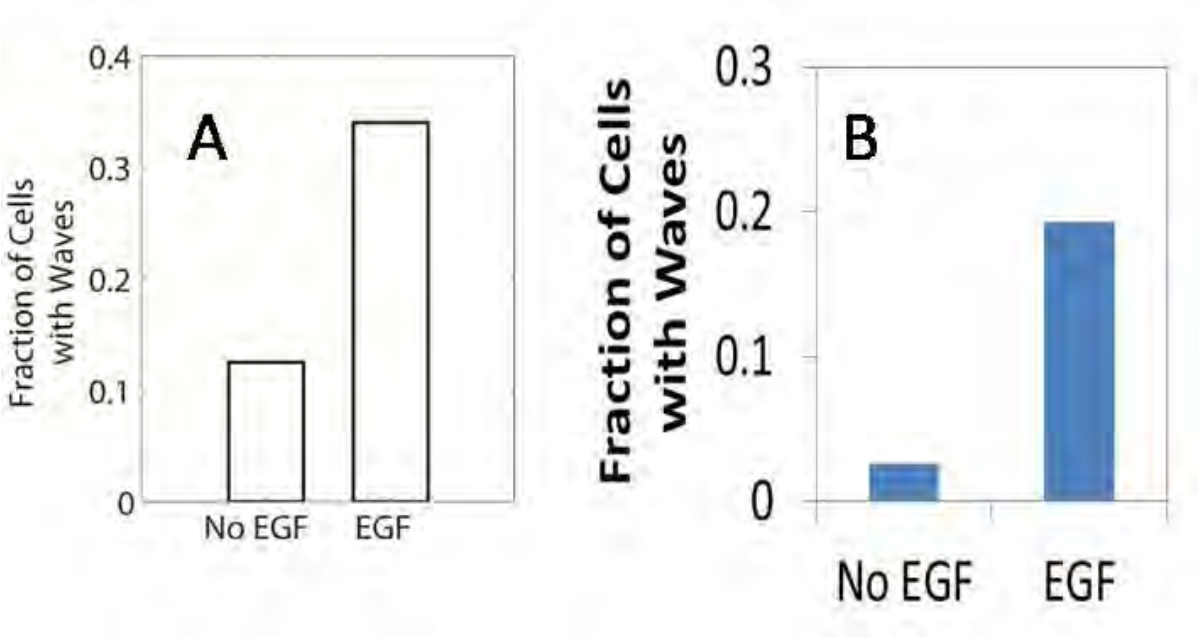

Figure 4.7 **EGF stimulation enhanced lateral protrusion waves.** A. Fraction of cells with lateral protrusion waves in chapter 2 and B. Fraction of cells with lateral protrusion waves in this chapter. $N_{A,NoEGF} = 5$; $N_{A,EGF} = 18$; $N_{B,NoEGF} = 38$; $N_{B,EGF} = 83$.

in the presence of adhesion-blocking peptides or over nonadhesive surfaces. They were slightly shorter and retracted rapidly under those conditions (Bailly, Condeelis et al. 1998). Therefore, the initial adhesivity of the substrates might only affect the shape of the outcoming protrusion rather than the presence of the waves.

Gupton et al. has described a direct relationship between adhesion strength and the total amount of FA molecules at the ventral cell surface (Gupton and Waterman-Storer 2006) and FAs are significant larger at low adhesion, which is consistent with my observation that increasing adhesivity resulted in more and smaller FAs (Fig. 4.6A). Increases in contractility may promote FA maturation and turnover by producing more contractile power than the FA can resist. Therefore, when decreasing ROCK-mediated contractility, FAs had smaller area due to the inhibition of maturation and had longer lifetime due to the inhibition of turnover (Fig. 4.6C and D). Without FA turnover, there is less retraction and the cells cannot pull the rear from the substrates, resulting in slow migration speed.

4.5 Conclusions

I measured EGF-stimulated cell migration speed and persistence as well as protrusion and FA characteristics under conditions where adhesion and contraction were altered. I found that increasing non-specific adhesion or decreasing ROCK mediated contractility have the same effect of EGF-mediated migration. Both resulted in a decrease in migration speed, but the dose response remained biphasic. While protrusion waves were originally thought to correlate with cell migration speed, here they do not. Increasing non-specific adhesion decreases migration speed, but dramatically increases protrusion waves, whereas decreasing contractility by blocking ROCK seems to block protrusion waves. Consequently, ROCK may be the causative agent in generating protrusion waves. Instead, FA characteristics seem to regulate migration speed as both increasing adhesion and decreasing contractility lead to more and smaller focal adhesions with longer lifetimes. Consequently, the disassembly rate, which is dependent on the FA number and is exhibited by the lifetime, might be leading to a decrease in migration speed.

When studying the cell migration behavior on different types of substrates, I observed that cells formed clusters with different sizes and morphology. In addition, cell clustering plays an important role in the formation of secondary tumor site and as well as dispersing cells in tissue engineered constructs. Consequently, I wanted to investigate what causes the clustering. So in chapter 5, I will show data associated with the quantification of cell clustering on different substrates as well as how the mechanism of collagen attachment to different substrates regulates clustering.

4.6 Acknowledgements

I thank Dr. Ian Schneider for his guidance and revision for this chapter; Juan Wang for her help with the experiments and data analysis for cell migration assay. I thank Dr. Antonio Sechi and Thomas Wurflinger for help with the FA analysis; Dr. Gaudenz Danuser and Shann-Ching Chen for help with the protrusion analysis and Nick Romsey for his help with the cell migration analysis.

4.7 References

Ando, Y. and P. J. Jensen (1993). "Epidermal growth-factor and insulin-like growth factor-I enhance keratinocyte migration" Journal of Investigative Dermatology 100(5): 633-639.

Arteaga, C. L. (2002). "Epidermal Growth Factor Receptor Dependence in Human Tumors: More Than Just Expression?" The Oncologist 7(suppl 4): 31-39.

Bailly, M., J. S. Condeelis and J. E. Segall (1998). "Chemoattractant-induced lamellipod extension." Microscopy Research and Technique 43(5): 433-443.

Bailly, M., L. Yan, G. M. Whitesides, J. S. Condeelis and J. E. Segall (1998). "Regulation of protrusion shape and adhesion to the substratum during chemotactic responses of mammalian carcinoma cells." Experimental Cell Research 241(2): 285-299.

Chinkers, M., J. A. McKanna and S. Cohen (1979). "Rapid induction of morphological changes in human carcinoma cells A-431 by epidermal growth factors." The Journal of Cell Biology 83(1): 260-265.

Giannone, G., B. J. Dubin-Thaler, H. G. Dobereiner, N. Kieffer, A. R. Bresnick and M. P. Sheetz (2004). "Periodic lamellipodial contractions correlate with rearward actin waves." Cell 116(3): 431-443.

Giannone, G., B. J. Dubin-Thaler, O. Rossier, Y. Cai, O. Chaga, G. Jiang, W. Beaver, H.-G. Dobereiner, Y. Freund, G. Borisy and M. P. Sheetz (2007). "Lamellipodial Actin Mechanically Links Myosin Activity with Adhesion-Site Formation." Cell 128(3): 561-575.

Gupton, S. L. and C. M. Waterman-Storer (2006). "Spatiotemporal feedback between actomyosin and focal-adhesion systems optimizes rapid cell migration." Cell 125(7): 1361-1374.

Han, J., L. Li, J. Hu, L. Yu, Y. Zheng, J. Guo, X. Zheng, P. Yi and Y. Zhou "Epidermal Growth Factor Stimulates Human Trophoblast Cell Migration through Rho A and Rho C Activation." Endocrinology 151(4): 1732-1742.

Harms, B. D., G. M. Bassi, A. R. Horwitz and D. A. Lauffenburger (2005). "Directional persistence of EGF-Induced cell migration is associated with stabilization of lamellipodial protrusions." Biophysical Journal 88(2): 1479-1488.

Herbst, R. S. (2004). "Review of epidermal growth factor receptor biology." International

Journal of Radiation Oncology Biology Physics 59(2): 21-26.

Hinz, B., W. Alt, C. Johnen, V. Herzog and H.-W. Kaiser (1999). "Quantifying Lamella Dynamics of Cultured Cells by SACED, a New Computer-Assisted Motion Analysis." Experimental Cell Research 251(1): 234-243.

Joslin, E. J., L. K. Opresko, A. Wells, H. S. Wiley and D. A. Lauffenburger (2007). "EGF-receptor-mediated mammary epithelial cell migration is driven by sustained ERK signaling from autocrine stimulation." Journal of Cell Science 120(20): 3688-3699.

Kaibuchi, K., S. Kuroda and M. Amano (1999). "Regulation of the cytoskeleton and cell adhesion by the Rho family GTPases in mammalian cells." Annu Rev Biochem 68: 459-486.

Katz, M., I. Amit, A. Citri, T. Shay, S. Carvalho, S. Lavi, F. Milanezi, L. Lyass, N. Amariglio, J. Jacob-Hirsch, N. Ben-Chetrit, G. Tarcic, M. Lindzen, R. Avraham, Y.-C. Liao, P. Trusk, A. Lyass, G. Rechavi, N. L. Spector, S. H. Lo, F. Schmitt, S. S. Bacus and Y. Yarden (2007). "A reciprocal tensin-3-cten switch mediates EGF-driven mammary cell migration." Nat Cell Biol 9(8): 961-969.

Kim, H. D., T. W. Guo, A. P. Wu, A. Wells, F. B. Gertler and D. A. Lauffenburger (2008). "Epidermal growth factor-induced enhancement of glioblastoma cell migration in 3D arises from an intrinsic increase in speed but an extrinsic matrix- and proteolysis-dependent increase in persistence." Mol Biol Cell 19(10): 4249-4259.

Lauffenburger, D. A. and A. F. Horwitz (1996). "Cell migration: A physically integrated molecular process." Cell 84(3): 359-369.

Lim, J., M. Sabouri-Ghomi, M. Machacek, C. Waterman and G. Danuser (2010). "Protrusion and actin assembly are coupled to the organization of lamellar contractile structures." Experimental Cell Research 316(13): 2027-2041.

Machacek, M. and G. Danuser (2006). "Morphodynamic profiling of protrusion phenotypes." Biophysical Journal 90(4): 1439-1452.

Maheshwari, G., A. Wells, L. G. Griffith and D. A. Lauffenburger (1999). "Biophysical integration of effects of epidermal growth factor and fibronectin on fibroblast migration." Biophysical Journal 76(5): 2814-2823.

Maheshwari, G., H. S. Wiley and D. A. Lauffenburger (2001). "Autocrine epidermal growth

factor signaling stimulates directionally persistent mammary epithelial cell migration." Journal of Cell Biology 155(7): 1123-1128.

Neri, A., D. Welch, T. Kawaguchi and G. L. Nicolson (1982). "Development and Biologic Properties of Malignant-Cell Sublines and Clones of a Spontaneously Metastasizing Rat Mammary Adenocarcinoma." Journal of the National Cancer Institute 68(3): 507-517.

Othmer, H. G., S. R. Dunbar and W. Alt (1988). "Models of dispersal in biological systems." J Math Biol 26(3): 263-298.

Peppelenbosch, M. P., L. G. J. Tertoolen, W. J. Hage and S. W. de Laat (1993). "Epidermal growth factor–induced actin remodeling is regulated by 5-lipoxygenase and cyclooxygenase products." Cell 74(3): 565-575.

Pollard, T. D. and G. G. Borisy (2003). "Cellular motility driven by assembly and disassembly of actin filaments." Cell 112(4): 453-465.

Price, J. T., T. Tiganis, A. Agarwal, D. Djakiew and E. W. Thompson (1999). "Epidermal Growth Factor Promotes MDA-MB-231 Breast Cancer Cell Migration through a Phosphatidylinositol 3-Kinase and Phospholipase C-dependent Mechanism." Cancer Research 59(21): 5475-5478.

Segall, J., S. Tyerech, L. Boselli, S. Masseling, J. Helft, A. Chan, J. Jones and J. Condeelis (1996). "EGF stimulates lamellipod extension in metastatic mammary adenocarcinoma cells by an actin-dependent mechanism." Clinical and Experimental Metastasis 14(1): 61-72.

Segall, J. E., S. Tyerech, L. Boselli, S. Masseling, J. Helft, A. Chan, J. Jones and J. Condeelis (1996). "EGF stimulates lamellipod extension in metastatic mammary adenocarcinoma cells by an actin-dependent mechanism." Clinical and Experimental Metastasis 14(1): 61-72.

Totsukawa, G., Y. Yamakita, S. Yamashiro, D. J. Hartshorne, Y. Sasaki and F. Matsumura (2000). "Distinct roles of ROCK (Rho-kinase) and MLCK in spatial regulation of MLC phosphorylation for assembly of stress fibers and focal adhesions in 3T3 fibroblasts." Journal of Cell Biology 150(4): 797-806.

Turnert, T., P. Chen, L. J. Goodly and A. Nwells (1996). "EGF receptor signaling enhances in vivo invasiveness of DU-145 human prostate carcinoma cells." Clinical and Experimental Metastasis 14(4): 409-418.

Vallotton, P., S. L. Gupton, C. M. Waterman-Storer and G. Danuser (2004). "Simultaneous mapping of filamentous actin flow and turnover in migrating cells by quantitative fluorescent speckle microscopy." Proceedings of the National Academy of Sciences of the United States of America 101(26): 9660-9665.

Ware, M. F., A. Wells and D. A. Lauffenburger (1998). "Epidermal growth factor alters fibroblast migration speed and directional persistence reciprocally and in a matrix-dependent manner." Journal of Cell Science 111: 2423-2432.

Wells, A., K. Gupta, P. Chang, S. Swindle, A. Glading and H. Shiraha (1998). "Epidermal growth factor receptor-mediated motility in fibroblasts." Microscopy Research and Technique 43(5): 395-411.

Wells, A., J. Kassis, J. Solava, T. Turner and D. A. Lauffenburger (2002). "Growth Factor-Induced Cell Motility in Tumor Invasion." Acta Oncologica 41(2): 124-130.

Wurflinger, T., I. Gamper, T. Aach and A. S. Sechi (2011). "Automated segmentation and tracking for large-scale analysis of focal adhesion dynamics." Journal of Microscopy 241(1): 37-53.

Xie, H., M. A. Pallero, K. Gupta, P. Chang, M. F. Ware, W. Witke, D. J. Kwiatkowski, D. A. Lauffenburger, J. E. Murphy-Ullrich and A. Wells (1998). "EGF receptor regulation of cell motility: EGF induces disassembly of focal adhesions independently of the motility-associated PLC gamma signaling pathway." Journal of Cell Science 111: 615-624.

Xie, H., T. Turner, M.-H. Wang, R. K. Singh, G. P. Siegal and A. Wells (1995). "In vitro invasiveness of DU-145 human prostate carcinoma cells is modulated by EGF receptor-mediated signals." Clinical and Experimental Metastasis 13(6): 407-419.

Zhang, F., H. Yang, Z. Pan, Z. Wang, J. M. Wolosin, P. Gjorstrup and P. S. Reinach "Dependence of Resolvin-Induced Increases in Corneal Epithelial Cell Migration on EGF Receptor Transactivation." Investigative Ophthalmology and Visual Science 51(11): 5601-5609.

CHAPTER 5. COLLAGEN ATTACHMENT TO SUBSTRATES CONTROLS CELL CLUSTERING THROUGH MIGRATION

This chapter was modified from the paper submitted to *Biophysical Journal*.

Yue Hou, Laura Lara Rodriguez, Juan Wang, Ian C Schneider

Cell clustering and scattering play important roles in cancer progression and tissue engineering. While the extracellular matrix (ECM) is known to control cell clustering, much of the quantitative work has focused on the analysis of clustering between cells with strong cell-cell junctions. Much less is known about how the ECM regulates cells with weak cell-cell contact. Clustering characteristics were quantified in rat adenocarcinoma cells, which form clusters on physically adsorbed collagen substrates, but not on covalently attached collagen substrates. Covalently attaching collagen allowed for higher initial collagen surface coverage and decreased desorption of collagen. This lower initial density of collagen as well as its decrease over time with physically adsorption resulted in more clustering. While changes in proliferation rate could not explain differences seen in the clustering, changes in cell speed and persistence could. Cells plated under conditions that resulted in more clustering had a lower persistence time and slower migration rate than those under conditions that resulted in less clustering. In addition, the use of a scaling model showed that quantitative changes in migration speed explain quantitative changes in clustering. Understanding how the ECM regulates clustering will not only impact the fundamental understanding of cancer progression, but also will guide the design of tissue engineered constructs that require either the clustering or dissemination of cells in the construct.

5.1 Introduction

Tissues reorganize continuously by disassembling and assembling cellular structures. The disassembly process is often referred to as scattering and describes the well-studied epithelial to mesenchymal (EMT) transition (Thiery, Acloque et al. 2009). The assembly process is often referred to as aggregation or clustering. Both cell scattering and clustering play important roles in pathologies like cancer metastasis (Hanahan and Weinberg 2000), but also in regenerative medicine and tissue engineering (Sasai 2013). In carcinomas, the primary tumor develops as cluster of cells from an epithelial layer, where cells are attached. Mutations in oncogenes disrupt cell-cell adhesion (Ma, Maulik et al. 2003), causing cells to break off the primary tumor as single cells or clusters, metastasize to distant organs and form nascent secondary tumors (Hanahan and Weinberg 2000). Clustering during metastasis might also be advantageous. For example, squamous cell carcinomas can escape apoptosis by forming multicellular clusters (Zhang, Lu et al. 2004, Zhang, Xu et al. 2010). Some cancer cells also undergo EMT, where epithelial cells lose polarity and diminish cell-cell adhesion, and gain migratory and invasive properties of mesenchymal cells (Vincent-Salomon and Thiery 2003). In addition to pathological *in vivo* environments, engineered environments must be able to orchestrate cell scattering and clustering during the formation of functional tissues (Sasai 2013). Many types of cells are known to self-assemble into organ-like structures in engineered environments outside of the body (Moscona and Moscona 1952, Giudice 1962, Wei, Larsen et al. 2007). For instance, mouse embryonic cells from submandibular gland can assemble into branched structures that resemble salivary gland buds *in vitro* (Wei, Larsen et al. 2007). While cell clustering is desired for certain specific tissue engineering applications, other applications require limiting cell clustering, particularly in the case of stem cell expansion (Ferrari, Balandras et al. 2012). Understanding the signals that contribute to scattering and clustering will not only provide therapeutic targets for pathologies, but also will guide the design of engineered tissue environments that can regulate the degree of cell scattering and clustering.

In the most general sense, scattering is the process by which cells transit from a state of close proximity to state where cells are well-dispersed. In most studies, the cells in close

proximity form cell-cell junctions, so scattering is described as a disassembly process that includes loss of cell-cell junctions (Thiery, Acloque et al. 2009). This type of scattering can proceed either through transcriptional control, usually by altering the expression of the cell-cell adhesion molecule E-cadherin (Guaita, Puig et al. 2002, Grotegut, von Schweinitz et al. 2006), or through signaling (Boyer, Roche et al. 1997, Khwaja, Lehmann et al. 1998) or cytoskeletal (Ryan, Foty et al. 2001, de Rooij, Kerstens et al. 2005) events upstream of transcription, usually by altering the relative magnitudes of the cell-cell or cell-substrate adhesion forces. Numerous extracellular ligands such as hepatocyte growth factor (Montesano, Matsumoto et al. 1991) or epidermal growth factor (Boyer, Roche et al. 1997, Pope, Graham et al. 2008) can induce scattering. Clustering, on the other hand, is the process by which cells transit from a well-dispersed state to a state of close proximity. Cell clustering can be induced by extracellular ligands like insulin like growth factor (Guvakova and Surmacz 1997). Again, in most studies the cells in close proximity form cell-cell junctions, so clustering is described as an assembly process that includes formation of cell-cell junctions. When cell-cell adhesion is significant and in the absence of proliferation, the assembly of clusters can result either from random migration (de la Rosa, Yanez-Mo et al. 2005, Mina-Osorio, Shapiro et al. 2006, Wei, Larsen et al. 2007, Gassei, Ehmcke et al. 2008, Pope and Asthagiri 2012) or paracrine-mediated directed migration (Silver and Montell 2001, Hardikar, Marcus-Samuels et al. 2003). Both induce cell-cell contact and cluster formation when cells collide (Kudo, Kigoshi et al. 2009). In the presence of proliferation, the continual division of well-attached daughter cells can also act to enhance clustering (Andl, Mizushima et al. 2003). When cell-cell adhesion is insignificant, the mechanisms are somewhat different. The only routes for cell clustering are proliferation coupled with slow migration (Wu, Yu et al. 2013) or paracrine-mediated attraction of cells.

Since migration, cell-substrate adhesion and perhaps proliferation are important processes in the disassembly and assembly of cell clusters, the ECM plays a role in regulating scattering and clustering (de Rooij, Kerstens et al. 2005, Shields, Dangi-Garimella et al. 2011, Pope and Asthagiri 2012, Shields, Krantz et al. 2012). The ECM determines the speed and persistence of cell migration which can act to cluster cells (Pope and Asthagiri 2012). It also sets the cell-substrate adhesive force, so the type of the ECM ligand and its mechanical stiffness are

important regulators of cell scattering (de Rooij, Kerstens et al. 2005, Gilchrist, Darling et al. 2011). For example, epithelial cell scattering is enhanced on collagen and fibronectin, as compared with laminin I and rigid substrates that produce high traction forces promoted scattering, in comparison to more compliant substrates (de Rooij, Kerstens et al. 2005). In addition, cell clustering is also enhanced in environments where cells can exert large contractile forces (Salmenpera, Kankuri et al. 2008, Rhee, Ho et al. 2010, da Rocha-Azevedo, Ho et al. 2013). These contractile forces coupled with matrix degradation act to remodel the ECM (Xu, Boudreau et al. 2009), which in turn can either enhance scattering or clustering.

While there have been several recent quantitative efforts made to characterize scattering and clustering on different ECM (de Rooij, Kerstens et al. 2005, Pope and Asthagiri 2012), this has mainly focused on cells that can generate strong cell-cell junctions. I was interested in probing mechanisms that lead to the clustering of cells that lack robust cell-cell junctions. Therefore, I constructed four types of substrates that varied in the way in which collagen was attached to the surface and in their adhesivity. A rat adenocarcinoma cell line (MTLn3) was used as a model system to study scattering and clustering in cells that lack strong cell-cell adhesion. I developed a method to quantify the clustering and found higher clustering on physically adsorbed collagen substrates than on covalently attached substrates. Higher clustering correlated with substrates that were initially lower in collagen density and that showed larger rates of collagen cleavage or desorption from the surface. No significant difference in cell proliferation was observed between the conditions. However, cell migration was enhanced on collagen that was covalently attached to the surface. This indicates that the attachment mechanism of collagen can alter the clustering behavior of cells by regulating the migration rate. This has importance in understanding how matrix remodeling might alter clustering *in vivo*, but also how the immobilization of ECM in engineered constructs is a critical factor in disseminating cells across a surface or throughout a matrix.

5.2 Materials and Methods

Materials:

Cell culture media was MEMα medium (Life Technologies, Grand Island, NY, USA) con-

taining 5 % fetal bovine serum (Life Technologies, Grand Island, NY, USA) and 1 % penicillin-streptomycin(Life Technologies, Grand Island, NY, USA). Collagen (Col) and poly-L-lysine (PLL) solution contained 1.8 μg/mL of rat tail collagen I (Life Technologies, Grand Island, NY, USA) and 2 μg/mL of PLL hydrochloride (Sigma-Aldrich, St. Louis, MO, USA) and was dissolved in UV-sterilized 0.5 M acetic acid (Fisher Scientific, Hampton, New Hampshire, USA). Imaging media was MEMα medium without phenol red containing 5 % fetal bovine serum, 1 % penicillin-streptomycin, and 12 mM HEPES (Fisher Scientific, Hampton, New Hampshire, USA). The matrix metalloproteinase inhibitor, GM-6001 (Calbiochem, EMD Millipore Corporation, Billerica, MA, USA) was prepared at 0.25 μM, dissolved in Dulbecco's Phosphate-Buffered Saline (DPBS) with calcium and magnesium (Life Technologies, Grand Island, NY, USA).

Collagen Substrates Treatment:

No. 1.5, 22 mm square coverslips (Corning Inc., Corning, New York, USA) were sonicated 30 minutes in the following solutions to make squeaky cleaned coverslips: hot tap water with Versa Clean detergent (Fisher Scientific, Hampton, New Hampshire, USA), hot tap water, distilled water, double distilled water, 1 mM ethylenediaminetetraacetic acid (EDTA) solution (Fisher Scientific, Hampton, New Hampshire, USA), 70% ethanol in water and 100% ethanol. An adaptation of a protocol to functionalize coverslips with glutaraldehyde was used (Branch, Corey et al. 1998). Cleaned coverslips were soaked in a 3:1 sulfuric acid (Fisher Scientific, Hampton, New Hampshire, USA):30% hydrogen peroxide (Fisher Scientific, Hampton, New Hampshire, USA) solution for one hour, washed with double distilled water and placed in 10 mL of 1% aminopropyltriethylsilane (APTES) (Fisher Scientific, Hampton, New Hampshire, USA) in 10 mM acetic acid for two hours. They were then rinsed with double distilled water, spin dried and heat-treated in an oven at 100°C for one hour. Finally, the coverslips were treated with 5 mL of 6% glutaraldehyde (Fisher Scientific, Hampton, New Hampshire, USA) in phosphate buffered saline (PBS) without calcium and magnesium (Gibco, Grand Island, New York, USA) for two hours. The functionalized coverslips were stored in double distilled water at 4°C until use. A 1.8 μg/mL Col solution with or without 2 μg/mL PLL was added onto a 35 mm cell culture dish (Fisher Scientific, Hampton, New Hampshire, USA) and covered either by

a cleaned coverslip or a functionalized coverslip. Alternatively, collagen was printed onto the surface. Polydimethylsiloxane (PDMS) stamps were made via soft lithography by mixing 184 Silicone Elastomer Base (Dow Corning) with its curing agent in a 10:1 weight ratio and then allowing it to spread on top of a fused silica master. The master coated with PDMS was exposed to a vacuum to remove any air pockets and then cured for an hour at 60°C. PDMS stamps were sonicated in double distilled water and in 100% ethanol. A 200 μL collagen solution of 45 μg/mL collagen I and 15 μg/mL alexa 555-labeled collagen I in 0.5 M acetic acid was applied to each stamp. After 40 min incubation, the collagen solution was removed and then the stamp was placed on the functionalized coverslip and allowed to incubate for 15 minutes. Later, the stamp was removed and the coverslips were incubated in the dark for 2 hours. Before seeding MTLn3 cells, the coverslips were washed with PBS.

Cell Culture:

Rat mammary adenocarcinoma cell line (MTLn3) was obtained from Dr. Jeffrey E. Segall (Albert Einstein College of Medicine). Cells were maintained in cell culture media at 37°C in 5 % CO_2 and were passed every two or three days.

Clustering Assay:

MTLn3 cells between passage 2 and 20 were seeded onto Phys-COL or Cov-COL substrates in 35 mm cell culture dishes at an approximate density of 50,000 cells per dish and maintained in cell culture media at 37°C in 5 % CO2. Dishes with cells were imaged every 8 hours from 0 hour to 48 hours. Phase contrast images were captured at 10× magnification (NA 0.30, Nikon) with a charge-coupled device (CoolSNAP HQ2, Photometrics) attached to an inverted microscope (Eclipse Ti, Nikon). Cell centroids were identified manually by MTrackJ plugins of ImageJ. Quantification of clustering was analyzed by MATLAB. Briefly, if the centroid of a cell was 26 μm further from other centroids, this cell was defined as single cell and its centroid was deleted from the centroid matrix. Then the clusters were identified using the `kmeans` function in MATLAB. Cluster number was determined by an iteration process. The percentage of

variance is governed by the following equation 5.1:

$$\%Var = 1 - \frac{\frac{\sum_{i=1}^{N_{cell}} D^2_{i,cell-cluster}}{N_{cell}}}{\frac{\sum_{j=1}^{N_{cell}} \sum_{k=1}^{N_{cell}} D^2_{jk,cell-cell}}{N^2_{cell}}} \tag{5.1}$$

Where $D_{cell-cluster}$ is the within-cluster sums of point-to-cluster-centroid distances; N_{cell} is the number of cells in each image; $D_{cell-cell}$ is the pair-wise distance between individual cells. Cluster number was tested from two to N_{cell} and the percentage of variance was calculated. When the percentage of variance reached 0.995, the iteration stopped and that cluster number was the set as the final cluster number. The decay distance and scatter index of cells and clusters were calculated using the MATLAB function `rdfcalc` (from GUI: Radial Distribution Function, File ID: #31494, File exchange, MATLAB CENTRAL). The area under the RDF curve is the scatter index (SI) defined as equation 5.2:

$$SI = \frac{\sum_i g_i(r) r_i}{\sum_i g_i(r)} \tag{5.2}$$

The decay distance ($R_{1/2max}$) is the distance where the probability equals the half height of the peak. The cell number in clusters and percentage of cells in clusters were quantified based on the identified clusters and total cell number.

Collagen Degradation and Uptake Assay:

Collagen was labeled using Alexa Fluor 555 carboxylic acid, succinimidyl ester (Life Technologies, Grand Island, NY, USA) as before (Nicholas R. Romsey, submitted) and was attached to the surface at a concentration of 1.8 μg/mL. For substrates with cells, MTLn3 cells in imaging media were then flowed into this chamber at an approximate density of 25,000 cells per coverslip. For substrates with cells plus GM-6001, 0.25 μM GM-6001 solution was added into the chamber. For substrates without cells, only the imaging media was flowed into the chamber. The chambers were then sealed with VaLaP and imaged on a heated stage. For the degradation assay, differential interference contrast (DIC) images were captured at 0, 6 and 21 hours using a 40× oil objective (NA 1.30, Nikon, Melville, NY, USA) using the same imaging system as mentioned above. Epifluorescence (EPI) images were captured at 0, 6 and 21 hours using a 40×

oil objective with an excitation filter 555/25 and an emission filter 605/52. The fluorescence intensity of the whole image was quantified using ImageJ. For the uptake assay, MTLn3 cells were incubated for 6 hrs in cell culture media at 37°C in 5 % CO_2, mounted into the chambers and time lapse images were taken using a 40× oil objective with the same imaging system as mentioned above. DIC images were captured every two minutes, while EPI images were taken every two hours. The cells were manually selected according to the DIC images and then the fluorescent intensity of the cells was quantified based on the EPI images using ImageJ.

Cell migration assay:

The cell migration assay was performed based on the previous work (Hou, Hedberg et al. 2012). Briefly, MTLn3 cells were incubated on collagen substrates for 6 hrs and were mounted into perfusion chambers (Warner Instruments, Hamden, CT, USA) in imaging media. Chambers were imaged on an automated heating stage every 2 minutes for 12 hours. Phase contrast images were captured at 10× objective (NA 0.30, Nikon) with a charge-coupled device (CoolSNAP HQ2, Photometrics) attached to an inverted microscope (Eclipse Ti, Nikon). Cell centroids were identified manually by MTrackJ plugins of ImageJ. Model speed, S, and model persistence time, P, of single cell were obtained by fitting these to the persistence random walk equation 5.3 (Dunn 1983, Othmer, Dunbar et al. 1988):

$$< d^2(t) >= 2S^2P[t - P(1 - e^{-t/P)}], \tag{5.3}$$

using a nonlinear least square regression analysis. I fit the model over a 30 minute time lag.

5.3 Results

Mechanism of collagen attachment regulates cell clustering

Collagen is a large charged protein that can physically adsorb to bare glass surfaces (Phys-COL) or covalently react with functionalized glass surfaces (Cov-COL). Both approaches are used to render substrates adhesive towards cells. I observed that these different collagen attachment mechanisms altered the clustering behavior of a rat adenocarcinoma cell line (MTLn3). MTLn3 cells adhered to Phys-COL substrates and formed noticeable clusters after 8 hrs. (Fig. 5.1A), whereas those adhered to Cov-COL substrates did not cluster (Fig. 5.1B). Interestingly,

this clustering was not due to cell-cell contact as in other epithelial cells, because MTLn3 cells are highly metastatic and do not form cell-cell contacts. I was interested in quantifying the clustering, so I logged the position of the nucleus of each cell and used a *k-means* clustering algorithm outlined in the materials and methods to identify the clusters (Fig. 5.2A and B). From this position data, a radial distribution function (RDF) was calculated (Fig. 5.2C). The RDF describes the probability of finding a cell at a distance from a given reference cell. This quantitative clustering approach formed the basis of my analysis. Different parameters, such as scatter index (SI) and decay distance ($R_{1/2max}$) were analyzed from the RDF to characterize the clustering behavior (Fig. 5.2C). Larger SI and $R_{1/2max}$ values indicate more scattered and less clustered cells.

Since cells were less clustered on Cov-COL surface, but appeared to spread more quickly (Fig. 5.1), I decided to examine whether the clusters were caused by differences in adhesivity of the substrate. Therefore, I added an adhesive component, poly-L-lysine (PLL), to both substrates and observed cell morphology on four different substrates: Phys-COL, Cov-COL, Phys-COL+PLL and Cov-COL+PLL (Fig. 5.3). No large difference in cell spreading area was seen (Fig. 5.4). Cells on Phys-COL substrates had tighter clusters and were less spread than cells on Cov-COL substrates (Fig. 5.3). The PLL treatment only marginally altered the clustering (Fig. 5.3). In order to support these qualitative observations, I quantitatively analyzed the clustering behavior using the metrics described above.

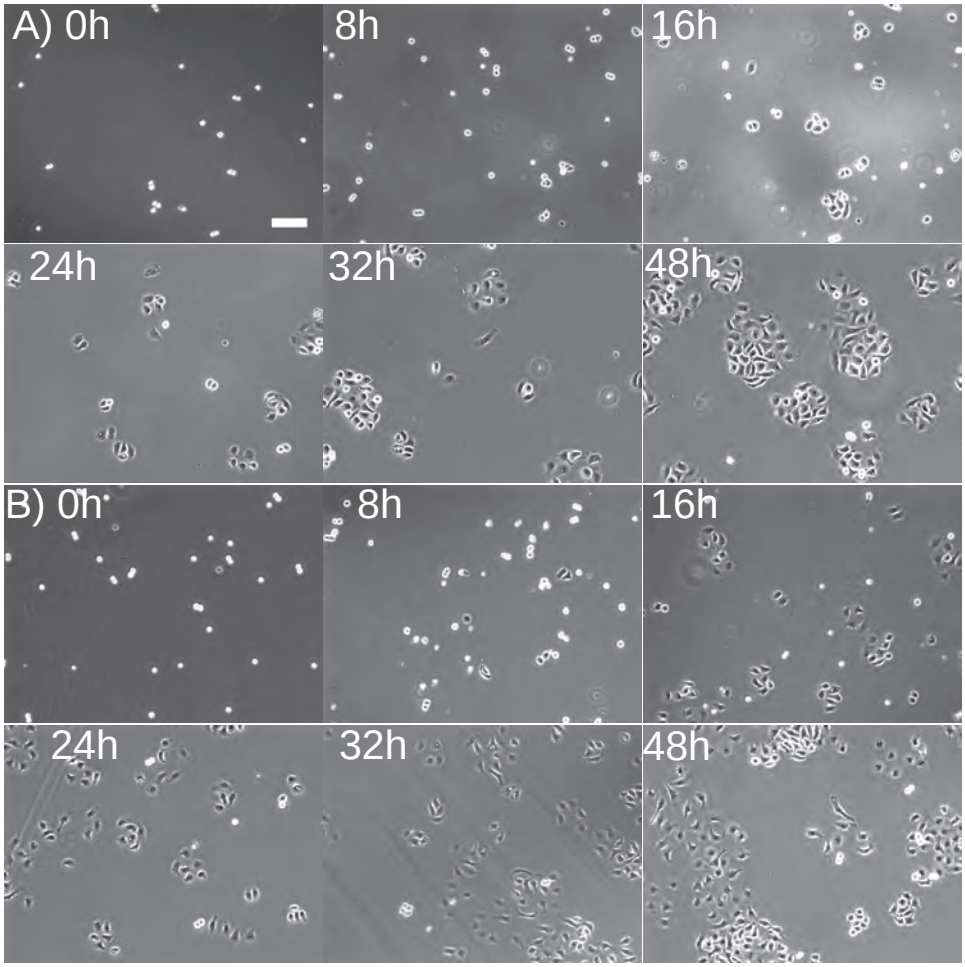

Figure 5.1 **Attachment mechanism of collagen produces differences in clustering in MTLn3 cells.** A) Phys-COL and B) Cov-COL substrates. Cells were imaged after incubation for 0, 8, 16, 24, 32 and 48 hrs in 5% serum α-MEM medium. Scale bar is 100 μm.

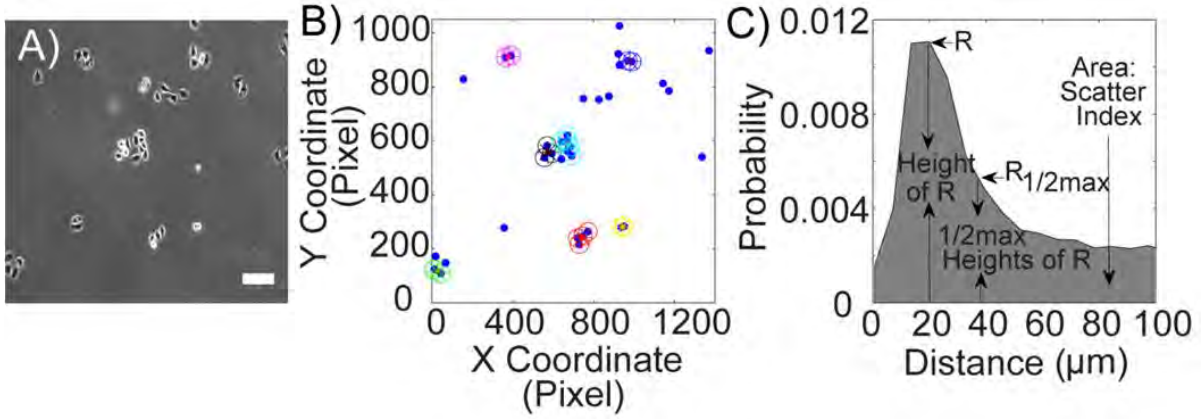

Figure 5.2 **Schematic illustrating cluster analysis.** A) Original phase contrast image, B) plot of cell and cluster positions, and C) plot of radial distribution function (RDF) showing decay distance ($R_{1/2max}$) and the area under the curve (Scatter Index (SI)). The blue dots in B) represent the centroids of cells in A) and the circles in B) represent the cells in a cluster. The asterisks in B) represent the centroids of clusters. Each color represents a cluster. Scale bar is 100 μm.

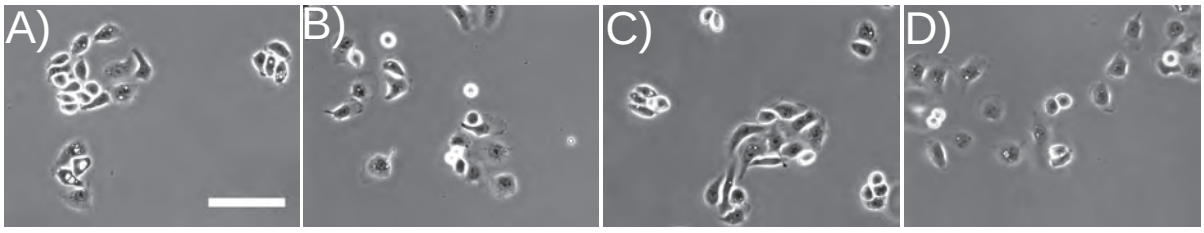

Figure 5.3 **PLL does not dramatically affect clustering on different substrates.** A) Phys-COL, B) Cov-COL, C) Phys-COL+PLL and D) Cov-COL+PLL. Cells were imaged after incubation for 24 hrs in 5% serum MEM α medium. Scale bar is 100 μm.

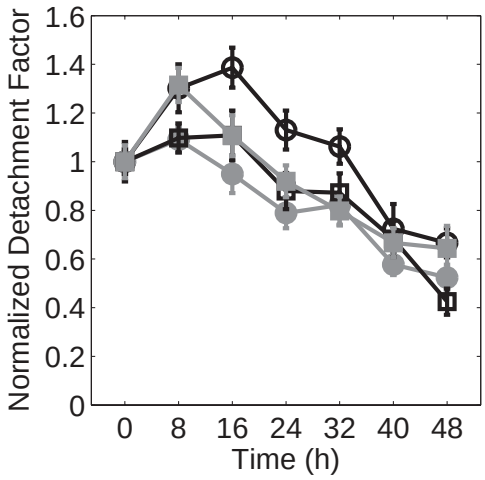

Figure 5.4 **Quantification of cell spreading on different substrates.** Normalized detachment factor per cell was the total areas of the unspread cells divided by the total cell number. The blank circle line represents Phys-COL. The filled circle line represents Cov-COL. The blank square line represents Phys-COL+PLL. The filled square line represents Cov-COL+PLL. Error bars are 95% confidence intervals.

To quantify the clustering behavior on the four different substrates, I measured the *SI* of cells, normalized *SI* of cells, *SI* of clusters, $R_{1/2max}$, cell number in clusters, percentage of cells in clusters, RDF of cells and RDF of clusters over time (Fig. 5.5, 5.6 and 5.7). Clear differences were seen. Cells on substrates with covalently attached collagen produced larger *SI* values than those on substrates with adsorbed collagen (Fig. 5.5A). In addition, the *SI* values increased over time and above what was seen initially when collagen was covalently attached (Fig. 5.5B). While PLL addition to physically adsorbed collagen substrates did increase the scattering above that seen with collagen alone, it did not reach the same level as that seen when collagen was covalently attached to the substrate (Fig. 5.5A). However, while there was a noticeable difference in the SI value of cells among the different substrates, there was no significant difference in the *SI* value of clusters among the different substrates (Fig. 5.5C), suggesting that the distances between neighboring clusters changed in a similar manner. Enhanced clustering on physically adsorbed collagen also resulted in smaller values of $R_{1/2max}$ (Fig. 5.5D) and a larger mean cell number in clusters (Fig. 5.5E). Finally, the most dramatic difference was seen in the percentage of cells that existed in clusters. After 8 hrs, the percentage of cells in clusters on covalently attached collagen decreased by roughly 50% over the next 16 hrs., whereas the

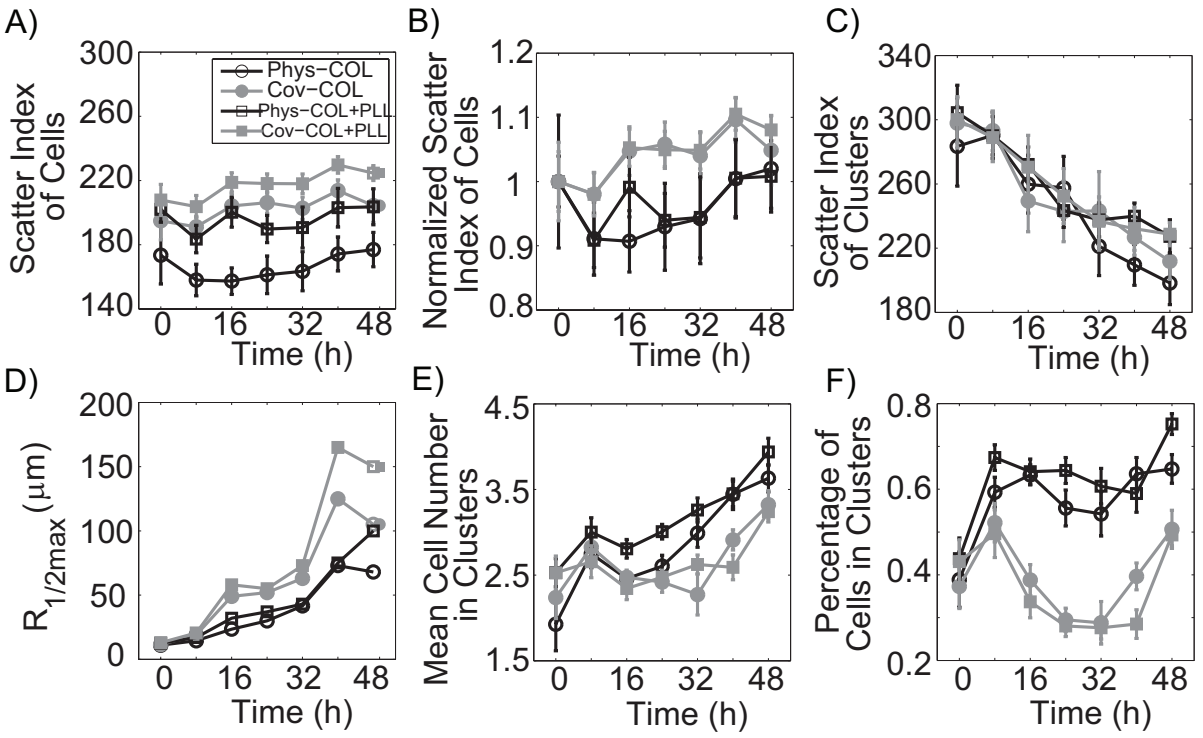

Figure 5.5 **Quantification of cell clustering over time on different substrates.** A) Scatter Index (SI) of cells, B) normalized SI of cells, C) SI of clusters, D) decay distance ($R_{1/2max}$), E) mean cell number in clusters and F) percentage of cells in clusters. The black open circle represents Phys-COL. The gray filled circle represents Cov-COL. The black open square represents Phys-COL+PLL. The gray filled square represents Cov-COL+PLL. Error bars are 95% confidence intervals.

percentage of cells in clusters on physically adsorbed collagen remained constant (Fig. 5.5F). These data suggest that the largest effect on clustering was the mechanism of attachment of collagen, with a smaller effect due to non-specific adhesivity of the substrate.

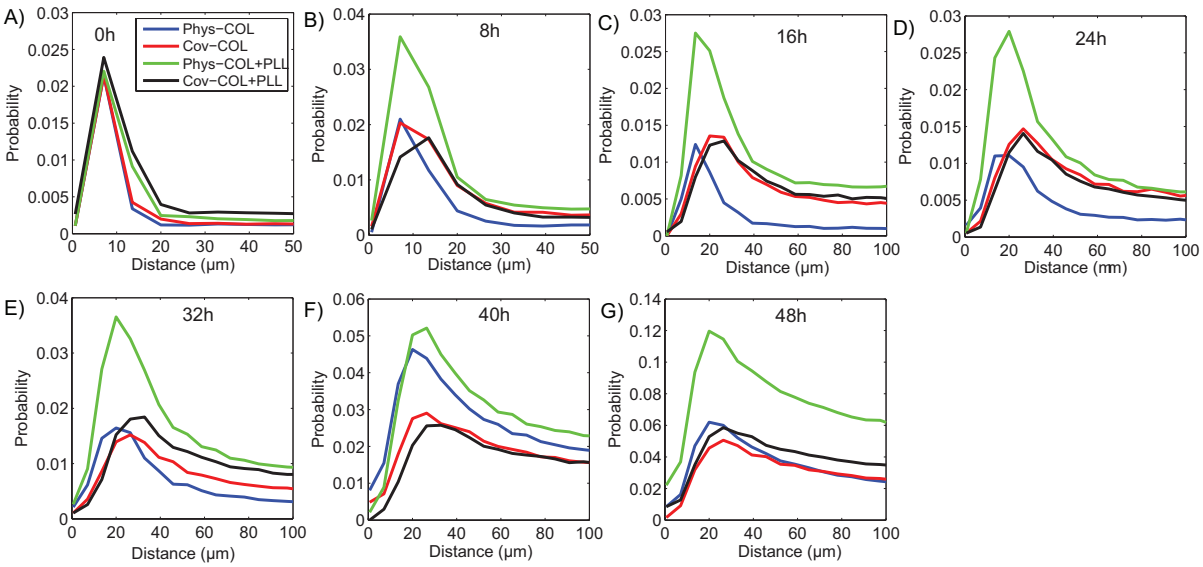

Figure 5.6 **Radial distribution functions of cells on different substrates at different time points.** A) 0h, B) 8h, C) 16h, D) 24h, E) 32h, F) 40h and G) 48h. The blue line represents Phys-COL. The red line represents Cov-COL. The green line represents Phys-COL+PLL. The black line represents Cov-COL+PLL.

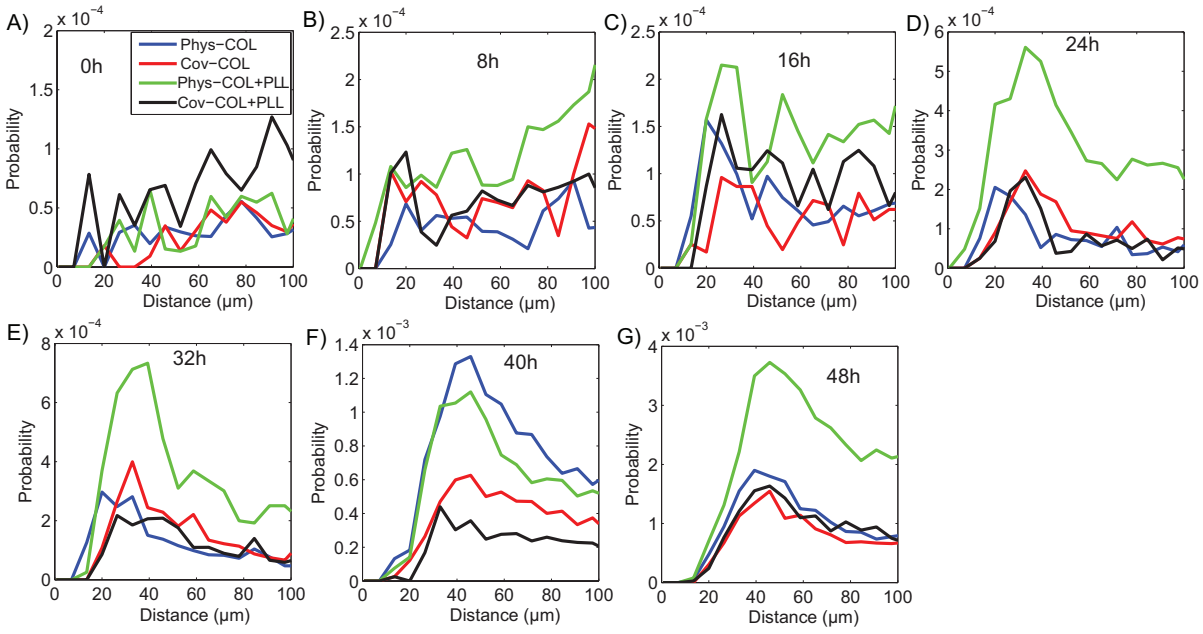

Figure 5.7 **Radial distribution functions of clusters on different substrates at different time points.** A) 0h, B) 8h, C) 16h, D) 24h, E) 32h, F) 40h and G) 48h. The blue line represents Phys-COL. The red line represents Cov-COL. The green line represents Phys-COL+PLL. The black line represents Cov-COL+PLL.

Covalent collagen attachment inhibits desorption and uptake by cells

Given that collagen attachment to the surface drives clustering, I was interested in determining if the surface coverage of collagen was different between conditions and whether it changed over time. To determine this, I used Alexa Fluor 555-labeled collagen to construct Phys-COL and Cov-COL substrates and quantified the fluorescent intensity of the whole image over time. I examined substrates with and without cells. However, because MTLn3 cells are known to express matrix metalloproteinases which could cleave and potentially release collagen from the surface, I also treated cells with a broad spectrum MMP inhibitor, GM-6001. Although the bulk concentrations of fluorescent collagen used to treat both substrates were the same, the amount of collagen binding to the Cov-COL surface was roughly two fold larger than that on Phys-COL substrates (Fig. 5.8). If the clustering was only caused by low coverage of collagen, I should observe clustering on low concentration Cov-COL and scattering on high concentration Phys-COL substrates. Indeed, cells formed clusters on low concentration Cov-COL substrates and on functionalized glass (Fig. 5.9). However, cells also formed clusters on high concentration and stamped Phys-COL substrates. Therefore, the collagen coverage might only partially explain why some substrates result in clustering, while others do not. Low collagen surface coverage and Phys-COL may coordinately be driving the cluster formation. Collagen physically adsorbed to glass decreases in the absence of cells, whereas collagen attached to the surface remains constant over time (Fig. 5.8). In the presence of cells the collagen surface coverage decreases under both conditions, albeit to a lesser extent when collagen is covalently attached to the surface. This decrease in collagen coverage on both Phys-COL and Cov-COL substrates is abrogated when matrix metalloproteinase activity is blocked using GM-6001, indicating that some of the collagen is cleaved from the surface and some passively desorbs (Fig. 5.8). These data indicate that surface coverage of collagen plays a part in clustering and that collagen on Phys-COL substrates decreases due to desorption, matrix metalloproteinase activity and other cellular processes.

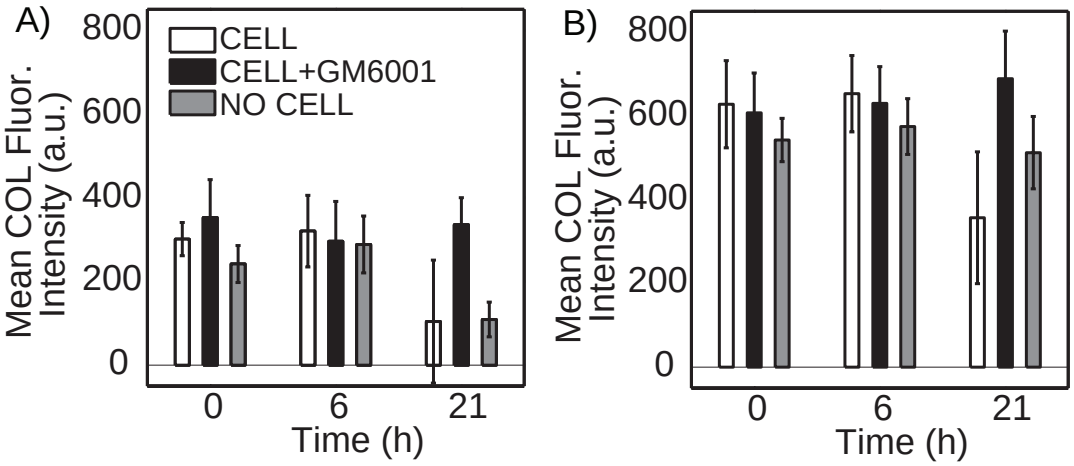

Figure 5.8 **Quantification of surface collagen density.** A) Phys-COL and B) Cov-COL. The white bar represents substrates with MTLn3 cells. The black bar represents substrates with cells and adding MMP inhibitor GM-6001. The gray bar represents substrates without cells. Error bars are 95% confidence intervals.

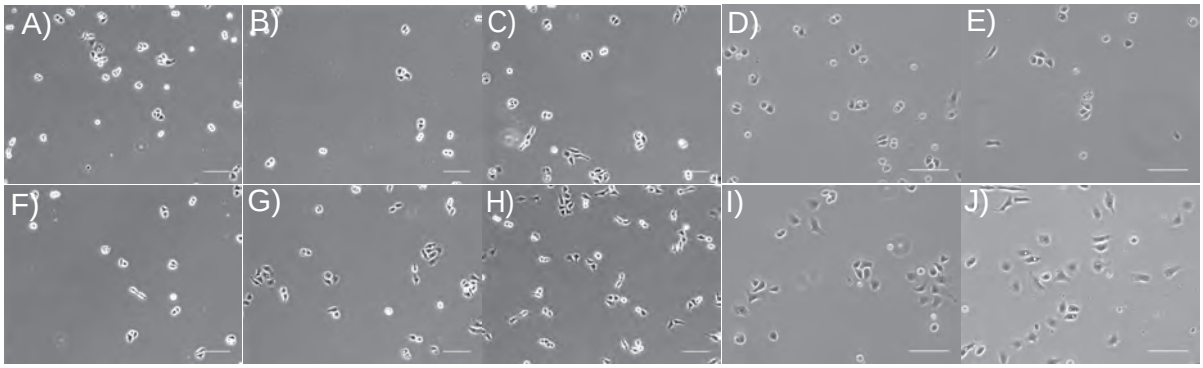

Figure 5.9 **Morphology of cells at 12-16 hrs on different substrates.** A) no COL Phys, B) 0.3 μg/mL COL Phys, C) 0.3 μg/mL COL+PLL Phys, D)30 μg/mL COL Phys, E) stamped COL Phys, F) no COL Cov, G) 0.3 μg/mL COL Cov, H) 0.3 μg/mL COL+PLL Cov, I) 30 μg/mL COL Cov and J) stamped COL Cov, Scale bar is 100 μm.

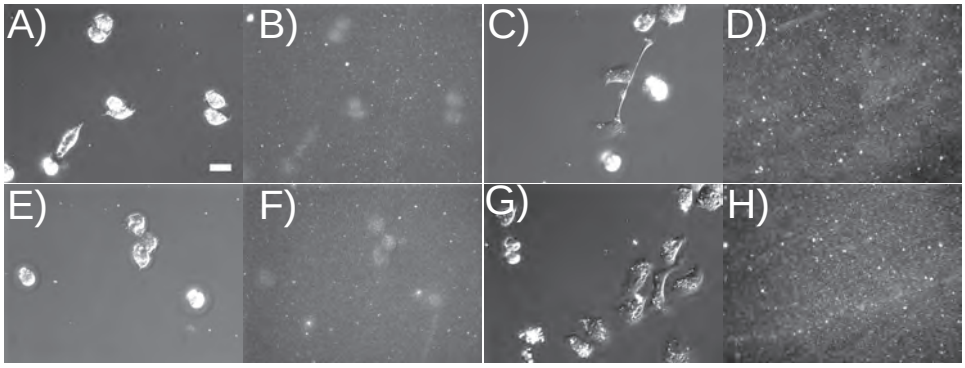

Figure 5.10 **Uptake of collagen by cells on different substrates.** A) Differential interference contrast image of cells (A, C, E and G) and epifluorescence image of Alexa Fluor 555-labeled collagen (B, D, F and H) on Phys-COL (A and B), Cov-COL (C and D), Phys-COL+PLL (E and F) and Cov-COL+PLL (G and H). B) and F) were scaled to the same background level. D and H were scaled to the same background level. Scale bar is 20 μm.

Another approach to quantify the desorption or cleavage of collagen from the surface is to measure the uptake of fluorescent collagen by the cells. To investigate how cells uptake collagen after desorption or cleavage from the surface, I imaged cells on the four different substrates with fluorescently labeled collagen and quantified the mean fluorescent intensity of the cells on four substrates over time. The fluorescent intensity of the cells on physically adsorbed collagen substrates was higher than the surrounding areas, while the fluorescent intensity of the cells on covalently attached substrates did not differ from the surrounding area (Fig. 5.10). The intensity of collagen inside the cells was quantified and increased with time on physically adsorbed collagen substrates (Fig. 5.11A and C). However, cell fluorescence was much more stable on substrates with covalently attached collagen (Fig. 5.11B and D). This coupled with quantification of collagen on the surface indicate that surfaces with covalent collagen attachment have a higher collagen density and are more resistant to desorption or cleavage than surfaces with adsorbed collagen. This difference in collagen surface coverage then contributes to the differences in clustering. However, why do cells exposed to different collagen surface coverages cluster differently? Two possible mechanisms that lead to clustering are proliferation and migration.

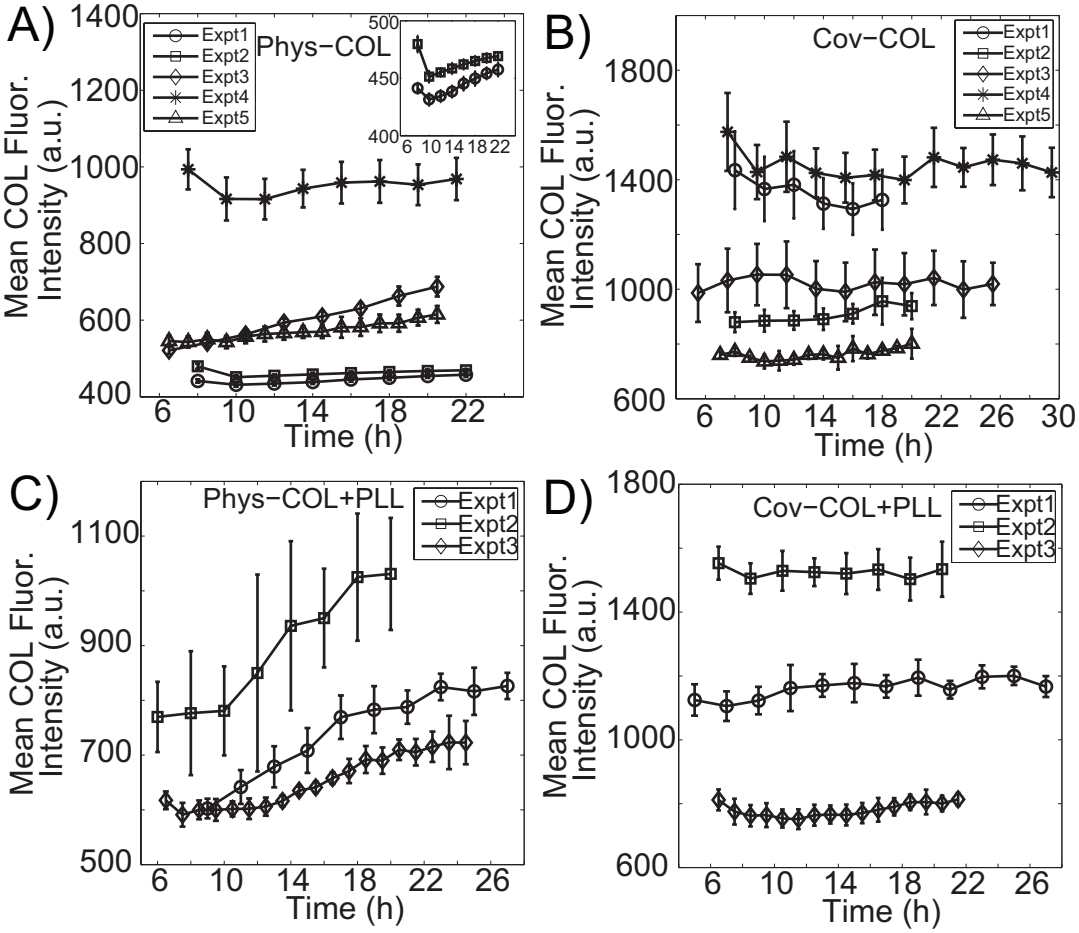

Figure 5.11 **Quantification of the uptake of collagen by cells on different substrates.** A) Phys-COL, B) Cov-COL, C) Phys-COL+PLL and D) Cov-COL+PLL. Different symbols and lines represent different experiments. Insert of A) is the enlarged image of experiment 1 and 2 in A). Error bars are 95% confidence intervals.

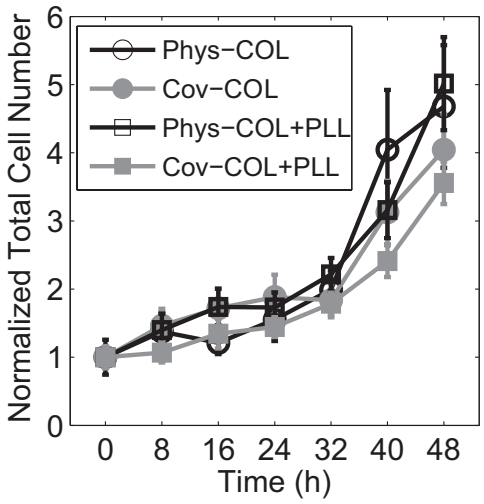

Figure 5.12 **Quantification of cell proliferation over time on different substrates.** Normalized total cell number was calculated. The black opencircle represents Phys-COL. The gray filled circle represents Cov-COL. The black open square represents Phys-COL+PLL. The gray filled square represents Cov-COL+PLL. Error bars are 95% confidence intervals.

Cell proliferation does not explain clustering differences on different substrates

Given that the mechanism of collagen attachment to the surface results in different surface coverage of collagen over time, I was interested in determining whether this had an effect on proliferation. A simple conceptual model for scattering and clustering of non-adherent cells involves the two processes of proliferation and diffusion. The diffusion rate is driven by cell migration and contains two parts, cell migration speed and persistence. When a cell divides, it forms a cluster of two. If the cell migrates slowly, this cluster will grow in size and the average distance between cells will become smaller. Increased proliferation rate can act to enhance clustering, whereas increased diffusion rate acts to enhance scattering. One might assume that cells on physically adsorbed collagen proliferate faster than cells on covalently attached collagen. Therefore, I counted the total cell number over time on the four different substrates to examine whether there was a difference in proliferation rate. There was no significant difference in normalized total cell number between substrates until 40 hrs, much after distinctions in clustering arise (Fig. 5.12). Therefore, clusters are not caused by differences in cell proliferation rates.

Cell migration does explain clustering differences on different substrates

Given that proliferation rates were the same among cells plated on collagen attached to substrates through different mechanisms, I wanted to determine if diffusion rates, set by the magnitude of the cell migration velocity and persistence time, were the same among different substrates. I tracked cell nuclei over time on Phys-COL and Cov-COL substrates and fitted the mean-squared displacement to a model for a persistent random walk. Both the speed and the persistence of MTLn3 cells on Phys-COL were lower than that on Cov-COL (Fig. 5.13A). The persistent random walk model only fits mean-squared displacement data well if the sampling time is sufficiently smaller than the persistence time. If this is not the case, fitting algorithms often push persistence times to arbitrarily low values and migration speeds to arbitrarily high values. When this happened, these data were taken from the pool. However, I noticed that this occurred more frequently with Phys-COL substrates as compared to Cov-COL substrates (Fig. 5.13B). This indicates that cells plated on Phys-COL substrates in general had a much lower persistence than cells plated on Cov-COL substrates. This data indicates that an diminished diffusion rate caused by decreased cell migration speed and persistence and not an enhanced proliferation rate drives the clustering of cells on collagen physically adsorbed to the substrate.

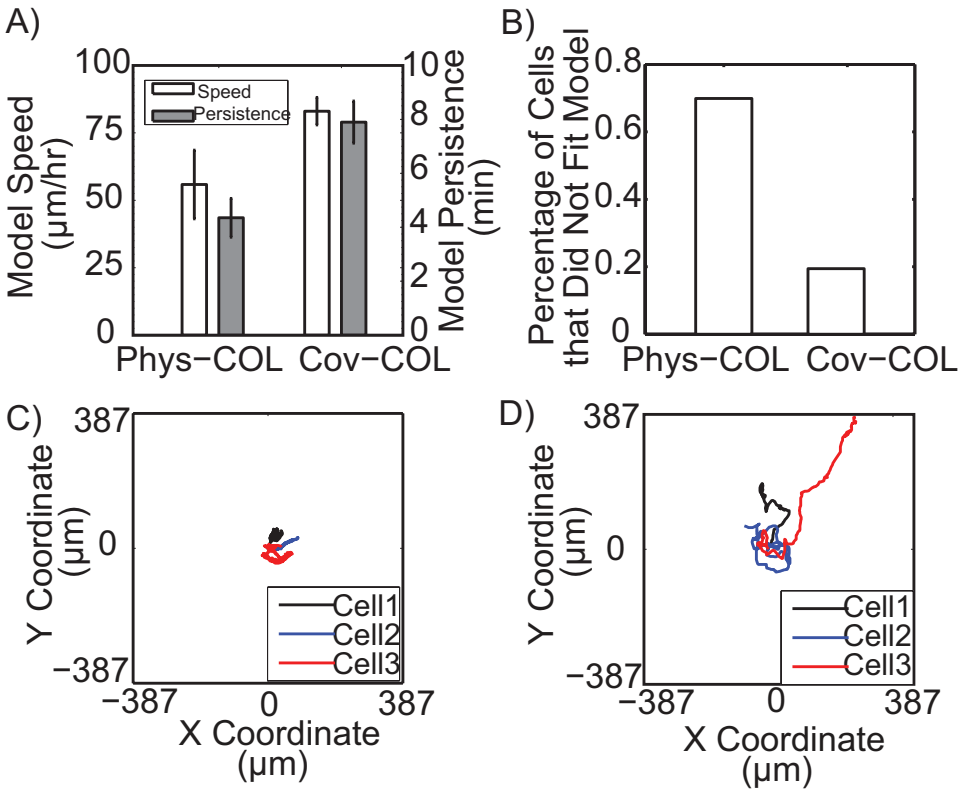

Figure 5.13 **Quantification of cell migration on different substrates.** Cells were tracked and mean squared displacements were fitted to a persistent random walk model. A) Cell speed (open bars) and persistence (gray bars) were measured for cells plated on both Phys-COL and Cov-COL substrates. Error bars represent 95% confidence intervals. B) The percentage of cells that did not fit the model on both Phys-COL and Cov-COL substrates is also shown. Cell migration tracks for cells plated on C) Phys-Col substrates and D) Cov-Col substrates.

5.4 Discussion

In cells that generate firm cell-cell contact, scattering or clustering is a competition between cell-cell vs. cell-substrate adhesivity (de Rooij, Kerstens et al. 2005). If the cell-cell adhesive force is stronger than the cell-substrate adhesive force, cells will tend to remain clustered as opposed to scattering when contractility increases. If contractility increases dramatically and cells do not detach from each other, retraction will occur (Schneider, Hays et al. 2009). Growth factors or other regulators can initiate scattering by either decreasing the cell-cell adhesive force or increasing the cell-substrate adhesive force. When the ECM is presented under conditions of high cell-substrate adhesion (high concentration and stiffness), cells are more able to scatter in response to stimulants (de Rooij, Kerstens et al. 2005). In the case of clustering, migration drives the assembly of clusters. Cells from different regions must find each other, so they search for neighbors using a random walk. Consequently, larger clusters are formed when migration rate is maximal (Pope and Asthagiri 2012). However, in order to cluster cells that form weak cell-cell contact, random migration is not sufficient. With no intercellular adhesion, random migration acts to disperse cells. Consequently, there are only two mechanisms that can explain cell clustering in cells that lack strong cell-cell junctions. The first involves paracrine attraction between cells (Silver and Montell 2001, Hardikar, Marcus-Samuels et al. 2003). Here the paracrine attraction acts as the assembling factor rather than cell-cell adhesion. In addition to this paracrine mediated interaction, high proliferation rates with correspondingly low migration rates could also cause cell clustering. Above it is shown that changes in cell clustering correlate with changes in random cell migration. However, can paracrine attraction be ruled out in favor of a model that includes only fast proliferation and slow random migration?

Perhaps a scaling approach using parameters that describe the rate of proliferation and dispersion could explain changes in average cell spacing. Proliferation rate is characterized by a first order rate constant, μ [=] hr^{-1}. Fits to the time-dependent cell number (Fig. 5.12) resulted in rate constants of 0.028 hr^{-1} and 0.031 hr^{-1} for Cov-Col and Phys-Col substrates, respectively. These equate to doubling times of 25 hr and 22 hr for Cov-Col and Phys-Col substrates, respectively. Dispersion rate or diffusion rate is characterized by a diffusion coef-

ficient, D [=] $\mu m^2/hr$. For random migration the diffusion coefficient, D is also referred to as the random motility coefficient and is equal to the migration speed squared multiplied by the persistence time. Using speeds and persistence times in Fig. 5.13, I was able to calculate the random motility coefficient for Cov-Col and Phys-Col of 910 μm^2/hr and 230 μm^2/hr, respectively. The length scale of dispersion is given by the following equation 5.4:

$$R = \sqrt{\frac{D}{\mu}} \tag{5.4}$$

Consequently, the ratio of dispersion length scales between the Cov-Col and Phys-Col conditions are governed by the following equation 5.5:

$$\frac{R_{Cov-Col}}{R_{Phys-Col}} = \sqrt{\frac{D_{Cov-Col}\mu_{Phys-Col}}{D_{Phys-Col}\mu_{Cov-Col}}} \tag{5.5}$$

This ratio can be directly calculated using the $R_{1/2max}$ for each of the two conditions. This ratio at 16 hrs, after sufficient time for migration and proliferation, but before confluency, was calculated to be 2.1. Using the random motility coefficient and the proliferation rate constant for both conditions a ratio of 2.1 is also calculated. This indicates that simple changes in random motility coefficient can explain the quantitative difference in clustering. In addition, it suggests that while paracrine interactions could act to assemble clusters together, they are probably not at play here since changes in random motility appear to explain the changes in clustering.

The clustering of cells in response to different ECM environments has relevance in cancer. Many clinical and experimental observations suggest that both the weakening of cell-cell contacts and enhanced migration lead to metastasis driven by single cells (Friedl and Wolf 2003). However, others have found less invasive clusters of cells in lymph nodes (Cavallaro and Christofori 2001). This suggests that either multicellular clusters can escape from the primary tissues and form emboli in blood vessels or lymph nodes (Tomlinson, Alpaugh et al. 2001). The idea that metastases might be in fact multicellular clusters provides motivation for the work showing carcinoma cells can escape suspension-induced apoptosis by forming multicelluar clusters. Single cells in suspension that do not form clusters undergo apoptosis (Zhang, Lu et al. 2004, Zhang, Xu et al. 2010). Moreover, the clustering of stromal cells might be just

as important as the clustering of cancer cells as there is some indication that these clusters can initiate tumor invasiveness (Lizonova, Bizik et al. 1990, Kankuri, Cholujova et al. 2005). Therefore, cell clustering plays an important role in the formation of secondary tumor site by either assembling the cancer cells themselves or reorganizing stromal cells. In addition, a firm understanding of clustering is required in tissue engineering applications. Under certain circumstances clusters might be desired, while other circumstances might require the dispersion of cells (Sasai 2013). The examination of clustering on 2D surfaces does have relevance to tissue engineering. While 3D matrices are the first and most common type of construct in tissue engineering applications, engineered surfaces are also important (Ma, Mao et al. 2007, Bauer, Schmuki et al. 2013). Often ECM like collagen is used to make materials like titanium for implants biocompatible (Morra, Cassinelli et al. 2003). Knowing the best approach by which to attach collagen or other ECM to the surface in order for the body to populate it with the appropriate cells that are either dispersed or clustered will have noticeable impact on the design of biomaterials like artificial hips and dental implants (Puleo and Nanci 1999, Li and Kawashita 2011).

5.5 Conclusions

I observed that MTLn3 cells formed clusters on physically adsorbed collagen substrates, while on covalently attached collagen surfaces, cells were more scattered. This clustering appears to be independent of cell-cell attachments as these cells make few cell-cell junctions due to their highly metastatic nature. I quantified several clustering parameters based on radial distribution function and the quantification confirmed my qualitative observations. Cells on covalently attached collagen surfaces had larger scatter index and resulted in lower percentage of cells in clusters. I found that surfaces with covalently attached collagen had a higher collagen coverage and were more resistant to desorption or cleavage than surfaces with adsorbed collagen. While proliferation was the same on physically adsorbed collagen in comparison to covalently attached collagen, the migration speed and persistence were much lower resulting in clustering. This study shows that cell clustering, even in cells that make few cell-cell contacts, is regulated through ECM attachment to substrates through the modulation of cell migration

characteristics.

Given that uniformly distributed ECM substrates affect cell migration and clustering, I wondered how directional cues such as micropatterned collagen lines influence cell adhesion, protrusion and migration behavior. Therefore, in chapter 6, I present an analysis of cell adhesion, protrusion and migration under contact guidance.

5.6 Acknowledgements

I thank Dr. Ian C. Schneider for his guidance, patience and revision throughout this chapter; I thank Laura Lara Rodriguez and Juan Wang for help with the experiments; Matthew Constant and Juan Wang for help in data analysis and Elizabeth Whitley for a helpful discussion. I acknowledge support from the Roy J. Carver Charitable Trust for general project funding and from NSF ARI-R2 (CMMI-0963224) for funding the renovation of the research laboratories used for these studies.

5.7 References

Andl, C. D., T. Mizushima, H. Nakagawa, K. Oyama, H. Harada, K. Chruma, M. Herlyn and A. K. Rustgi (2003). "Epidermal Growth Factor Receptor Mediates Increased Cell Proliferation, Migration, and Aggregation in Esophageal Keratinocytes in Vitro and in Vivo."

Bauer, S., P. Schmuki, K. von der Mark and J. Park (2013). "Engineering biocompatible implant surfaces Part I: Materials and surfaces." Progress in Materials Science 58(3): 261-326.

Boyer, B., S. Roche, M. Denoyelle and J. P. Thiery (1997). "Src and Ras are involved in separate pathways in epithelial cell scattering." Embo Journal 16(19): 5904-5913.

Branch, D. W., J. M. Corey, J. A. Weyhenmeyer, G. J. Brewer and B. C. Wheeler (1998). "Microstamp patterns of biomolecules for high-resolution neuronal networks." Med Biol Eng Comput 36(1): 135-141.

Cavallaro, U. and G. Christofori (2001). "Cell adhesion in tumor invasion and metastasis: loss of the glue is not enough." Biochimica Et Biophysica Acta-Reviews on Cancer 1552(1): 39-45.

da Rocha-Azevedo, B., C.-H. Ho and F. Grinnell (2013). "Fibroblast cluster formation on 3D collagen matrices requires cell contraction dependent fibronectin matrix organization." Experimental Cell Research 319(4): 546-555.

de la Rosa, G., M. Yanez-Mo, R. Samaneigo, D. Serrano-Gomez, L. Martinez-Munoz, E. Fernandez-Ruiz, N. Longo, F. Sanchez-Madrid, A. L. Corbi and P. Sanchez-Mateos (2005). "Regulated recruitment of DC-SIGN to cell-cell contact regions during zymosan-induced human dendritic cell aggregation." Journal of Leukocyte Biology 77(5): 699-709.

de Rooij, J., A. Kerstens, G. Danuser, M. A. Schwartz and C. M. Waterman-Storer (2005). "Integrin-dependent actomyosin contraction regulates epithelial cell scattering." The Journal of Cell Biology 171(1): 153-164.

Dunn, G. A. (1983). "Characterising a kinesis response: time averaged measures of cell speed and directional persistence." Agents Actions Suppl 12: 14-33.

Ferrari, C., F. Balandras, E. Guedon, E. Olmos, I. Chevalot and A. Marc (2012). "Limiting Cell Aggregation During Mesenchymal Stem Cell Expansion on Microcarriers." Biotechnology

Progress 28(3): 780-787.

Friedl, P. and K. Wolf (2003). "Tumour-cell invasion and migration: Diversity and escape mechanisms." Nature Reviews Cancer 3(5): 362-374.

Gassei, K., J. Ehmcke and S. Schlatt (2008). "Initiation of testicular tubulogenesis is controlled by neurotrophic tyrosine receptor kinases in a three-dimensional Sertoli cell aggregation assay." Reproduction 136(4): 459-469.

Gilchrist, C. L., E. M. Darling, J. Chen and L. A. Setton (2011). "Extracellular Matrix Ligand and Stiffness Modulate Immature Nucleus Pulposus Cell-Cell Interactions." PLoS ONE 6(11): e27170.

Giudice, G. (1962). "Restitution of whole larvae from disaggregated cells of sea urchin embryos." Developmental Biology 5(3): 402.

Grotegut, S., D. von Schweinitz, G. Christofori and F. Lehembre (2006). "Hepatocyte growth factor induces cell scattering through MAPK/Egr-1-mediated upregulation of Snail." Embo Journal 25(15): 3534-3545.

Guaita, S., I. Puig, C. Franci, M. Garrido, D. Dominguez, E. Batlle, E. Sancho, S. Dedhar, A. G. de Herreros and J. Baulida (2002). "Snail induction of epithelial to mesenchymal transition in tumor cells is accompanied by MUC1 repression and ZEB1 expression." Journal of Biological Chemistry 277(42): 39209-39216.

Guvakova, M. A. and E. Surmacz (1997). "Overexpressed IGF-I receptors reduce estrogen growth requirements, enhance survival, and promote E-cadherin-mediated cell-cell adhesion in human breast cancer cells." Experimental Cell Research 231(1): 149-162.

Hanahan, D. and R. Weinberg (2000). "The hallmarks of cancer." Cell 100(1): 57-70.

Hardikar, A. A., B. Marcus-Samuels, E. Geras-Raaka, B. M. Raaka and M. C. Gershengorn (2003). "Human pancreatic precursor cells secrete FGF2 to stimulate clustering into hormone-expressing islet-like cell aggregates." Proceedings of the National Academy of Sciences of the United States of America 100(12): 7117-7122.

Hou, Y., S. Hedberg and I. C. Schneider (2012). "Differences in adhesion and protrusion properties correlate with differences in migration speed under EGF stimulation." BMC Biophys 5: 8.

Kankuri, E., D. Cholujova, M. Comajova, A. Vaheri and J. Bizik (2005). "Induction of hepatocyte growth factor/scatter factor by fibroblast clustering directly promotes tumor cell invasiveness." Cancer Research 65(21): 9914-9922.

Khwaja, A., K. Lehmann, B. M. Marte and J. Downward (1998). "Phosphoinositide 3-kinase induces scattering and tubulogenesis in epithelial cells through a novel pathway." Journal of Biological Chemistry 273(30): 18793-18801.

Kudo, T., H. Kigoshi, T. Hagiwara, T. Takino, M. Yamazaki and S. Yui (2009). "Cathepsin G, a neutrophil protease, induces compact cell-cell adhesion in MCF-7 human breast cancer cells." Mediators Inflamm 2009: 850940.

Li, Z. X. and M. Kawashita (2011). "Current progress in inorganic artificial biomaterials." Journal of Artificial Organs 14(3): 163-170.

Lizonova, A., J. Bizik, M. Grofova and A. Vaheri (1990). "Coexpresion of tumor-associated alpha-2-macroglobulin and growth-factors in human-melanoma cell-lines." Journal of Cellular Biochemistry 43(4): 315-325.

Ma, P. C., G. Maulik, J. Christensen and R. Salgia (2003). "c-Met: Structure, functions and potential for therapeutic inhibition." Cancer and Metastasis Reviews 22(4): 309-325.

Ma, Z. W., Z. W. Mao and C. Y. Gao (2007). "Surface modification and property analysis of biomedical polymers used for tissue engineering." Colloids and Surfaces B-Biointerfaces 60(2): 137-157.

Mina-Osorio, P., L. H. Shapiro and E. Ortega (2006). "CD13 in cell adhesion: aminopeptidase N (CD13) mediates homotypic aggregation of monocytic cells." Journal of Leukocyte Biology 79(4): 719-730.

Montesano, R., K. Matsumoto, T. Nakamura and L. Orci (1991). "Identification of a fibroblast-derived epithelial morphogen as hepatocyte growth-factor." Cell 67(5): 901-908.

Morra, M., C. Cassinelli, G. Cascardo, P. Cahalan, L. Cahalan, M. Fini and R. Giardino (2003). "Surface engineering of titanium by collagen immobilization. Surface characterization and in vitro and in vivo studies." Biomaterials 24(25): 4639-4654.

Moscona, A. and H. Moscona (1952). "The dissociation and aggregation of cells from organ rudiments of the early chick embryo." Journal of Anatomy 86(3): 287.

Othmer, H. G., S. R. Dunbar and W. Alt (1988). "Models of dispersal in biological systems." J Math Biol 26(3): 263-298.

Pope, M., N. Graham, B. Huang and A. Asthagiri (2008). "Automated quantitative analysis of epithelial cell scatter." Cell Adhesion and Migration 2(2): 110-116.

Pope, M. D. and A. R. Asthagiri (2012). "Short-Lived, Transitory Cell-Cell Interactions Foster Migration-Dependent Aggregation." Plos One 7(8).

Puleo, D. A. and A. Nanci (1999). "Understanding and controlling the bone-implant interface." Biomaterials 20(23-24): 2311-2321.

Rhee, S., C. H. Ho and F. Grinnell (2010). "Promigratory and procontractile growth factor environments differentially regulate cell morphogenesis." Experimental Cell Research 316(2): 232-244.

Ryan, P., R. Foty, J. Kohn and M. Steinberg (2001). "Tissue spreading on implantable substrates is a competitive outcome of cell-cell vs. cell-substratum adhesivity." Proceedings of the National Academy of Sciences of the United States of America 98(8): 4323-4327.

Salmenpera, P., E. Kankuri, J. Bizik, V. Siren, I. Virtanen, S. Takahashi, M. Leiss, R. Fassler and A. Vaheri (2008). "Formation and activation of fibroblast spheroids depend on fibronectin-integrin interaction." Experimental Cell Research 314(19): 3444-3452.

Sasai, Y. (2013). "Cytosystems dynamics in self-organization of tissue architecture." Nature 493(7432): 318-326.

Schneider, I. C., C. K. Hays and C. M. Waterman (2009). "Epidermal Growth Factor-induced Contraction Regulates Paxillin Phosphorylation to Temporally Separate Traction Generation from De-adhesion." Molecular Biology of the Cell 20(13): 3155-3167.

Shields, M. A., S. Dangi-Garimella, S. B. Krantz, D. J. Bentrem and H. G. Munshi (2011). "Pancreatic cancer cells respond to type I collagen by inducing snail expression to promote membrane type 1 matrix metalloproteinase-dependent collagen invasion." J Biol Chem 286(12): 10495-10504.

Shields, M. A., S. B. Krantz, D. J. Bentrem, S. Dangi-Garimella and H. G. Munshi (2012). "Interplay between β1-integrin and Rho signaling regulates differential scattering and motility of pancreatic cancer cells by snail and Slug proteins." J Biol Chem 287(9): 6218-6229.

Silver, D. L. and D. J. Montell (2001). "Paracrine signaling through the JAK/STAT pathway activates invasive behavior of ovarian epithelial cells in Drosophila." Cell 107(7): 831-841.

Thiery, J. P., H. Acloque, R. Y. J. Huang and M. A. Nieto (2009). "Epithelial-Mesenchymal Transitions in Development and Disease." Cell 139(5): 871-890.

Tomlinson, J., M. Alpaugh and S. Barsky (2001). "An intact overexpressed E-cadherin/alpha, beta-catenin axis characterizes the lymphovascular emboli of inflammatory breast carcinoma." Cancer Research 61(13): 5231-5241.

Vincent-Salomon, A. and J. Thiery (2003). "Host microenvironment in breast cancer development - Epithelial-mesenchymal transition in breast cancer development." Breast Cancer Research 5(2): 101-106.

Wei, C., M. Larsen, M. P. Hoffman and K. M. Yamada (2007). "Self-organization and branching morphogenesis of primary salivary epithelial cells." Tissue Engineering 13(4): 721-735.

Wu, Z., Y. Yu, J. Zhang, Y. Zhai, Y. Tao and J. Shi (2013). "Clustered immature myeloid precursors in intertrabecular region during remission evolve from leukemia stem cell near endosteum and contribute to disease relapse in acute myeloid leukemia." Medical hypotheses 80(5): 624-628.

Xu, R., A. Boudreau and M. Bissell (2009). "Tissue architecture and function: dynamic reciprocity via extra- and intra-cellular matrices." Cancer and Metastasis Reviews 28(1-2): 167-176.

Zhang, X., L. H. Xu and Q. Yu (2010). "Cell aggregation induces phosphorylation of PECAM-1 and Pyk2 and promotes tumor cell anchorage-independent growth." Molecular Cancer 9: 11.

Zhang, Y., H. Lu, P. Dazin and Y. Kapila (2004). "Squamous cell carcinoma cell aggregates escape suspension-induced, p53-mediated anoikis - Fibronectin and integrin alpha(v) mediate survival signals through focal adhesion kinase." Journal of Biological Chemistry 279(46): 48342-48349.

CHAPTER 6. CELL ADHESION STRENGTH AND LINE SPACING DRIVE THE EFFICIENCY OF CONTACT GUIDANCE THROUGH PROTRUSION AND ADHESION

This chapter was modified from the paper submitted to *Cellular and Molecular Bioengineering.*

Nick Romsey, Yue Hou, Ian C Schneider

Cell migration is an important biological function that impacts many physiological and pathological processes. Often migration is directed along aligned fibers of collagen, a process called contact guidance. However, cells also adhere to other components in the extracellular matrix, possibly affecting migrational behavior. This study examines differences in directed migration, protrusion and adhesion in response to varying the spacing of collagen lines, background adhesion strength and the density of collagen lines. Collagen lines were microcontact printed onto glass substrates and timelapse live-cell microscopy was used to measure migration characteristics. Changes in speed and directionality were context different, either increasing or decreasing with line spacing as a function of background adhesivity. However, directionality decreased and speed increased as the cell contacted more lines for all background adhesivity. Both decreasing line spacing and increasing the number of lines a cell contacted resulted in a higher fraction of lateral protrusion waves, but background adhesivity had no effect on protrusion waves. FA dynamics were also regulated by line spacing as well as the number of lines contacted. Fewer and brighter FAs were related to high directionality. This suggests that line spacing, adhesion strength and the number of lines contacted drive the efficiency of contact guidance through protrusion and adhesion.

6.1 Introduction

Cell migration is an important cell behavior that regulates numerous physiological and pathological processes such as cancer metastasis (Friedl and Gilmour 2009). Insight into how cell migration is regulated in these environments will not only lead to therapeutic approaches to enhance or slow down migration during these biological processes, but also will inform models to predict migration behavior from static images of tissue biopsies (Anderson, Weaver et al. 2006) or will guide the design of artificial tissues (Lutolf and Hubbell 2005). In order to achieve these goals cell migration behavior must be quantitatively characterized under different environmental conditions.

Cells migrate by extending protrusions forward. Protrusion can either occur continuously in spatially confined regions as in keratocyte migration or it can occur in cycles or waves of protrusion that move laterally along the edge (Dbereiner, Dubin-Thaler et al. 2006, Machacek and Danuser 2006, Hou, Hedberg et al. 2012). These protrusions adhere to the surrounding extracellular matrix (ECM) through receptors or other non-specific charge-based interactions. Integrins constitute one large family of receptors, which bind specifically to ECM proteins such as fibronectin, laminin and collagens. However, cell adhesion can also be made through non-specific interactions between charged ligands and surface proteoglycans or other receptors (Massia and Hubbell 1992, Mager, LaPointe et al. 2011). While these charge-based interactions can cooperate to adhere new protrusions to the substrate, they lack the ability to form focal adhesions (FAs) (Massia and Hubbell 1992, Lehnert, Wehrle-Haller et al. 2004). On the other hand, integrin interactions with ECM readily form FAs that can be attached to the actin cytoskeleton for structural support and can engage in intracellular signaling that can drive continued protrusion (Zaidel-Bar, Ballestrem et al. 2003, Nayal, Webb et al. 2006). Some FA characteristics like intensity are associated with fast migrating cells and lateral protrusion waves (Hou, Hedberg et al. 2012). When cells migrate with fast speed, changing either adhesion or contractility (or matrix stiffness) can lead to decreased cell migration speed, resulting in a biphasic response (Dimilla, Barbee et al. 1991, Peyton and Putnam 2005, Gupton and Waterman-Storer 2006, Zaman, Trapani et al. 2006).

In vivo migration is not random, but often times directed by extracellular cues such as aligned collagen fibers. For instance, metastatic carcinoma cells translate along collagen fibers as they exit the tumor (Wolf, Mazo et al. 2003, Sahai, Wyckoff et al. 2005, Provenzano, Eliceiri et al. 2008). This migration behavior is called contact guidance (Dunn and Heath 1976). If the contact guidance cue is weak, cell migration is only weakly biased and not all migration steps are in the direction of the cue. If the contact guidance cue is strong, cell migration is strongly biased and most or all steps are in the direction of the cue. Early in the development of the tumor, collagen is organized circumferentially around the tumor mass. During tumor progression, these collagen fibers are reorganized by surrounding stromal cells resulting in large fiber bundles that extend radially from the tumor mass. This new collagen fiber morphology can then direct migration of cells out of the tumor (Provenzano, Eliceiri et al. 2006). While protease activity and fiber reorganization are both vital to the overall process of invasion and metastasis, protease activity seems to be most important during penetration through the basement membrane during initial exit out of the epithelial tissue or entrance into endothelial tissue of blood and lymph vessels (Mierke, Rosel et al. 2008). This suggests that between these two points, cancer cell migration is determined to a large extent by the existing ECM. How fast cells migrate in that environment (speed) and how well the aligned fibers bias migration direction (directionality) are two primary indicators of if or how fast metastatsis will occur. Environmental characteristics such as fiber density (fiber-to-fiber spacing) and the concentration of charged accessory molecules in and around the ECM will impact both speed and directionality. The ECM impacts speed and directionality by altering protrusion and FA dynamics, which plays an important role in the adhesion-based modulation of directionality, because a cell must form nascent FAs and extend an adherent new leading lamellipod to change its direction of locomotion. Dynamics like lateral protrusion waves might lead to a decrease in the directionality. Developing *in vitro* environments where collagen organization can be controlled and cell migration, protrusion and FA characteristics measured will be a powerful approach to understand how cells sense directional ECM cues.

There are various approaches by which to organize and present fibers, including electrospinning collagen fibers (Matthews, Wnek et al. 2002), drawing suspended fibers across posts (Nain,

Phillippi et al. 2008), creating aligned thin films of collagen (Amyot, Small et al. 2008) and growing collagen fibers on atomically smooth mica (Jiang, Horber et al. 2004). Microcontact printing lines of ECM that mimic fibers have also been used. Microcontact printing in general is a powerful way by which to direct cell migration (Kushiro, Chang et al. 2010). Microcontact printing adhesive lines has been used to examine cytoskeleton structure or dynamics (Csucs, Quirin et al. 2007, Pouthas, Girard et al. 2008, Rossier, Gauthier et al. 2010), cell alignment and bridging across lines (Oneill, Jordan et al. 1990, Clark, Connolly et al. 1992, Csucs, Quirin et al. 2007, Doyle, Wang et al. 2009, Rossier, Gauthier et al. 2010, Desai, Khan et al. 2011), traction forces (Borghi, Lowndes et al. 2010, Rossier, Gauthier et al. 2010) or cell migration (Csucs, Quirin et al. 2007, Kandere-Grzybowska, Campbell et al. 2007, Doyle, Wang et al. 2009, Borghi, Lowndes et al. 2010, Maiuri, Terriac et al. 2012). Doyle et al. suggested that line spacing could control migration rate, but these reports along with Mairuri et al. examined cells engaged in complete directional persistence. In addition, Kandere-Grzybowska et al. examined how both speed and persistence length varied as a function of line width, but only on very wide lines. Borghi et al. did show evidence that directionality was a function of adhesiveness and line spacing, but conducted experiments in slow moving cells < 15 μm/hr. These reports did not fully address how line spacing, adhesion strength between lines and protrusion and FA dynamics might impact migration speed or directionality, when cells have the ability to span several ECM lines and move between lines. Given that cells can attach to several ECM fibers simultaneously and move between fibers *in vivo* (Doyle, Wang et al. 2009), I was interested in characterizing the directed migration of cells on substrates where I could probe how fiber density (line spacing), surrounding chemical composition (different backfilling molecules) and the number of lines cells contacted regulate the ability of cells to sense directional ECM cues through protrusion and adhesion. Consequently, I used live cell microscopy to quantitatively measure cell migration behavior under different environmental conditions.

6.2 Materials and Methods

Microcontact printing

All chemicals were purchased from Sigma (St. Louis, Missouri, US) or Fisher (Hampton,

New Hampshire, US) unless otherwise noted. Coverslips used for microcontact printing were aldehyde functionalized. No. 1, 22 mm square coverslips (Corning Inc., Corning, New York, US) were sonicated in the following solutions: hot tap water with Neutrad (Decon Labs, King of Prussia, Pennsylvania, US), hot tap water, distilled water, 1 mM EDTA solution, 70% ethanol in water and 100% ethanol. An adaptation of a protocol to functionalize coverslips with glutaraldehyde was used (Branch, Corey et al. 1998). The coverslips were soaked in a 3:1 sulfuric acid:30% hydrogen peroxide solution, washed with double distilled water and placed in a solution of 1% aminopropyltriethylsilane (APTES) in 10 mM acetic acid. They were then heat-treated in an oven at 100°C. Finally, the coverslips were treated with 6% glutaraldehyde in phosphate buffered saline (PBS) (Gibco, Grand Island, New York, US). The coverslips were stored in double distilled water at 4°C until use.

Masks for the patterns were purchased through Microtronics, Inc. (Newton, Pennsylvania, US). SU-8 photoresist (MicroChem, Newton, Massachusetts, US) was spun on fused silica wafers, exposed to UV light through the mask and developed per the manufacturers recommendations. Polydimethylsiloxane (PDMS) stamps were created by mixing 184 Silicone Elastomer Base (Dow Corning, Ellsworth Adhesives, Germantown, Wisconsin, US) with its curing agent in a 10:1 weight ratio and then allowing it to spread on top of a fused silica master. The master coated with PDMS was exposed to a vacuum to remove any air bubbles and heated for an hour at 60°C to cure the PDMS. PDMS stamps were sonicated in double distilled water and in 100% ethanol. A 200 μL collagen solution of 45 μg/mL collagen I and 15 μg/mL alexa 555-labeled collagen I in 0.5 M acetic acid was applied to each stamp. After a 40 min incubation, the collagen solution was wicked off and then applied to an aldehyde-functionalized coverslip. This system was allowed to incubate for fifteen minutes, and then the stamp was removed. The coverslip incubated for an additional two hours and was then backfilled with either poly-L-lysine (PLL) or PLL polyethylene glycol (PLL-PEG, Alamanda Polymers, Huntsville, AL, US) for one hour. PLL was >30,000 MW and PLL-PEG was 16,000 MW PLL attached to 5000 MW PEG. The PLL, PLL-PEG or FN solutions were each applied for one hour at concentrations of 1,000, 250 and 1000 μg/ml, respectively.

Cell culture and seeding

MTLn3 cells were subcultured in α-MEM media (Gibco, Grand Island, New York, US) containing 5% fetal bovine serum and 1% penicillin and streptomycine (Gibco, Grand Island, New York, US). Cells between passage three and twenty were plated onto patterned coverslips at an approximate density of 100,000 cells per coverslip. Cells were allowed to attach to the coverslip for three to four hours. The coverslip was then inverted onto a microscope slide with strips of double-sided sticky tape. This chamber was filled with α-MEM media with 12 mM HEPES while lacking phenol red (Gibco, Grand Island, New York, US) and sealed using VALAP.

Cell imaging

The microscopy stage was heated with an air curtain (Nevtech, Gardnerville, Nevada, US) or through use of a perfusion chamber with temperature control (Warner Instruments, Hamden, Connecticut, US). The heater was allowed to reach a steady-state 37°C before the sample was imaged. Before cells were imaged, lines were imaged using epifluorescence microscopy. Cells were imaged using phase microscopy at two minute intervals. Images were captured at 20× (NA 0.50) with a charge-coupled device (CoolSNAP HQ2, Photometrics, Tuscan, Arizona, US) attached to an inverted microscope (Eclipse Ti, Nikon, Tokyo, Japan). Image equipment was controlled by μManager 1.3.

Fluorescence microscopy

MTLn3 cells were incubated on patterned coverslips for one day and transfected with paxillin-EGFP as performed previously (Hou, Hedberg et al. 2012). Transfected cells were imaged by total internal reflection fluorescence imaging using a 60× oil objective (NA 1.49, Nikon). Images were taken using the same microscope, camera and software and described above. An automated segmentation and tracking algorithm was utilized for large-scale analysis of FA dynamics (Wurflinger, Gamper et al. 2011). FAs smaller than 0.05 μm^2 and larger than 10 μm^2 were excluded from our analysis because they represent either FAs consisting of less than three pixels or several FAs clustered together. FA fluorescence intensities were calibrated to the standard condition of 1 mW laser power with a 300 ms exposure time, so FA intensity should be directly proportional to protein level across all samples. Number of FAs on and off collagen lines were counted by eyes.

Migration data analysis The cells in the image sequences were manually tracked using MtrackJ, an ImageJ add-on. The nucleus of each qualifying migrating cell was tracked. Only cells that lived for or stayed within the bounds of the imaging field for at least six hours and migrated were tracked. A cell that divided must have migrated by itself for six consecutive hours, without interruption by cellular division to be tracked. A cell resulting from division must migrate for six hours on its own, following the same criteria as a non-dividing cell. The position of each cell was logged using MtrackJ and the directionality and migration speed was calculated using a MATLAB script. The movement of the cell from one position (x_1, y_1) to another position (x_2, y_2) over a given time interval (t_1 to t_2) was used to calculate the angle of displacement with respect to the long axis of the collagen lines, θ and the migration speed, S. Cell directionality, DI, was calculated for each cell using the following equation 6.1:

$$DI = \frac{1}{N}\sum_{i=1}^{N}\cos(2\theta_i), \tag{6.1}$$

where N is the number of non-overlapping time intervals contained in an individual cell track and θ_i is the angle of cell movement with respect to the collagen lines between two times (t_{i+1} - $t_i = \tau$). This value was then averaged among cells to construct an average DI for a given condition. Cell migration speed, S, was calculated for each cell using the following equation 6.2:

$$S = \frac{1}{N}\sum_{i=1}^{N}\frac{\sqrt{\Delta x_i{}^2 + \Delta y_i{}^2}}{\tau}, \tag{6.2}$$

where N is the number of non-overlapping time intervals contained in an individual cell track and Δx and Δy are the x and y displacements between two times (t_{i+1} - $t_i = \tau$). This value was then averaged among cells to construct an average S for a given condition.

To quantify protrusion rate we used a constrained optimization program to measure the protrusion and retraction rates from masked images as done in previous chapters (Machacek and Danuser 2006). The cell edge was segmented into 100 sectors. The average protrusion rate in these sectors was calculated over time.

Statistical analysis

All graphs and statistical analyses were done using JMP and MATLAB software. FA number as described in the results section is more precisely a FA number per cell. Consequently, the

number of measurements of FA number per cell is the product of the average number of frames and the cell number. All the other FA properties were generated by using the time-averaged FA property for each FA in each cell. Consequently, the number of measurements of FA properties is the product of the average FA number and the cell number. Differences between line spacing or number of lines contacted were quantified by calculating the Kolmogorov-Smirnov statistic using the MATLAB function `kstest2`. To determine the statistical differences of the mean values between groups of line spacing or number of lines contacted, a student′s t-test or ANOVA test was utilized and a $p < 0.01$ was deemed significant.

6.3 Results

Collagen line spacing, adhesion strength and the number of lines contacted result in differences in cell morphology, directionality and migration speed

Collagen fiber density is never uniform over space *in vivo* (Wolf, Mazo et al. 2003, Sahai, Wyckoff et al. 2005, Provenzano, Eliceiri et al. 2008). Additionally, other ECM components might be present to varying degrees in different regions *in vivo*. Consequently, another student in our lab (Nick Romsey) examined how cell migration was altered when cells were allowed to migrate on various line spacing and surrounding adhesion strength. Rat adenocarcinoma cells (MTLn3) were plated on various patterns with tunable line spacing (3×5 and 3×10 μm) of fluorescently labeled collagen backfilled with poly-L-lysine (PLL) or poly-L-lysine polyethylene glycol (PLL-PEG). We called these substrates Col:PLL-PEG and Col:PLL substrates, respectively. Cells adopted circular shapes on patterns with small distances between collagen lines on both Col:PLL-PEG and Col:PLL substrates (Fig. 6.1). However, cells on Col:PLL-PEG substrates often formed protrusions directly over the collagen lines only and had concave edges in areas over the PLL-PEG (Fig. 6.1B and D). Cells on Col:PLL substrates had smoother edges (Fig. 6.1A and C). As the line spacing increased cells became more elongated on both Col:PLL-PEG and Col:PLL substrates (Fig. 6.1C and D). However, cells on Col:PLL substrates at large line spacing usually spanned the same line, extending small protrusions over the PLL that were eventually retracted (Fig. 6.1C), whereas cells on Col:PLL-PEG substrates usually spanned more than one line (Fig. 6.1D). This is interesting because PLL is much more adhesive than

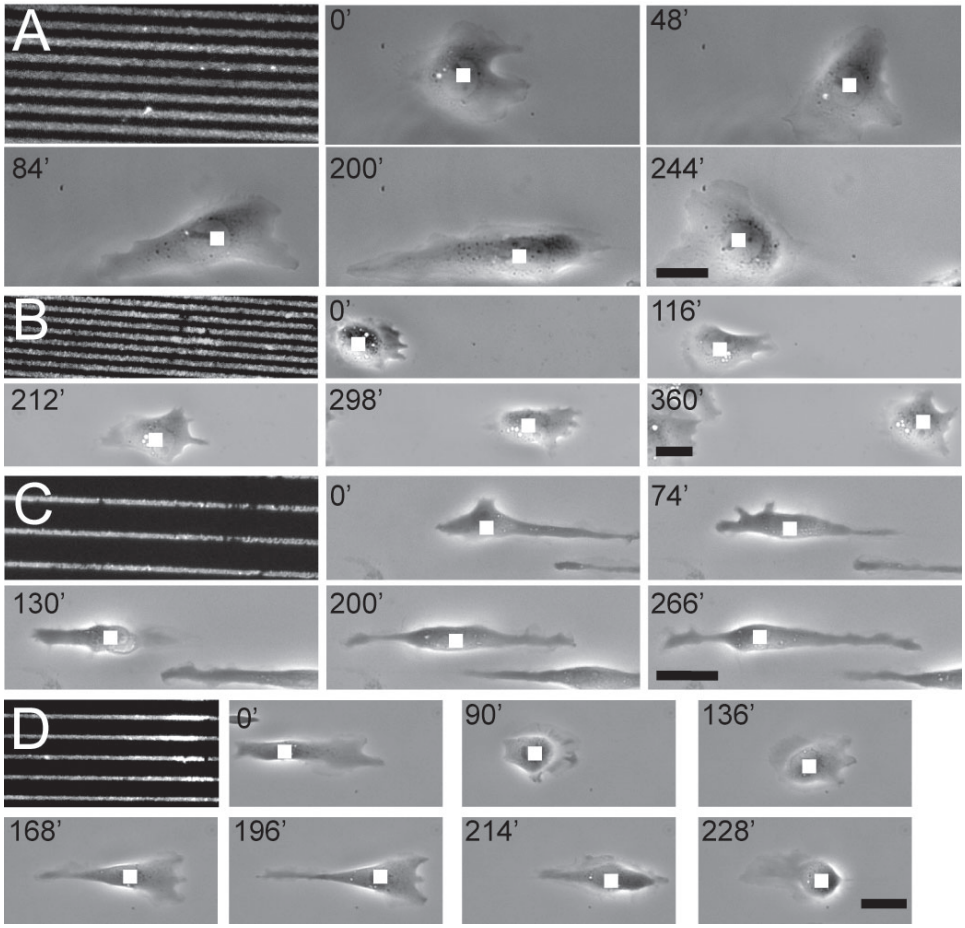

Figure 6.1 **Cell morphology on Col:PLL-PEG and Col:PLL substrates**: MTLn3 cells migrating on A. 3×5 μm Col:PLL, B. 3×5 μm Col:PLL-PEG, C. 3×10 μm Col:PLL and D. 3×10 μm Col:PLL-PEG substrates. White squares are positioned on the tracked coordinates. Scale bars represent 20 μm. Courtesy: Nick Romsey.

PLL-PEG. Given the distinct morphology of the cells on different line spacing and background adhesion strength, the migrational behavior such as directionality and cell migration speed on different line spacing was quantified.

Narrow line spacing resulted in directionality that is roughly independent of adhesivity, however, at wide line spacing, directionality was low for Col:PLL-PEG and high for Col:PLL substrates indicating that Col:PLL and not Col:PLL-PEG substrates are better at directing cell migration (Fig. 6.2A). Speed behaved much differently. The average speed was generally between 25-40 μm/hr. For line spacing less than 10 μm, cells migrated on Col:PLL-PEG and Col:PLL substrates at similar speeds (Fig. 6.2B). However, on a lines spacing of 10 μm, cells on Col:PLL-PEG substrates had roughly similar migration speed, whereas cells on Col:PLL substrates had decreased migration speed (Fig. 6.2B). Plotting directionality as a function of cell migration speed revealed an inverse and roughly linear behavior for all conditions to this point (Fig. 6.2C).

As shown in Fig. 6.1, patterns with different line spacing resulted in cells that contacted different numbers of lines. The number of lines that a cell contacts should regulate the fidelity of contact guidance. The number of lines that each cell contacted was determined by visual inspection and averaged over the imaging time. The average number of lines that each cell contacted decreased with increasing line spacing as would be expected (Fig. 6.2F). Since the number of lines contacted varied greatly, we grouped data based on this metric and examined cell directionality and migration speed. The bins were determined by splitting the distribution of lines contacted into thirds (lines contacted: <3, 3 - 5, >5). Cells attached to one line have little chance to move in directions perpendicular to that line. In contrast, cells attached to many lines can generate force between the lines and perhaps pull themselves perpendicularly to the long axis of the lines. Consequently, one would expect higher directionality in cells touching fewer lines. On both substrates, the directionality decreases as a function of the number of lines that a cell contacts and higher adhesion generally produces better directionality (Fig. 6.2D). Speed has a slightly different relationship. It has been shown that migration speed has a biphasic response to the density of ECM concentration or more generally, the adhesivity of the substrate. On one side of this biphasic curve, increasing adhesivity decreases cell migration speed. For cells migrating on few lines speed is higher on the less adhesive PLL-PEG substrate and lower on the more adhesive PLL. At high numbers of lines contacted cell migration speed converges for both substrates (Fig. 6.2E).

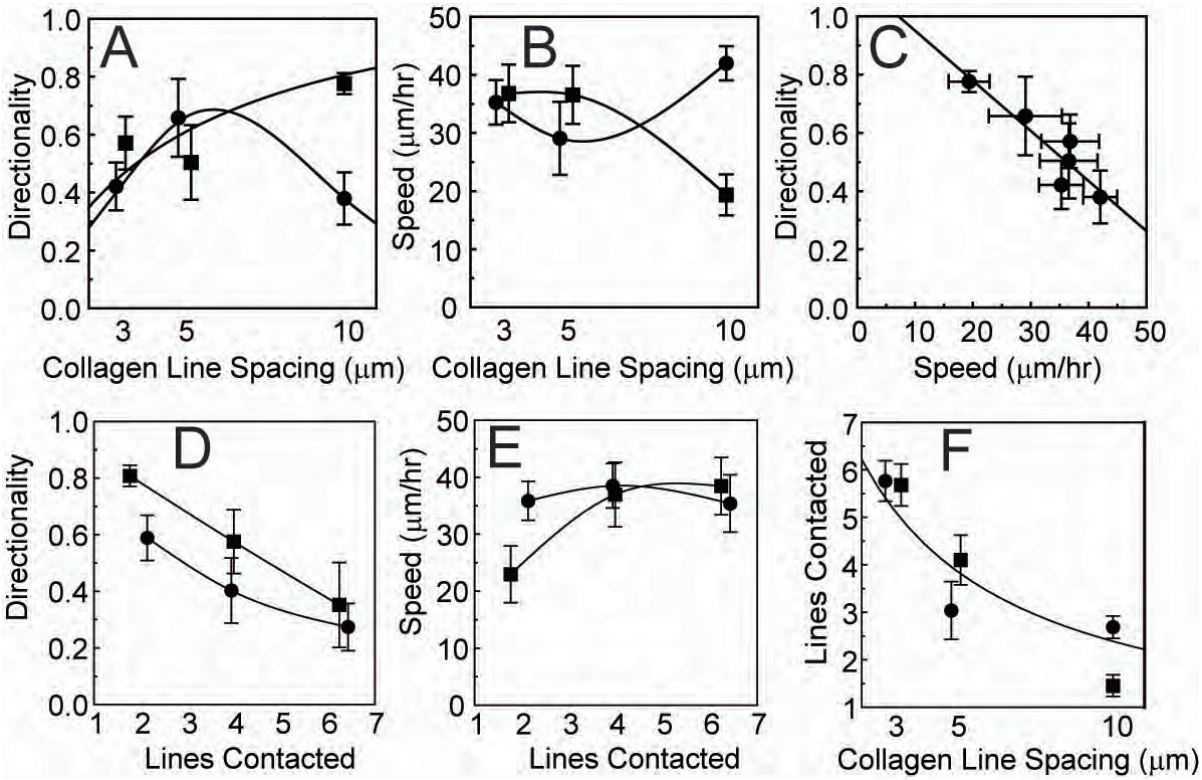

Figure 6.2 **Directionality and cell migration speed are functions of adhesion strength, line spacing and number of lines contacted.** A. and D. Directionality and B. and E. cell migration speed are shown for various backfill molecules (Col:PLL-PEG (circles) and Col:PLL (squares)), line spacing widths and number of lines contacted ((<3, low; 3-5, medium; >5, high)). C. Directionality is plotted as a function of cell migration speed. F. The number of lines a cell contacts is plotted as a function of collagen line spacing. Lines guide the eyes and error bars are 95% confidence intervals. Col:PLL-PEG: 3×3 μm (N_{cells} = 52 and $N_{substrates}$ = 6), 3×5 μm (N_{cells} = 16 and $N_{substrates}$ = 2) and 3×10 μm (N_{cells} = 42 and $N_{substrates}$ = 3); low (N_{cells} = 41 and $N_{substrates}$ = 6), medium (N_{cells} = 38 and $N_{substrates}$ = 10) and high (N_{cells} = 35 and $N_{substrates}$ = 6). Col:PLL: 3×3 μm (N_{cells} = 17 and $N_{substrates}$ = 2), 3×5 μm (N_{cells} = 34 and $N_{substrates}$ = 4) and 3×10 μm (N_{cells} = 11 and $N_{substrates}$ = 2); low (N_{cells} = 17 and $N_{substrates}$ = 4), medium (N_{cells} = 26 and $N_{substrates}$ = 6) and high (N_{cells} = 19 and $N_{substrates}$ = 5). Courtesy: Nick Romsey.

Collagen line spacing and the number of lines contacted regulate the protrusion waves and protrusion waves on Col:PEG decreased directionality

Given that the directionality and cell speed are functions of line spacing, background adhesion strength and the number of lines that a cell contacts, I was interested to see if protrusion or focal adhesion signatures correlate with or explain this behavior. I examined the differences in protrusion and retraction velocities as well as the morphology of FAs on 3×10 μm lines of Col:PLL-PEG or Col:PLL substrates (Fig. 6.3). One prominent feature that I observed was traveling waves of protrusion along the edge of the cell (Fig. 6.3A and B). As I have described in earlier chapters. I quantified the fraction of cells with waves on Col:PLL-PEG and Col:PLL substrates and found that the fraction of cells with waves doesn′t depend on adhesion strength (Fig. 6.4A). The cells on the adhesive backfilling (Col:PLL) only had a slightly lower percentage of traveling waves than the cells on non-adhesive backfilling (Col:PLL-PEG). I also quantified the fraction of cells with waves on different line spacing and the number of lines contacted. At narrow line spacing, the fraction of cells with waves was higher for Col:PLL than Col:PLL-PEG, whereas at wide line spacing, the fraction of cells with waves was higher on Col:PLL-PEG than on Col:PLL (Fig. 6.4B) (based on one cell). Interestingly, the fraction of cells with waves increases as a function of the number of lines that a cell contacts and is independent of background adhesivity (Fig. 6.4C).

Given that the protrusion waves tend to correlate with fast migration as shown in chapter 2, I wondered how fraction of cells with waves will be affected by different cell migration speed. I binned the cell speed into two groups (slow and fast) using a `kstest` function in MATLAB as mentioned in previous paper (Hou, Hedberg et al. 2012). The threshold speed is 42 μm/hr as mentioned in previous chapter. By plotting fraction of cells with waves based on cell speed, I found that at low cell speed, half of the cells had waves and half did not. While at high speed, there is a higher percentage of cells with waves than without wave and this phenomenon is independent of adhesivity (Fig. 6.4D).

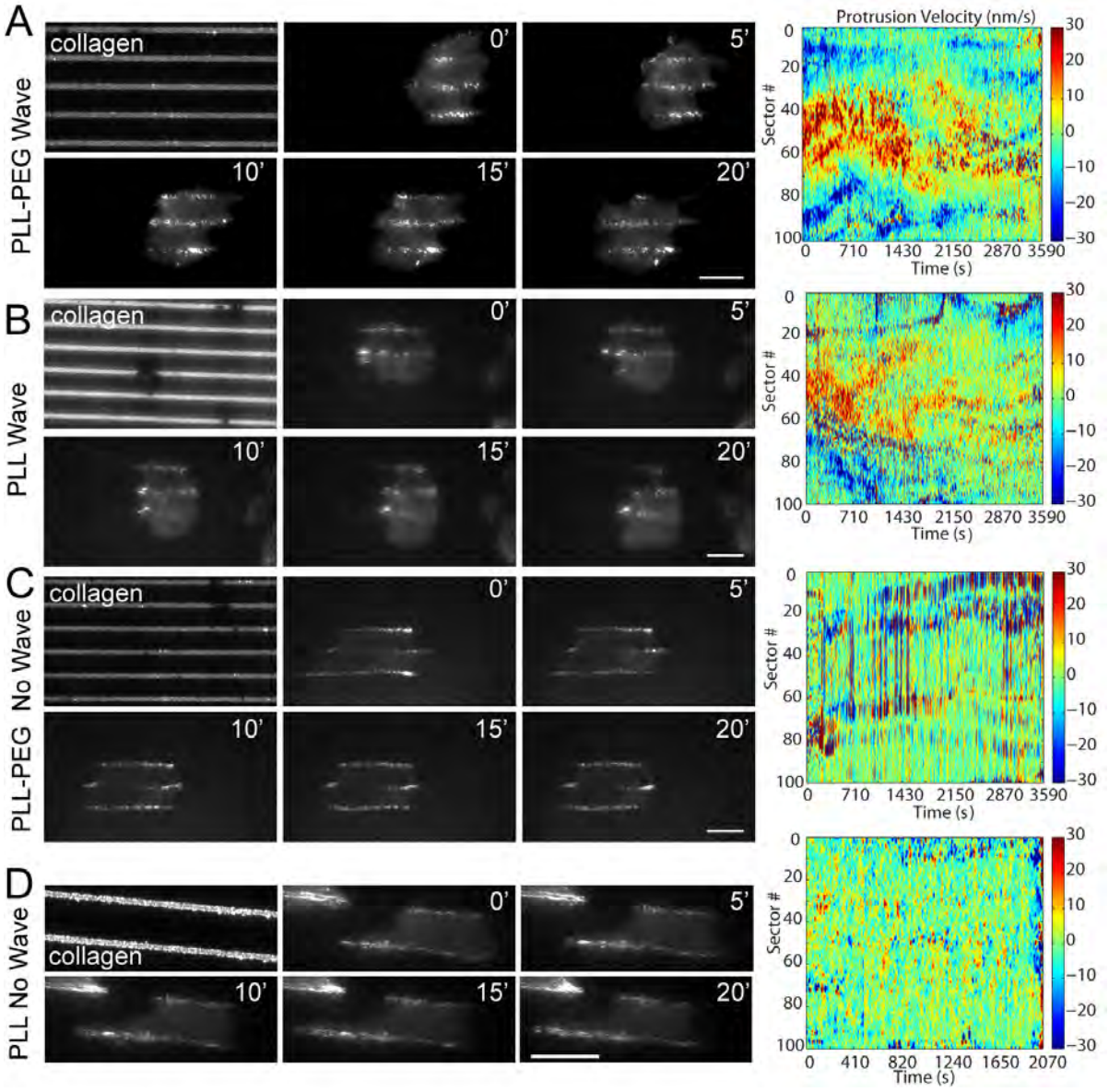

Figure 6.3 **Morphology and focal adhesion dynamics of MTLn3 cells with or without waves on 3 × 10 μm collagen patterned substrates**: A. Col:PLL-PEG with waves, B. Col:PLL with waves, C. Col:PLL-PEG without waves and D. Col:PLL substrates without waves. MTLn3 cells expressing paxillin-EGFP were imaged at various time points (in minutes) during active migration. Scale bars are 20 μm. The right column showed the protrusion velocity maps for each substrate. The cell edge was divided into 100 segments and the average protrusion rate in each segment was determined over time. Red represents fast protrusion, green represents quiescence and blue represents fast retraction.

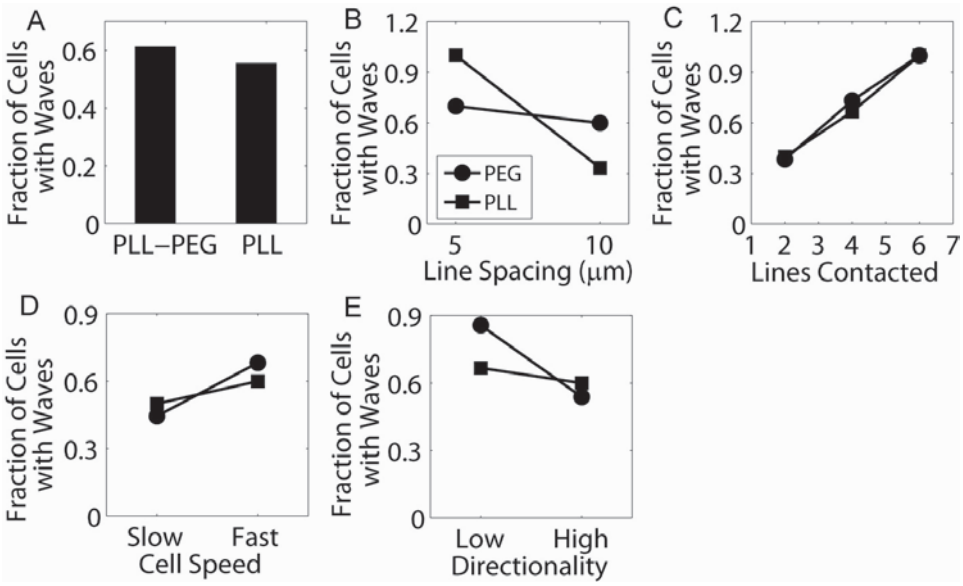

Figure 6.4 **Fraction of cells with waves is a function of collagen line patterns, cell speed and directionality.** A. Fraction of cells with waves on Col:PLL-PEG and Col:PLL substrates. Fraction of cells with waves depends on B. line spacing, C. number of lines contacted (<3, low; 3-5, medium; >5, high), D. cell speed and E. directionality on Col:PLL-PEG (circles) and Col:PLL (squares) substrates. Cell numbers for Col:PLL-PEG: $N = 31$, $N_{3\times5} = 10$, $N_{3\times10} = 10$, $N_{<3}$= 13, N_{3-5}= 15, $N_{>5} = 3$, $N_{Slow} = 9$, $N_{Fast} = 22$, $N_{LowDI} = 7$ and $N_{HighDI} = 13$; for Col:PLL: $N = 9$, $N_{3\times5} = 1$, $N_{3\times10} = 6$, $N_{<3} = 5$, $N_{3-5} = 3$, $N_{>5} = 1$, $N_{Slow} = 4$, $N_{Fast} = 5$, $N_{LowDI} = 3$ and $N_{HighDI} = 5$.

Given that directionality is a decreasing function of the number of lines contacted, while the fraction of waves is an increasing function of the number of lines contacted, I wondered whether the protrusion waves negatively correlate with directionality. Therefore, I binned the directionality into two groups (low and high) the same as I binned the migration speed. The cutoff directionality is 0.4. The cells with directionality less than 0.4 were counted as low directionality and higher than 0.4 were counted as high directionality. By plotting the fraction of waves based on directionality, I found that when cells were plated on Col:PLL-PEG, the fraction of cells with waves was high for low directionality cells. However, when cells were plated on Col:PLL, the fraction of cells with waves was roughly the same for both low and high directionality. (Fig. 6.4E).

Collagen line spacing and the number of lines that a cell contacts regulate FA dynamics

Since cell directionality, speed and protrusion were modulated by collagen line spacing and the number of lines that a cell contacts, I wondered whether FA dynamics were regulated by these two factors as well. Therefore, I examined FA morphology on both Col:PLL-PEG and Col:PLL substrates (Fig. 6.3). When cells spanned numerous collagen lines, individual FAs were seen to form primarily over the collagen lines. However at times some FAs formed over the backfilled portions of the substrates, especially when cells were migrating perpendicularly to the lines (Fig. 6.3A and B). The FAs on Col:PLL were dimmer and harder to detect than on Col:PLL-PEG. As a result, I quantified several FA properties only on Col:PLL-PEG substrate.

The importance of FA characteristics can be based on the magnitude of the difference between different line spacing or the number of lines contacted. This magnitude was quantified by the Kolmogorov-Smirnov statistic (Fig. 6.5). When this statistic is large, it is more likely that there is a difference in distributions between groups. FA number per cell, intensity and lifetime showed the largest values, so I decided to focus on these characteristics. Furthermore, the number of lines contacted caused larger differences in all FA properties in comparison to the line spacing (Fig. 6.5). When binned on line spacing, I found that at narrow line spacing, there were fewer FAs per cell, brighter, larger, more elongated, less orientated FAs and FAs with longer lifetime than at wide line spacing. Only FA speed showed no significant differences between 3×5 and 3×10 patterns (Fig. 6.6). FA number on and off lines has a significant difference on narrow line spacing. When binned on number of lines contacted, there are fewer FAs per cell, brighter FAs and FAs with shorter lifetime on lower number of lines contacted, which associated with high directionality (Fig. 6.7). However, there is only a significant difference between the number of FAs on and off lines on higher number of lines contacted (Fig. 6.7H). Given that narrow spacing and lower number of lines contacted showed high directionality, fewer FAs per cell, and brighter FAs seem to correlate with high directionality.

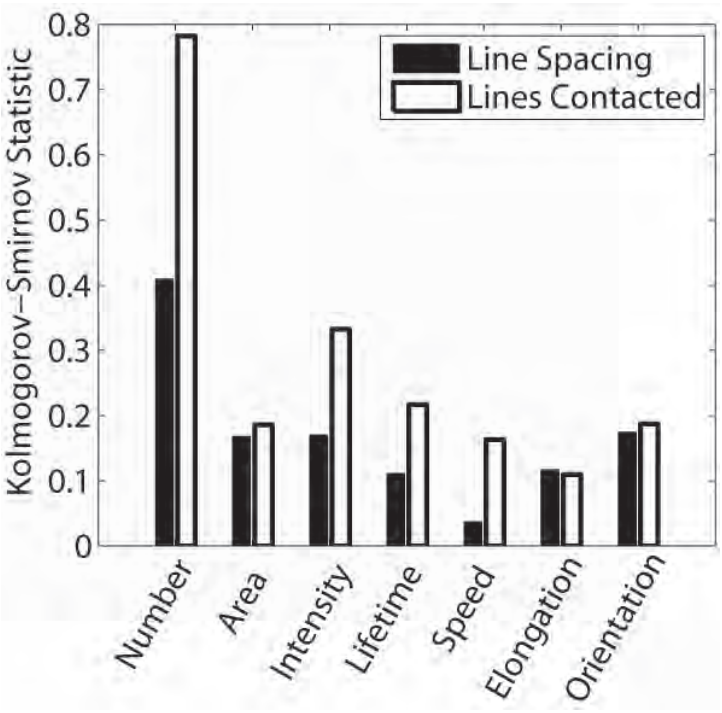

Figure 6.5 **Quantification of the difference between experimental distributions of FA properties.** Cells were binned based on line spacing (3×10 or 3×5 μm) or the number of lines contacted (< 3, 3 - 5, > 5). The Kolmogorov-Smirnov statistic was simply the pair-wise comparison (line spacing) or the average of three pair-wise comparisons (number of lines contacted). A larger value for the Kolmogorov-Smirnov statistic signifies a higher probability that there are differences between groups.

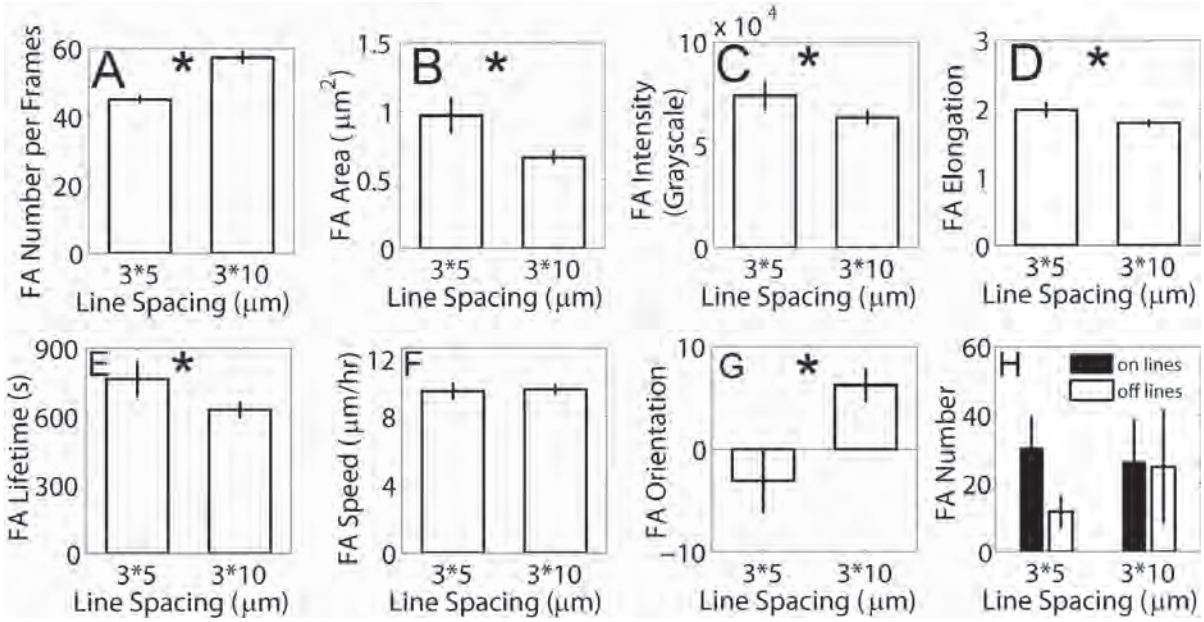

Figure 6.6 **FA properties depend on line spacing.** Mean FA A. number per frames, B. area, C. intensity, D, elongation, E. lifetime, F. speed, G. orientation and H. number on lines (black bar) or off lines (white bar) on Col:PLL-PEG substrate with 1 nM EGF stimulation. Error bars are 95% confidence intervals and asterisks denote $p < 0.01$. For number per frame, $N_{cell,3\times5} = 2$; $N_{FA,3\times5} = 565$; $N_{cell,3\times10} = 4$; $N_{FA,3\times10} = 1441$; for other properties, $N_{cell,3\times5} = 2$; $N_{FA,3\times5} = 334$; $N_{cell,3\times10} = 4$; $N_{FA,3\times10} = 1303$.

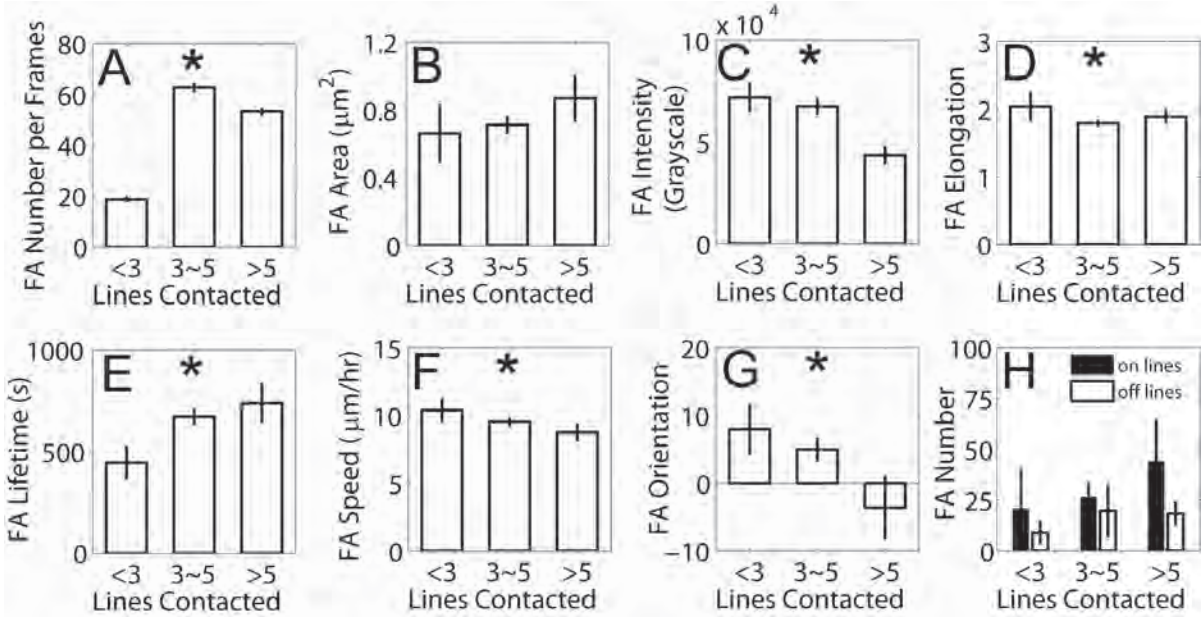

Figure 6.7 **FA properties depend on the number of lines over which a cell spans.** Mean FA A. number per frames, B. area, C. intensity, D, elongation, E. lifetime, F. speed, G. orientation and H. number on lines (black bar) or off lines (white bar) on Col:PLL-PEG substrate with 1 nM EGF stimulation. Error bars are 95% confidence intervals and asterisks denote $p < 0.01$ between three groups. For number per frame, $N_{cell,<3} = 1$; $N_{FA,<3} = 358$; $N_{cell,3-5} = 4$; $N_{FA,3-5} = 1409$; $N_{cell,>5} = 1$; $N_{FA,>5} = 239$; for other properties, $N_{cell,<3} = 1$; $N_{FA,<3} = 151$; $N_{cell,3-5} = 4$; $N_{FA,3-5} = 1313$; $N_{cell,>5} = 1$; $N_{FA,>5} = 173$.

6.4 Discussion

Here we demonstrate that the contact guidance of cells on microcontact printed collagen lines is regulated by adhesivity between the lines, line spacing and the number of lines contacted by cells. Directionality decreases as line spacing increases on Col:PLL-PEG substrates and increases on Col:PLL substrates. Consequently, directionality is a decreasing function of the number of lines contacted by cells and is higher on more adhesive substrates. This somewhat contradicts Borghi et al. who showed that directionality decreased as line spacing increased (Borghi, Lowndes et al. 2010), however they did not keep the collagen line width the same as we did in this report and the backfilling agent was a more specific adhesive molecule, E-cadherin antibody, not PLL. Interestingly, the percentage of cells with protrusion waves is an increasing function of the number of lines contacted by cells. Consequently, low directionality could be caused by protrusion waves.

In addition to directionality and protrusion, cell migration speed remains constant on Col:PLL-PEG substrates and increases on Col:PLL substrates with increasing number of lines contacted. The response of cell migration speed to the number of lines seems to vary based on context. Borghi et al. showed that speed decreases (Borghi, Lowndes et al. 2010), Csucs et al. showed that speed remains constant(Csucs, Quirin et al. 2007) and Doyle et al showed that speed increases with increasing line spacing (Doyle, Wang et al. 2009). This is most likely due to the differences in the ECM type as well as the backfilling agent used in each of these studies. Additionally, cells migrated as fast (Csucs, Quirin et al. 2007, Borghi, Lowndes et al. 2010) or faster (Doyle, Wang et al. 2009) on these contact guidance substrates as compared to the uniform substrates. For instance, Doyle et al. showed that cell migration speeds were dramatically enhanced when cell migration was confined to 1D as opposed to 2D. Optimal speed (65 μm/hr) was attained during 1D migration on 2.5 μm lines, a line width very similar to the one used in this study. The authors argue this enhanced migration rate is most likely due to alterations in adhesion stability and mechanical coupling between the cytoskeleton and FAs (Doyle, Wang et al. 2009, Doyle, Kutys et al. 2012). Our cell migration speeds on contact guiding substrates are roughly similar or slightly less than what we have measured in 2D using

collagen and PLL in the same cells (Hou, Hedberg et al. 2012). However, our cells were not completely confined to 1D migration except when cells only contacted few lines. Here, the enhanced adhesion to PLL explains the slower migration than that seen in 2D. Indeed, when cells contact few lines, cell migration speed appears to be inversely related to adhesion strength, where faster migration occurs on PLL-PEG and slow migration occurs on PLL.

Why does directionality decrease as speed and the frequency of protrusion waves increase?

Random migration can be characterized by a persistence time (or length) and a cell speed and can occur in either 1D, 2D or 3D. Persistence time is the time over which both the magnitude and direction of cell velocity remain constant. Correlations between persistence and cell migration speed in 2D have revealed that as migration speed increases persistence time decreases across several different cell lines (Lauffenburger 1993). Fibroblasts move slowly with high persistence, whereas neutrophils move quickly with low persistence. However, directional persistence is associated with lamellipodial protrusion. Harms et al. have found that EGF stimulation increases both persistence and stablility of lamillipodial protrusions with increasing fibronectin concentration and cell-substratum adhesion concomitantly influences lamellipodial dynamics and directional persistence in 2D (Harms, Bassi et al. 2005). This seems to contradict my results because I found that directionality decreases when protrusion waves increases, especially for cells contact with multiple lines. However, lateral waves are different than persistent protrusion as measured in Harms′ paper, which means that the cells extend protrusions perpendicularly to the collagen lines. Lateral waves dramatically decrease the directionality during contact guidance. The short-timescale kinetics of FA formation may also play an important role in modulating directional persistence over much longer timescales. For example, microtubule motor Kif1C contributes to persistent cell migration primarily through stabilization of an extended cell rear and maturation of trailing FAs (Theisen, Straube et al. 2012). This relates to my observation that brighter and more mature FAs are related to high directionality. These bright, mature FAs probably exist at the rear of the cells and are resistant to tail retraction. Furthermore, FAs play a role in stabilizing the protrusion as well as in the control of its final shape and amplitude (Bailly, Yan et al. 1998). There might be more

and dimer nascent FAs formed on multiple lines and initiate traveling protrusion waves, which decrease the directionality.

6.5 Conclusions

This study examines differences in directed migration, protrusion and adhesion in response to varying the spacing of collagen lines, background adhesion strength and the density of collagen lines. Collagen lines were microcontact printed onto glass substrates and timelapse live-cell microscopy was used to measure migration characteristics. Changes in speed and directionality were context specific, either increasing or decreasing with line spacing as a function of background adhesivity. However, directionality decreased and speed increased as the cell contacted more lines for all background adhesivity. Both decreasing line spacing and increasing the number of lines a cell contacted resulted in a higher fraction of lateral protrusion waves, but background adhesivity had no effect on protrusion waves. FA dynamics were also regulated by line spacing as well as the number of lines contacted. Fewer and brighter FAs were related to high directionality. This suggests that line spacing, adhesion strength and the number of lines contacted drive the efficiency of contact guidance through protrusion and adhesion.

6.6 Acknowledgements

I thank Dr. Ian C. Schneider for his guidance and revision of this chapter. I thank Nicholas R. Romsey for his help with the directionality and migration speed assay and generating some figures. I thank Dave Schmidt and Yong Luo for technical help. I acknowledge support from the Roy J. Carver Charitable Trust for general project funding and from NSF ARI-R2(CMMI-0963224) for funding the renovation of the research laboratories used for these studies.

6.7 References

Amyot, F., A. Small, H. Boukari, D. Sackett, J. Elliott, D. McDaniel, A. Plant and A. Gandjbakhche (2008). "Thin films of oriented collagen fibrils for cell motility studies." Journal of Biomedical Materials Research Part B-Applied Biomaterials 86B(2): 438-443.

Anderson, A. R. A., A. M. Weaver, P. T. Cummings and V. Quaranta (2006). "Tumor morphology and phenotypic evolution driven by selective pressure from the microenvironment." Cell 127(5): 905-915.

Bailly, M., L. Yan, G. M. Whitesides, J. S. Condeelis and J. E. Segall (1998). "Regulation of protrusion shape and adhesion to the substratum during chemotactic responses of mammalian carcinoma cells." Experimental Cell Research 241(2): 285-299.

Borghi, N., M. Lowndes, V. Maruthamuthu, M. L. Gardel and W. J. Nelson (2010). "Regulation of cell motile behavior by crosstalk between cadherin- and integrin-mediated adhesions." Proceedings of the National Academy of Sciences of the United States of America 107(30): 13324-13329.

Branch, D. W., J. M. Corey, J. A. Weyhenmeyer, G. J. Brewer and B. C. Wheeler (1998). "Microstamp patterns of biomolecules for high-resolution neuronal networks." Medical and Biological Engineering and Computing 36(1): 135-141.

Clark, P., P. Connolly and G. R. Moores (1992). "Cell guidance by micropatterned adhesiveness in vitro." Journal of Cell Science 103: 287-292.

Csucs, G., K. Quirin and G. Danuser (2007). "Locomotion of fish epidermal keratocytes on spatially selective adhesion patterns." Cell Motility and the Cytoskeleton 64: 856-867.

Desai, R. A., M. K. Khan, S. B. Gopal and C. S. Chen (2011). "Subcellular spatial segregation of integrin subtypes by patterned multicomponent surfaces." Integrative Biology 3(5): 560-567.

Dimilla, P. A., K. Barbee and D. A. Lauffenburger (1991). "Mathematical model for the effects of adhesion and mechanics on cell migration speed." Biophysical Journal 60(1): 15-37.

Doyle, A. D., M. L. Kutys, M. A. Conti, K. Matsumoto, R. S. Adelstein and K. M. Yamada (2012). "Micro-environmental control of cell migration - myosin IIA is required for efficient

migration in fibrillar environments through control of cell adhesion dynamics." Journal of Cell Science 125(9): 2244-2256.

Doyle, A. D., F. W. Wang, K. Matsumoto and K. M. Yamada (2009). "One-dimensional topography underlies three-dimensional fibrillar cell migration." Journal of Cell Biology 184(4): 481-490.

Dunn, G. A. and J. P. Heath (1976). "New hypothesis of contact guidance in tissue-cells." Experimental Cell Research 101(1): 1-14.

Dbereiner, H. G., B. J. Dubin-Thaler, J. M. Hofman, H. S. Xenias, T. N. Sims, G. Giannone, M. L. Dustin, C. H. Wiggins and M. P. Sheetz (2006). "Lateral membrane waves constitute a universal dynamic pattern of motile cells." Phys Rev Lett 97(3): 038102.

Friedl, P. and D. Gilmour (2009). "Collective cell migration in morphogenesis, regeneration and cancer." Nature Reviews Molecular Cell Biology 10(7): 445-457.

Gupton, S. L. and C. M. Waterman-Storer (2006). "Spatiotemporal feedback between actomyosin and focal-adhesion systems optimizes rapid cell migration." Cell 125(7): 1361-1374.

Harms, B. D., G. M. Bassi, A. R. Horwitz and D. A. Lauffenburger (2005). "Directional Persistence of EGF-Induced Cell Migration Is Associated with Stabilization of Lamellipodial Protrusions." Biophysical Journal 88(2): 1479-1488.

Hou, Y., S. Hedberg and I. C. Schneider (2012). "Differences in adhesion and protrusion properties correlate with differences in migration speed under EGF stimulation." BMC Biophys 5: 8.

Jiang, F. Z., H. Horber, J. Howard and D. J. Muller (2004). "Assembly of collagen into microribbons: effects of pH and electrolytes." Journal of Structural Biology 148(3): 268-278.

Kandere-Grzybowska, K., C. J. Campbell, G. Mahmud, Y. Komarova, S. Soh and B. A. Grzybowski (2007). "Cell motility on micropatterned treadmills and tracks." Soft Matter 3(6): 672-679.

Kushiro, K., S. Chang and A. R. Asthagiri (2010). "Reprogramming Directional Cell Motility by Tuning Micropattern Features and Cellular Signals." Advanced Materials 22(40): 4516-4519.

Lauffenburger, D. A. a. L., J.J. (1993). Receptors: Models for binding, trafficking, and

signaling. New York, New York, Oxford University Press, Inc.

Lehnert, D., B. Wehrle-Haller, C. David, U. Weiland, C. Ballestrem, B. A. Imhof and M. Bastmeyer (2004). "Cell behaviour on micropatterned substrata: limits of extracellular matrix geometry for spreading and adhesion." Journal of Cell Science 117(1): 41-52.

Lutolf, M. P. and J. A. Hubbell (2005). "Synthetic biomaterials as instructive extracellular microenvironments for morphogenesis in tissue engineering." Nature Biotechnology 23(1): 47-55.

Machacek, M. and G. Danuser (2006). "Morphodynamic profiling of protrusion phenotypes." Biophysical Journal 90(4): 1439-1452.

Mager, M. D., V. LaPointe and M. M. Stevens (2011). "Exploring and exploiting chemistry at the cell surface." Nature Chemistry 3(8): 582-589.

Maiuri, P., E. Terriac, P. Paul-Gilloteaux, T. Vignaud, K. McNally, J. Onuffer, K. Thorn, P. A. Nguyen, N. Georgoulia, D. Soong, A. Jayo, N. Beil, J. Beneke, J. C. H. Lim, C. P. Y. Sim, Y. S. Chu, A. Jimenez-Dalmaroni, J. F. Joanny, J. P. Thiery, H. Erfle, M. Parsons, T. J. Mitchison, W. A. Lim, A. M. Lennon-Dumenil, M. Piel, M. Thery and W. C. R. Participants (2012). "The first World Cell Race." Current Biology 22(17): R673-R675.

Massia, S. P. and J. A. Hubbell (1992). "Immobilized amines and basic amino-acids as mimetic heparin-binding domains of cell-surface proteoglycan-mediated adhesion." Journal of Biological Chemistry 267(14): 10133-10141.

Matthews, J. A., G. E. Wnek, D. G. Simpson and G. L. Bowlin (2002). "Electrospinning of collagen nanofibers." Biomacromolecules 3(2): 232-238.

Mierke, C. T., D. Rosel, B. Fabry and J. Brabek (2008). "Contractile forces in tumor cell migration." European Journal of Cell Biology 87(8-9): 669-676.

Nain, A. S., J. A. Phillippi, M. Sitti, J. MacKrell, P. G. Campbell and C. Amon (2008). "Control of cell behavior by aligned micro/nanofibrous biomaterial scaffolds fabricated by spinneret-based tunable engineered parameters (STEP) technique." Small 4(8): 1153-1159.

Nayal, A., D. J. Webb, C. M. Brown, E. M. Schaefer, M. Vicente-Manzanares and A. R. Horwitz (2006). "Paxillin phosphorylation at ser273 localizes a GIT1-PIX-PAK complex and regulates adhesion and protrusion dynamics." Journal of Cell Biology 173(4): 587-599.

Oneill, C., P. Jordan, P. Riddle and G. Ireland (1990). "Narrow linear strips of adhesive substratum are powerful inducers of both growth and total focal contact area." Journal of Cell Science 95: 577-586.

Peyton, S. R. and A. J. Putnam (2005). "Extracellular matrix rigidity governs smooth muscle cell motility in a biphasic fashion." Journal of Cellular Physiology 204(1): 198-209.

Pouthas, F., P. Girard, V. Lecaudey, T. B. N. Ly, D. Gilmour, C. Boulin, R. Pepperkok and E. G. Reynaud (2008). "In migrating cells, the Golgi complex and the position of the centrosome depend on geometrical constraints of the substratum." Journal of Cell Science 121(14): 2406-2414.

Provenzano, P. P., K. W. Eliceiri, J. M. Campbell, D. R. Inman, J. G. White and P. J. Keely (2006). "Collagen reorganization at the tumor-stromal interface facilitates local invasion." Bmc Medicine 4: 15.

Provenzano, P. P., K. W. Eliceiri, L. Yan, A. Ada-Nguema, M. W. Conklin, D. R. Inman and P. J. Keely (2008). "Nonlinear Optical Imaging of Cellular Processes in Breast Cancer." Microscopy and Microanalysis 14(6): 532-548.

Rossier, O. M., N. Gauthier, N. Biais, W. Vonnegut, M. A. Fardin, P. Avigan, E. R. Heller, A. Mathur, S. Ghassemi, M. S. Koeckert, J. C. Hone and M. P. Sheetz (2010). "Force generated by actomyosin contraction builds bridges between adhesive contacts." Embo Journal 29(6): 1055-1068.

Sahai, E., J. Wyckoff, U. Philippar, J. E. Segall, F. Gertler and J. Condeelis (2005). "Simultaneous imaging of GFP, CFP and collagen in tumors in vivo using multiphoton microscopy." Bmc Biotechnology 5: 9.

Theisen, U., E. Straube and A. Straube (2012). "Directional Persistence of Migrating Cells Requires Kif1C-Mediated Stabilization of Trailing Adhesions." Developmental Cell 23(6): 1153-1166.

Wolf, K., I. Mazo, H. Leung, K. Engelke, U. H. von Andrian, E. I. Deryugina, A. Y. Strongin, E. B. Brocker and P. Friedl (2003). "Compensation mechanism in tumor cell migration: mesenchymal-amoeboid transition after blocking of pericellular proteolysis." Journal of Cell Biology 160(2): 267-277.

Wurflinger, T., I. Gamper, T. Aach and A. S. Sechi (2011). "Automated segmentation and tracking for large-scale analysis of focal adhesion dynamics." Journal of Microscopy 241(1): 37-53.

Zaidel-Bar, R., C. Ballestrem, Z. Kam and B. Geiger (2003). "Early molecular events in the assembly of matrix adhesions at the leading edge of migrating cells." Journal of Cell Science 116(22): 4605-4613.

Zaman, M. H., L. M. Trapani, A. Siemeski, D. MacKellar, H. Y. Gong, R. D. Kamm, A. Wells, D. A. Lauffenburger and P. Matsudaira (2006). "Migration of tumor cells in 3D matrices is governed by matrix stiffness along with cell-matrix adhesion and proteolysis." Proceedings of the National Academy of Sciences of the United States of America 103(29): 10889-1089

CHAPTER 7. CONCLUSIONS

7.1 Differences in Adhesion and Protrusion Properties Correlate with Differences in Migration Speed under EGF Stimulation

Cell migration plays an essential role in many biological processes, such as cancer metastasis, wound healing and immune response. Cell migration is mediated through protrusion and focal adhesion (FA) assembly, maturation and disassembly. Chronic stimulation with epidermal growth factor (EGF) is known to enhance migration rate in many cell types; however it is not known how FA properties and protrusion dynamics are regulated during EGF-induced migration. In chapter 2, I described using rat adenocarcinoma cells as the model system. I measured cell migration speed and persistence on collagen substrates with an adhesive component poly-L-lysine (PLL) and used total internal reflection fluorescence (TIRF) microscopy and image analysis to quantify FA properties and protrusion dynamics under different doses of EGF stimulation.

EGF was found to broaden the distribution of cell migration rates, generating more fast and slow cells, but not dramatically affecting the average response. Several different adhesion and protrusion characteristics correlated with EGF stimulation and cell migration speed, however there is a hierarchy of these correlations. When data was binned based on EGF stimulation conditions, FA intensity and number per cell showed the largest difference among stimulation groups. FA intensity decreased with increasing EGF concentration and FA number per cell was highest under intermediate stimulation conditions. No difference in protrusion behavior was observed. However, when data was binned based on cell migration speed, FA intensity and not FA number per cell showed the largest difference among groups. FA intensity was lower for fast migrating cells. Additionally, waves of protrusion were found in fast migrating

cells. This effectively established signatures of FA properties and protrusion dynamics for EGF stimulation and fast migration. EGF concentration is considered an input that acts to regulate FA properties and protrusion dynamics, whereas cell speed is an output that acts to integrate information determined by inputs such as EGF concentration. While EGF stimulation could regulate FA intensity to modulate cell speed directly or by partially activating protrusion waves, other factors like contractility or extracellular matrix (ECM) most likely lead to protrusion waves.

The idea that EGF can both increase and decrease the migration speed of individual cells in a population has particular relevance to cancer metastasis where the microenvironment can select subpopulations based on some adhesion and protrusion characteristics, leading to a more invasive phenotype as would be seen if all cells responded like an average cell. Determining molecular signatures for fast migrating cells might enhance diagnostics which tend to emphasize average responses. Because fast invasive cancer cells are especially important for studying cancer metastasis, it is necessary to design a simple, high-throughput method to mark or isolate the subpopulation of fast migrating cells from other slow migrating cells in order to determine what differences in cell properties such as protein expression level lead to the cell-to-cell variability (chapter 3). In addition, other environmental factors such as adhesion and cell contractility might work through FA properties and protrusion dynamics to modulate migration (chapter 4).

7.2 Combination of Quantum Dot-based Phagokinetic Assay and Flow Cytometry to Assess Cell-to-cell Variability in Migration

Cancer metastasis is often driven by fast moving cells. Consequently, I began to optimize a QD-based phagokinetic assay with flow cytometry as a high-throughput method to identify fast moving cells with different level of fluorescence and use this information to assess cell-to-cell variability in migration. In this QD-based phagokinetic assay, cells are incubated on fluorescent QD substrates and allowed to uptake QDs through phagocytosis. I hypothesized that the fast migrating cells would uptake more QDs and be brighter due to the longer distances over which

they migrated in comparison to slow migrating cells.

By comparing different types, concentrations, buffers and coating methods of QDs, I found that 200 nM aminopropanediol (AP)-QDs in DMEM with a sandwich-like incubation method was the best condition for highest intensity and most homogeneous distribution of QDs on the surface. I compared the distances and the fluorescence intensities of tumor cells (MTLn3) and non-tumor cells mouse embryonic fibroblast cells (MEF) using the combination of the phagokinetic assay and flow cytometry. While cell migration speed was the largest contributor to the uptake, cell area affected the uptake too. This required fluorescence to be normalized based on cell area. This generated an measurable quantity that was a function of cell migration speed only. QD uptake amount was sensitive to cell speed, perticularly after long time migration for MTLn3 cells. Therefore, the combination of QD-based phagokinetic assay and flow cytometry might be a reasonable approach to analyze cell-to-cell variability in migration. However, much more optimization is required for a robust response.

7.3 EGF, Adhesivity and Contractility Integrally Modulate Cell Migration through Protrusion and Focal Adhesion Dynamics

Although it is established that cell migration, protrusion and adhesion are regulated by adhesivity and contractility, there exists little quantitative understanding concerning how these environmental factors are integrated to modulate migration. Adhesivity can be altered by increasing specific adhesion strength or adding a non-specific adhesive component and contractility can be altered by inhibiting Rho-Rho kinase (ROCK) signaling. I studied how cell migration speed and persistence changed on substrates of various adhesiveness or in response to ROCK inhibition during EGF stimulation.

I found that on less adhesive substrates, the migration speed was decreased and the biphasic response with EGF was eliminated. When non-specific adhesion increased, the migration response to EGF remained biphasic, but the speed was much lower. Contractility inhibition acted in the same manner as enhancing adhesiveness at the level of migration. When increasing adhesivity and decreasing contractility together, the dose response of migration speed to

EGF was eliminated and migration speed decreased significantly. While adhesivity and contractility impacted migration similarly, their impact on protrusion and adhesion were distinct. Enhanced adhesivity enhanced the fraction of cells with EGF-induced protrusion waves. Diminishing contractility abolished EGF-induced protrusion waves. Increasing adhesivity and decreasing contractility both generated more FAs and smaller FAs in response to EGF, but contractility also altered FA lifetime. This showed that although responses to environmental cues at the level of cell migraiton may be similar, upstream responses may vary.

When studying the cell migration behavior, I observed that some substrae conditions induced cell clustering with different sizes and morphology. In addition, clustering is an important phenomenon in metastasis and secondary tumor formation, so I wanted to investigate what causes clustering (chapter 5).

7.4 Collagen Attachment to the Substrate Controls Cell Clustering through Migration

Cell clustering and scattering play important roles in cancer progression and tissue engineering. While the ECM is known to control cell clustering, much of the quantitative work has focused on the analysis of clustering between cells with strong cell-cell junctions. Much less is known about how the ECM regulates cells with weak cell-cell contact. Therefore, I constructed four types of substrates that varied in the way in which collagen was attached to the surface and in their adhesivity. MTLn3 cells were used as a model system to study scattering and clustering in cells that lack strong cell-cell adhesion.

I observed that MTLn3 cells formed clusters on physically adsorbed collagen substrates, while on covalently attached collagen surfaces, cells were more scattered. This clustering appears to be independent of cell-cell attachments as these cells make few due to their highly metastatic nature. I quantified several clustering parameters based on a radial distribution function and a k-means clustering approach and the quantification confirmed the qualitative observations. Cells on covalently attached collagen surfaces had a larger scatter index and resulted in lower percentage of cells in clusters. Covalently attaching collagen allowed for higher

initial collagen surface coverage and decreased desorption of collagen. This lower initial density of collagen as well as its decrease over time when physically adsorbing resulted in more clustering. No significant difference in cell proliferation was observed between the conditions. However, cell migration was enhanced on collagen that was covalently attached to the surface. This indicates that the attachment mechanism of collagen can alter the clustering behavior of cells by regulating the migration rate.

Understanding how the ECM regulates clustering will not only impact the fundamental understanding of cancer progression, but also will guide the design of tissue engineered constructs that allow for the clustering or dissemination of cells throughout the construct. However, ECM sometimes organize into aligned fibers *in vivo*. These aligned fibers result in contact guidance, where metastatic carcinoma cells translate along as they exit the tumor. I wondered how directional cues such as micropatterned collagen lines influence cell adhesion, protrusion and migration behavior. Therefore, I conducted some experiments to study cell adhesion, protrusion and migration under contact guidance (chapter 6).

7.5 Cell Adhesion Strength and Line Spacing Drive the Efficiency of Contact Guidance through Protrusion and Adhesion

Cell migration is often directed along aligned fibers of collagen, a process called contact guidance. However, cells adhere to other components in the extracellular matrix, possibly affecting migrational behavior. I was interested in characterizing the directed migration of cells on substrates where I could probe how fiber density (line spacing), surrounding chemical composition (different backfilling molecules) and the number of lines cells contact regulate the ability of cells to sense directional ECM cues through protrusion and adhesion.

Collagen was microcontact printed onto glass substrates and timelapse live-cell microscopy was used to measure migration, protrusion and adhesion characteristics. Increasing the number of lines contacted resulted in a higher percentage of lateral protrusion waves, which led to decreases in directionality. Speed changes were context dependent. FA dynamics were also regulated by line spacing as well as the number of lines contacted and were related to direc-

tionality. This suggests that adhesion strength and line spacing drive the efficiency of contact guidance through the presence of protrusion waves.

7.6 Future Work

This work has attempted to quantitatively address how cancer cell migration is regulated through protrusion and adhesion under various perturbations and in various environments. However, several questions remain. First, the study of cell migration under directional cues is not complete. Do the same protrusion and FA signatures for random migration hold for directed migration? Are signatures for different types of directed migration such as contact guidance and chemotaxis the same? How do these signatures relate to other non-migratory functions? Immune cells secret soluble growth factors, generating concentration gradients. Cancer cells not only migrate out of tumor, but also remodel these fibers through protrusion and contraction to generate a more preferable invasive environment and lead to chemotaxis. *In vivo*, multiple cues for both contact guidance and chemotaxis are simultaneously presented and the substrate is not 2D. How do these signatures change in 3D environments? Furthermore, linking these observations of cell migration to diagnostic pathways will inform models to predict migration behavior from static images of tissue biopsies and will guide the design of artificial tissues. For example, can we extract cells from tissue biopsies and observe their protrusion and adhesion dynamics and can these dynamics be related to cancer prognosis? If they are invasive, we can then modulate their migrational behavior through modification of environmental factors, such as altering the stiffness of microenvironments or adding specific contractility inhibitors, which might prevent or delay the invasiveness of these cells after reintroducing them into the patient.